LUND UNIVERSITY

Fat bloom on chocolate confectionery systems - From core to surface

Dahlenborg, Hanna

2014

[Link to publication](#)

Citation for published version (APA):
Dahlenborg, H. (2014). *Fat bloom on chocolate confectionery systems - From core to surface*. [Doctoral Thesis (compilation)].

Total number of authors:
1

Fat bloom on chocolate confectionery systems

From core to surface

Hanna Dahlenborg
Department of Food Technology,
Engineering and Nutrition
Faculty of Engineering LTH
Lund University, Sweden 2014
Doctoral Thesis

LUND UNIVERSITY

2014

Fat bloom on chocolate confectionery systems

From core to surface

Hanna Dahlenborg

Department of Food Technology, Engineering and Nutrition

Faculty of Engineering LTH

Doctoral Thesis at Lund University

Lund, Sweden 2014

Akademisk avhandling som för avläggande av teknologie doktorsexamen vid tekniska fakulteten vid Lunds Universitet, kommer att offentligen försvaras tisdagen den 11 februari 2014, kl. 13:15 i hörsal B, på Kemicentrum, Getingevägen 60, Lund. Fakultetsopponent: Prof. Alejandro G. Marangoni, Department of Food Science, University of Guelph, Canada.

Academic thesis, which by due permission of the Faculty of Engineering at Lund University, will be publicly defended on Tuesday 11th of February 2014 at 13:15 p.m. in lecture hall B, at the Centre of Chemistry and Chemical Engineering, Getingevägen 60, Lund, for the degree of Doctor of Philosophy in Engineering. Faculty opponent: Prof. Alejandro G. Marangoni, Department of Food Science, University of Guelph, Canada.

"The best way to keep really good chocolate tasting really nice is not to stash it away in a safe place, but to eat it up in one go"

Chokladfabriken, Stockholm

Abstract

Fat bloom on chocolate is a major problem for the confectionery industry since the unappetising appearance and negative sensory effects lead to rejection by customers. The presence of fat bloom on chocolate confectionery systems is usually connected to migration of liquid fat due to the difference in composition between filling triacylglycerols (TAGs) and cocoa butter TAGs. The filling TAGs migrate into the chocolate shell where they can dissolve cocoa butter crystals. Consequently, cocoa butter TAGs migrate to the surface followed by a re-crystallisation into the most stable polymorph $\beta_1 VI$. Cocoa butter is the main fat in chocolate which can be considered as a composite material consisting of solid particles (i.e. cocoa particles, sugar crystals and in some cases milk solids) in a lipid continuous matrix of cocoa butter. The final quality of the product is highly dependent on the polymorphic forms of the cocoa butter TAGs in the fat phase and the distribution and size of the solid particles.

In this thesis the migration of filling oil into model shells of cocoa butter and of chocolate has been investigated as well as the fat bloom development. This was implemented through the development of novel analytical methods, where optical profilometry and confocal Raman microscopy give information regarding the shell microstructure at and below the surface, and energy dispersive X-ray spectroscopy (EDS) provides the opportunity to follow the movement of brominated TAGs from the filling into the shell. By combining these techniques with established methods such as low vacuum scanning electron microscopy (LV SEM) and differential scanning calorimetry (DSC) a toolkit for the investigation of oil migration connected to surface microstructure development has been established.

Imperfections, in form of pores and protrusions, at chocolate surfaces have been identified, confirming previous studies reporting these features. These imperfections were characterised using confocal Raman microscopy indicating that some protrusions are filled with fat and some are air-filled in conjunction with a fat shell, while the pores consist of air. These imperfections continued further into the chocolate shell, thus, it is

suggested that they could be connected to oil migration and further to fat bloom development.

The microstructure of model shells was shown to have a substantial impact on the TAG migration rate which was connected to fat bloom development. By applying seeding as pre-crystallisation technique to the shells the migration rates were decreased as well as the development of fat bloom crystals at the surface. In contrast, model pralines with poorly tempered shells indicated a higher oil migration rate and accelerated development of fat bloom. Furthermore, the presence of non-fat particles was shown to increase the migration rate and the fat bloom development. Additionally, the particle size of the non-fat particles proved to have an impact, where a smaller particle size gave rise to higher migration rates and thus, accelerated fat bloom development. The importance of controlled storage temperature was further demonstrated, where a minor increase in temperature from 20 to 23°C lead to substantially higher migration rates and accelerated fat bloom development.

The mechanisms of oil migration in chocolate confectionery systems have mainly been referred to as molecular diffusion or capillary flow in literature. However, through results from the work of this thesis, convective flow is suggested to be an important contribution to the migration of filling oil in addition to molecular diffusion and capillary flow.

Sammanfattning

Chokladprodukter som utvecklat fettblom är ett centralt problem för konfektyrindustrin då konsumenterna väljer bort dessa produkter på grund av oaptitligt utseende och negativa sensoriska effekter. Förekomsten av fettblom på fyllda chokladprodukter är vanligtvis kopplad till migrering av flytande fett från fyllning till skal vilket sker på grund av skillnader i sammansättning mellan fyllningens triacylglyceroler (TAG) och kakaosmörets TAG. Då fyllningens TAG migrerar in i chokladskalet löser de upp kristaller av kakaosmör, vilket är det huvudsakliga fettet i choklad. Flytande kakaosmör migrerar då till chokladytan där det genomgår en omkristallisation och antar den mest stabila polymorfen $\beta_1 VI$. Choklad kan ses som ett kompositmaterial bestående av partiklar (t.ex. kakaopulver, socker och i vissa fall mjölkpulver) i en lipidkontinuerlig matris av kakaosmör. Kvaliteten hos den slutliga produkten är i hög grad beroende av de polymorfa formerna i fettfasen samt av partiklarnas storlek och fördelning.

I denna avhandling har migrering av fyllningsfetter in i modellskal av kakaosmör och av choklad undersökts, liksom utveckling av fettblom. Detta har genomförts via utveckling av nya analysmetoder, där optisk profilometri och konfokal Raman-mikroskopi ger information om skalets mikrostruktur på och under ytan, och där EDS (energy dispersive X-ray spectroscopy) ger möjligheten att följa hur bromerade triacylglyceroler (BrTAG) rör sig från fyllningen in i skalet. Genom att kombinera dessa metoder med redan etablerade metoder, så som LV SEM (low vacuum scanning electron microscopy) och DSC (differential scanning calorimetry), har en verktygslåda tagits fram, som kan ge information om migrering av fyllningsfetter kopplat till mikrostrukturella förändringar på chokladytan.

Tidigare forskning har beskrivit ytliga oregelbundenheter på chokladytor, i form av porer och bubblor. Förekomsten av dessa kunde bekräftas i detta arbete. Vidare kunde dessa oregelbundenheter karakteriseras, genom användning av konfokal Raman-mikroskopi, vilket indikerade att vissa bubblor är fyllda med fett och vissa är luftfyllda under ett fettskal, medan porerna består av luft. Dessa oregelbundenheter förefaller fortsätta in i

chokladskalet, vilket antyder att de kan ha en koppling till migrering av flytande fett och därigenom till utveckling av fettblom.

Mikrostrukturen i modellpralinernas skal visade sig ha en betydande inverkan på migreringshastigheten av BrTAG, vilken i sin tur visades relatera till utvecklingen av fettblom. Genom att tillämpa s.k. seedning på modellskalen kunde man minska migreringshastigheten liksom utvecklingen av fettblomkristaller på ytan. I motsats till detta gav ett undertempererat skal upphov till ökad migreringshastighet och snabbare utveckling av fettblom. Även förekomsten av partiklar (kakaopartiklar och socker) bidrog till ökad migreringshastighet och tidigare utveckling av fettblom. Dessutom visade det sig att partikelstorleken har en betydande effekt. Mindre partikelstorlek gav upphov till ökad migreringshastighet och därmed en accelererad utveckling av fettblom. Vikten av kontrollerad lagringstemperatur visades ytterligare, där det räcker med en mindre ökning från 20 till 23°C för att nå väsentligt högre migreringshastigheter och accelererad utveckling av fettblom.

I litteraturen har migrering av fyllningsfetter i chokladpraliner huvudsakligen förklarats genom mekanismerna molekylär diffusion och kapillärflöde. Genom resultat från denna avhandling föreslås det att ett konvektivt flöde kan vara ett viktigt bidrag till migrering tillsammans med ovan nämnda mekanismer.

List of publications

I. **Investigation of Chocolate Surfaces Using Profilometry and Low Vacuum Scanning Electron Microscopy**
Hanna Dahlenborg, Anna Millqvist-Fureby, Björn Bergenståhl and Daniel J.E. Kalnin
Journal of the American Oil Chemists Society (2011) 88, 773-783.

II. **Study of the Porous Structure of White Chocolate by Confocal Raman Microscopy**
Hanna Dahlenborg, Anna Millqvist-Fureby, Birgit D. Brandner and Björn Bergenståhl
European Journal of Lipid Science and Technology (2012) 114, 919-926.

III. **Effect of Shell Microstructure on Oil Migration and Fat Bloom Development in Model Pralines**
Hanna Dahlenborg, Anna Millqvist-Fureby and Björn Bergenståhl
Submitted for publication.

IV. **Effect of Particle Size in Chocolate Shell on Oil Migration and Fat Bloom Development**
Hanna Dahlenborg, Anna Millqvist-Fureby and Björn Bergenståhl
Submitted for publication.

The authors contribution to the papers

I.   Planning of the experimental work was realised by the author with input from co-authors. The experimental work was performed by the author. Evaluation of the results was done with help from co-authors, and the author wrote the major part of the paper in cooperation with co-authors.

II.   The author planned and performed the experimental work, with some help from co-authors. Evaluation of the results was done with suggestions from co-authors, and the author wrote the major part of the paper in cooperation with co-authors.

III. The author planned and performed the experimental work. Evaluation of the results was done in cooperation with co-authors, and the author wrote the major part of the paper with input from the co-authors.

IV.   The author planned and performed the experimental work. Evaluation of the results was done in cooperation with co-authors, and the author wrote the major part of the paper with input from the co-authors.

Abbreviations

Abreviation	Meaning
AFM	Atomic Force Microscopy
BrTAG	Brominated triacylglycerol
CB	Cocoa butter
CLSM	Confocal Laser Scanning Microscopy
CP	Cocoa particles
CRM	Confocal Raman Microscopy
DCL	Double chain length
dCP	Defatted cocoa particles
DSC	Differential Scanning Calorimetry
EDS	Energy Dispersive X-ray Spectroscopy
H	Hexagonal
HPLC	High Pressure Liquid Chromatography
L	Linolenic acid
LSM	Laser Scanning Microscopy
LV SEM	Low Vacuum Scanning Electron Microscopy
MRI	Magnetic Resonance Imaging
O	Oleic acid
$O_\perp$	Orthorombic
OOO	Triolein
P	Palmitic acid
PGPR	Polyglycerol polyricinoleate
PSD	Particle size distribution

Abbreviation	Meaning
SEM	Scanning Electron Microscopy
SFC	Solid fat content
St	Stearic acid
$T_{//}$	Triclinic
TAG	Triacylglycerol
TCL	Triple chain length

Table of Contents

1 Introduction

Shelf life refers to the time frame that a product can be stored at optimum conditions before the quality is reduced, and for food products this is an important parameter. The shelf life of chocolate confectioneries can vary from a few months up to around one year depending on the composition, the production and the storage conditions. One of the most important parameters regarding shelf life of a chocolate confectionery product is the development of fat bloom. Once this has occurred the product is no longer possible to sell, mainly due to the unappetising appearance.

Chocolate is a confectionery product aiming to give an attractive sensorial experience and pleasure to its consumers. A freshly produced chocolate product should have a high gloss, a perfect snap and, when placed in the mouth, it should melt directly. Since chocolate is essentially solid at room temperature (below 25°C) and liquid at body temperature it is a unique product[1]. This property is due to the presence of cocoa butter, which when crystallised in the correct polymorphic form has a melting point just below the temperature of our mouth. In addition, chocolate consists of sugar crystals, cocoa particles and in some cases milk solids that are dispersed in a continuous phase of solid and liquid cocoa butter. An emulsifier, normally lecithin, is added during processing in order to obtain the desired rheological properties.

Cocoa butter is a polymorphic vegetable fat, i.e. it can form different crystalline structures with varied melting points, still with the same composition. The triacylglycerols (TAGs) of cocoa butter are usually referred to as being able to crystallise into six different polymorphic forms denoted by roman numbers, I to VI, or by the Greek letters α, β and β'. These crystal forms possess increasing thermodynamic stability and increasing melting points. Form $\beta_2 V$ is the desired form when producing chocolate, giving the product its unique properties mentioned above. Form $\beta_1 VI$ has the highest thermodynamic stability and thus the highest melting point and is normally connected to fat bloom. One of the major challenges during chocolate manufacturing is to achieve products where the cocoa butter TAGs are in form $\beta_2 V$, and to further control handling of the products and storage conditions in order to maintain the quality. However,

since the polymorphic form $\beta_1 VI$ is more stable than form $\beta_2 V$, the transformation from $\beta_2 V$ to $\beta_1 VI$ will eventually occur.

Due to the complexity of chocolate in terms of ingredients, production and temperature dependency, it can easily develop fat bloom, resulting in rejection from the consumers perspective. The appearance of fat bloom gives the product a dull, greyish-whitish haze in addition to loss in textural quality. This appearance is generally explained by the scattering of light due to needle like fat crystals, at least 5 µm long, that are formed at the chocolate surface, normally explained by re-crystallisation of cocoa butter into polymorph $\beta_1 VI$[2]. Chocolate pralines, a hard chocolate shell surrounding a softer filling commonly containing nut oil, are more prone to quality problems than plain chocolate products. This is mostly owing to the characteristics of the fillings and the possible incompatibility with the surrounding chocolate shell. Due to migration of incompatible TAGs from filling into the chocolate shell fat bloom is enhanced. The mechanism of this fat migration is not yet fully understood and there are several theories behind this mechanism. Furthermore, microstructural properties of the chocolate shell matrix, such as physical properties of the fat crystal network and the non-fat particles, will affect the migration. Thus, by adjusting these properties, fat bloom stability of the product can be improved and consequentially, the shelf life of the products will increase.

1.1 Objective and outline of the thesis

The overall objective of this work was to provide a deeper understanding of the mechanisms behind fat bloom development and oil migration in chocolate confectionery systems. This was accomplished by developing new methods for analysis and by combining those with existing methods into an analytical toolkit. Furthermore, the impact of storage conditions and shell microstructure on oil migration and fat bloom development was investigated.

This thesis begins with a theoretical background to chocolate confectionery systems, where special emphasis is given to the physical properties of cocoa butter and the occurrence of fat bloom. Subsequently, established methods used within this work for evaluation of oil migration and fat bloom development will be described briefly. Novel methods that have been developed within the work of this thesis will be described more thoroughly. The state-of-the-art regarding causes for oil migration-induced fat bloom development will be described along with results from the work of this

thesis. In conclusion, there is a theoretical and state-of-the-art description of the most cited mechanisms behind oil migration in chocolate confectionery systems, which subsequently is linked to results achieved within this work. The last part of the thesis highlights concluding remarks and future perspectives.

2 Chocolate confectionery systems

This section will give background information to the work of this thesis. Some parts will be described in more detail under section 4.

2.1 Chocolate composition

Dark chocolate is a confectionery system consisting of cocoa particles and sugar suspended in a continuous fat phase of crystalline and liquid cocoa butter[2]. The proportion between solid and liquid fat in the continuous phase mainly depends on the temperature and the composition of the cocoa butter, and it is the physical properties of cocoa butter that give chocolate its special properties[3]. The sugar used in chocolate is usually crystalline and dense sucrose, while the cocoa particles are porous, normally containing 10-20% of fat[1, 4]. It is the cocoa particles that give the chocolate its characteristic aroma, flavour and colour. In addition, emulsifiers are added to reduce the interactions between the non-fat particles, primarily sugar. This leads to improved rheological properties with lower viscosity[1]. The most frequently used emulsifier is soy lecithin but also polyglycerol polyricinoleate (PGPR) is used occasionally. Dark chocolate typically consists of 47.5 wt% sugar, 30 wt% cocoa butter, 22 wt% cocoa particles and 0.5 wt% emulsifier[2]. Chocolate manufacturers characterise their products by mouth feel, i.e. the sensation in the mouth when consuming chocolate. If the product is too coarse with large particle size, it will give a gritty sensation, and if the product is too fine with small particle size, it will be described as sticky[5]. Thus, in order to achieve a pleasant mouth feel the non-fat particles should not be larger than 15-30 μm in diameter[1]. Furthermore, if the particle size is too small this might cause problems during production due to higher viscosity and yield value[6]. Fat crystal size also affects the rheological properties and consequently modifies taste, graininess and texture.

The main ingredient distinguishing milk chocolate from dark chocolate is milk powder consisting of proteins, lactose and milk fat. White chocolate is basically milk chocolate without any cocoa particles[1].

2.2 Chemical and physical properties of cocoa butter

Fats are present in most food products and clearly affect product properties such as taste, mouth feel and softness[3]. It is therefore of great importance to understand the chemical and physical properties of fats. Cocoa butter (CB) is the main fat in chocolate products providing physical properties such as high gloss, perfect snap and a sharp melting profile in the mouth. Chocolate consists of semisolid fats containing a liquid oil with a network of solid fat crystals[5].

Fat is a material composed of a mixture of liquid and solid (crystalline) phases whose main constituents are triacylglycerols (TAGs), consisting of three fatty acids that are esterified to a glycerol backbone[7]. Compared to many other fats, cocoa butter has a relatively simple fatty acid composition mainly consisting of palmitic acid (C16:0, P), stearic acid (C18:0, St) and oleic acid (C18:1, O). These fatty acids result in a homogenous TAG composition where the three dominating TAGs are POP, POSt and StOSt, representing more than 80% of the TAGs in cocoa butter[2]. However, the chemical composition and thus, the physical properties of cocoa butter vary with different origins due to factors such as temperature, sunshine, rainfall, and harvesting time[2, 8-9]. Figure 1 illustrates the general chemical structure of a TAG molecule, where for cocoa butter TAGs the positions 1 and 3 are sites for palmitic or stearic acid and position 2 is the site for oleic acid. However, due primarily to steric reasons, the fatty acid in the 2-position (i.e. oleic acid) is oriented on the opposite side of the glycerol backbone compared to the other two fatty acids. This gives the TAG molecule a chair-shaped conformation, as can be seen in Figure 1.
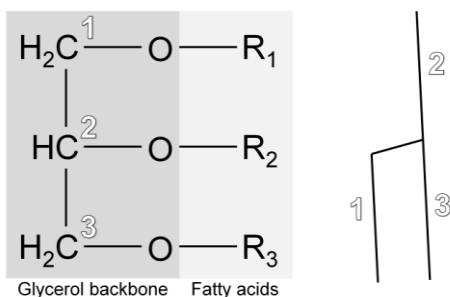

Figure 1. General structural formula and line structure of a TAG molecule. For cocoa butter TAGs the 1- and 3-positions are sites for palmitic or stearic acids and the 2-position is the site for oleic acid.

The positioned regularity, with the mono-unsaturated oleic acid in the 2-position, induces a tendency to form triple chain-length crystal structures (TCL) which gives the most favourable thermodynamic structure to cocoa butter TAGs. Double chain-length crystal structures (DCL) can also form from TAGs. Still, in the case of cocoa butter this gives a loose structure that is not thermodynamically stable[10]. The chain-length crystal structures, presented in Figure 2, enable cocoa butter TAGs to form several crystalline forms with different melting points, giving cocoa butter the characteristic melting properties. The ability of fats to exist in more than one crystalline form is called *polymorphism* (Greek: many forms)[3, 7, 11]. Each polymorph is due to a different way of packing the TAG molecules in the crystalline state. TAG, which is a long chain molecule, packs side by side in separate layers. The thickness of the layers depends on the length of the molecule (and therefore on the number of carbon atoms in the fatty acid chains) and on the angle of the tilt between the chain axes and the basal plane[7].
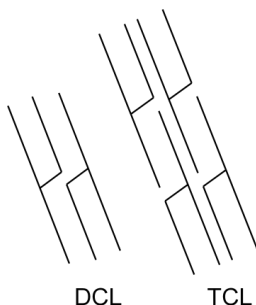
Figure 2. Double chain-length (DCL) and triple chain-length (TCL) crystal structures.

The three basic polymorphic forms of TAGs are named α, β' and β, with respect to increasing stability and increasing melting points[12]. Transformations take place in this order and are irreversible[7]. The different polymorphs can be described by subcell structures that represent the cross-sectional packing modes of the fatty acid chain, which has a zigzag appearance. This is due to the tetrahedral form of each C atom with its four bonds[3]. The subcell structures, defined by Larsson[12], together with the polymorphic forms are presented in Figure 3. The hexagonal subcell (H) is associated with polymorph α and the fatty acid chains are loosely packed and arranged hexagonally. The fatty acid chains are considered to be oscillating with no fixed position in the crystal and thus, there is a high mobility which leads to rapid transformation to a more stable polymorph. The orthorhombic subcell ($O_\perp$) is associated with the more stable polymorph β', where each hydrocarbon chain has its zigzag plane perpendicular to the zigzag planes of its neighbours. The most stable

polymorph is β which is associated with the triclinic subcell ($T_{//}$). In contrast to the orthorhombic subcell this has all zigzag planes parallel and thus, possesses the tightest packing.

Hexagonal (*H*)   Orthorombic ($O_\perp$)   Triclinic ($T_{//}$)
α   β'   β

⟲ = oscillating   ● = C   ○ = H
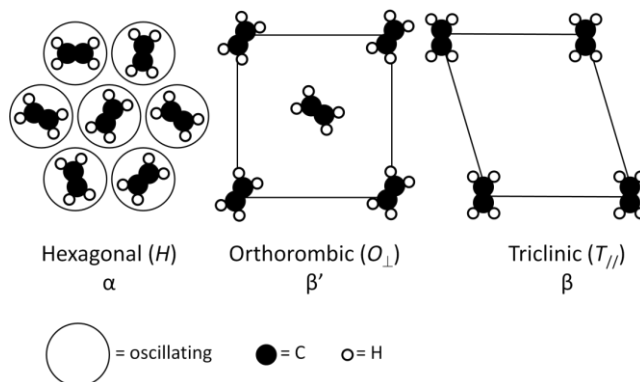
Figure 3. Subcell structures representing the cross-sectional packing modes of the fatty acid chains in TAGs.

Additionally, there are sub-forms of these basic forms that can be distinguished by subscripts. Cocoa butter can crystallise into several polymorphic forms. However, exactly how many polymorphs that can be formed is unclear. In 1966 six different polymorphic forms of cocoa butter TAGs were identified, named as form I-VI[13] or alternatively, sub-α, α, β'$_2$, β'$_1$, β$_2$, β$_1$[12], and in 1999 research suggested that only five forms existed[14]. In addition to these findings, there have been several reported results regarding the crystalline state and melting behaviour of cocoa butter, mainly obtained by using X-ray diffraction, differential scanning calorimetry (DSC) and microscopy[15-22]. This has resulted in a large variety of nomenclature and definitions of the different polymorphic forms and their melting temperatures. However, the nomenclatures from 1966 are often used in the field of chocolate research and within industry. In this thesis a combination of these two nomenclatures will be used to explain the different polymorphic forms of cocoa butter. Table 1 presents some of the reported polymorphic forms together with their nomenclature and melting temperature or melting range.

7

Table 1. Nomenclature and melting points/ranges (°C) of cocoa butter TAG polymorphs reported by different authors.

Vaeck (1960)		Larsson (1966)	Willie & Lutton (1966)		Lovegren et al. (1976)		Dimick & Manning (1987)		van Malssen et al. (1999)	
γ	16-18	sub-α	I	17.3	VI	13.0	I	17.6	γ	-5 to +5
α	21-24	α	II	23.3	V	20.0	II	19.9	α	17-22
		β'_2	III	25.5	IV	23.0	III	24.5	β'	20-27
β'	27-29	β'_1	IV	27.5	III	25.0	IV	27.9		
β	34-35	β_2	V	33.8	II	30.0	V	34.4	β-V	29-34
		β_1	VI	36.3	I	33.5	VI	34.1	β-VI	29-34

The three forms β'_1IV, β_2V and β_1VI are the most important forms in the production of chocolate. Form β_2V is the desired form of cocoa butter TAGs in chocolate which is achieved by controlled crystallisation during production. Form β'_1IV is characteristic for under-tempered chocolate and form β_1VI is a transformation from form β'_1IV and β_2V, normally associated with fat bloom.

2.3 Chocolate manufacturing

Since chocolate obtains its special properties from the cocoa bean, the production and processing of the bean is an essential first step[2]. The key steps for development of flavour in cocoa products are *fermentation* and *roasting*. After this the cocoa nibs are ground to produce cocoa mass, which can be separated into cocoa particles and cocoa butter by hydraulic pressing[23].

Chocolate is prepared as a liquid and then solidified to form the finished confectionery product[2]. In a first step the dry ingredients (sugar and cocoa particles) are *mixed* and *refined*, normally together with part of the cocoa butter. The purpose of the grinding is to reduce the particle size of the dry ingredients, which leads to increased specific surface area. Subsequently, the dry chocolate mass goes through the *conching* step where the refined ingredients will be constantly agitated for 2-72 hours under controlled heating (≤70°C)[5]. During this step flavour development, release of volatiles

and moisture occur. In order to get the chocolate mass to flow, the non-fat particles have to be able to move past one another[1]. Thus, the particles need to be coated with fat, which is facilitated by the addition of an emulsifier. Through the addition of emulsifiers in combination with added shear during conching, particle agglomerates are separated and the particles are coated by the fat phase, resulting in a smooth liquid[1-2]. Towards the end of the conching extra cocoa butter is added to obtain the desired viscosity. The chocolate is then kept at 45-50°C to ensure that no crystal nuclei are present before entering the *pre-crystallisation* step, where the cocoa butter TAGs are crystallised through a defined temperature controlled programme[2]. This is a crucial step which will be described in more detail in the following section. The pre-crystallised liquid chocolate is finally converted into confectionery products by moulding, enrobing or panning. Before de-moulding and storage the chocolate confectioneries are *cooled* under controlled conditions to ensure further crystallisation of the cocoa butter. Due to the contraction of the chocolate upon crystallisation the product will easily de-mould[11].

2.3.1 Pre-crystallisation of cocoa butter

When pre-crystallising the cocoa butter in chocolate, a large number of nuclei and seed crystals of the desired polymorph $\beta_2 V$ are formed, ensuring a homogenous fat crystal network and a product that is relatively stable against fat bloom. This gives the final product the desired characteristics such as gloss, fine texture, nice snap and a smooth melting profile in the mouth.

The two main processes involved in crystallisation are *nucleation* and *crystal growth,* which are followed by crystal ripening. During nucleation, formation of a stable nucleus takes place on which the remaining liquid fraction solidifies during crystal growth.

2.3.1.1 Nucleation

Before nucleation occurs, the liquid cocoa butter TAGs must be at supercooling conditions, i.e. below the maximum melting temperature[24-25]. Upon supercooling crystallisation occurs spontaneously and molecules begin to aggregate in clusters called embryos[26]. Once the energy of interaction between the TAG molecules is greater than the kinetic energy of the TAG molecules in the melt they will adapt to a specific and more stable conformation in order to form a stable nucleus. This is a relatively slow process, and as the supercooling is increased, stable nuclei of specific critical size are formed[27]. To minimize their free energy, clusters smaller

than the critical size will break down while clusters larger than the critical size continue to grow. Nucleation is usually heterogeneous for TAGs, i.e. the nucleation is catalysed by the presence of foreign particles in the system, such as sugar crystals or cocoa particles in chocolate. Compared to heterogeneous nucleation, primary homogeneous nucleation requires lower supersaturation due to the reduction of the effective surface free energy by foreign surfaces. Once primary homogenous nucleation takes place secondary homogeneous nucleation will proceed, where new crystal nuclei form on contact with existing crystals.[25, 27-28]

2.3.1.2 Crystal growth

Crystal growth involves diffusion of TAGs from the bulk solution to the crystal surface, in addition to the incorporation of TAGs into the crystal lattice[25-27]. The TAG crystal growth depends on factors such as degree of supercooling, rate of molecular diffusion to the crystal surface, the time required for a TAG molecule to fit into the growing crystal lattice, the liquid fat viscosity and the structure of the crystal surface[27]. The crystals grow layer by layer by secondary nucleation. At low degrees of supercooling each layer grows completely before a new layer is nucleated, whereas at higher degrees of supercooling several nuclei appear and layers grow simultaneously[26-27]. During crystallisation of TAGs, the formation of nuclei and the crystal growth usually occur nearly simultaneously due to a continuous variation of the conditions that produce crystallisation[24]. Along with the phase change from liquid to crystalline state, release of latent heat occurs, which must be transferred from the crystal surface[25].

2.3.1.3 Pre-crystallisation by tempering

The tempering procedure is the conventional way to pre-crystallise chocolate, where liquid chocolate mass is treated mechanically and thermally, i.e. under shear and through a defined temperature profile. During this process crystals are formed that can act as seed crystals, from which the remaining fat in the chocolate solidifies. The tempering procedure starts with a heating step since it is of great importance to ensure that there is no nucleus or crystal memory present in the cocoa butter. By keeping the chocolate mass at 45-50°C the presence of crystal nuclei can be avoided[2]. Subsequently, the chocolate is supercooled in order to induce crystallisation from nucleus and seed crystals. Depending on the type of chocolate the temperature is lowered to 22-26°C. Since exclusively crystal form $\beta_2 V$ is desired, the chocolate is then re-heated to a temperature just above the melting point of all unstable α and β' crystals (~30°C), ensuring growth of form $\beta_2 V$ and reduction of the unwanted polymorphs in the chocolate[1].

2.3.1.4 Pre-crystallisation by seeding

Another way of producing chocolate in the polymorphic form $\beta_2 V$ is by seeding. Pre-crystallisation by seeding can be realised in different ways, but all procedures use seeds in order to induce formation of crystal form $\beta_2 V$[29-33]. Zeng *et al.*[32] have developed a seeding technique where a pre-made seed cocoa butter crystal suspension, containing crystals of form $\beta_1 VI$, is added to the pre-cooled chocolate in quantities of 0.2-2%. This results in a large number of well defined nuclei, and although the seed crystals are in form $\beta_1 VI$, the cocoa butter in the chocolate solidifies and develops into the desired form, $\beta_2 V$.

When chocolate is over-tempered, the quantity of liquid fat is very small. This large quantity of crystals results in poor flow properties of the chocolate. In contrast, when chocolate is under-tempered, only a few crystal seeds have been formed leading to a poor crystal structure with large crystals, poor melting properties and unsatisfactory shelf life[2].

2.4 Fat bloom

Figure 4. Freshly produced (left) and heavily fat bloomed chocolate pralines. Photo: Dick Gillberg.

Chocolate products that have developed fat bloom are usually characterised by the loss of their initial gloss, having a dull, greyish-whitish haze at the surface (Figure 4). This appearance has been explained by the scattering of light by needle shaped fat crystals, >5 µm long, at the surface[34-36]. Research has demonstrated that in the presence of these large fat crystals, cocoa butter TAGs can be found in its most stable polymorphic form, i.e. form $\beta_1 VI$, and therefore fat bloom is often related to this polymorph[7, 13, 15, 21, 37-39]. However, researchers have found various forms and shapes of fat bloom

from surface to internal structures, depending on the product and the storage conditions[34, 36, 38, 40-41, Paper I]. Furthermore, the polymorphic transition from $\beta_2 V$ to $\beta_1 VI$ has also been shown to occur without visual fat bloom development[37].

The formation of fat bloom on chocolate is assumed to be caused by the migration of liquid cocoa butter to the surface which is followed by re-crystallisation into the most stable crystal form, $\beta_1 VI$[42]. It should be noted that fat bloom formation occurs both within and at the surface of chocolate. However internal fat bloom crystals are normally smaller and more irregular shaped than the ones at the surface, since at the surface, fat crystals have a larger freedom to grow. There are four main routes to fat bloom formation which are explained below.

2.4.1 Solid state transformation from $\beta_2 V$ to $\beta_1 VI$

Form $\beta_1 VI$, associated with fat bloom, is the most stable polymorph and due to the laws of thermodynamics this form will eventually develop during storage. However, under normal conditions, this polymorph can only form by a solid to solid transformation and not directly from liquid cocoa butter[1]. As the polymorphic transformation from $\beta_2 V$ to $\beta_1 VI$ proceeds, contractions in the crystal network occur, restricting the incorporation of low melting TAGs (i.e. liquid phase of cocoa butter). Thus, this liquid fat migrates to the surface where it re-crystallises into form $\beta_1 VI$[43]. This event has been shown to be time- and temperature dependent[1].

2.4.2 Polymorphic transformation from $\beta'_1 IV$ to $\beta_2 V$

When chocolate is subjected to poor pre-crystallisation during production there will be insufficient numbers of crystal nuclei seeding for stable, high-melting polymorphs, i.e. form $\beta_2 V$[2]. Thus, during the first days of storage, transformation from unstable polymorphs ($\beta'_1 IV$) into more stable polymorphs ($\beta_2 V$) takes place. As described for the solid transformation of polymorphs, the transformation from $\beta'_1 IV$ to $\beta_2 V$ leads to a more homogeneous and denser crystal network forcing liquid cocoa butter to the surface where it re-crystallises into the most stable polymorph $\beta_1 VI$.

2.4.3 Storage temperature

When chocolate products are subjected to higher temperatures and/or temperature fluctuations during storage, less stable fat crystals will melt and migrate to the surface where they re-crystallise at uncontrolled conditions. Considering the narrow melting temperature ranges between cocoa butter TAG polymorphs, small temperature variations may cause this event, i.e. ±2-3°C.

2.4.4 Oil migration in chocolate confectionery systems

Oil migration is the main source for undesirable changes in confectionery products, such as fat bloom development. This is typically observed when a product contains two or more lipid containing components in contact with each other, like in a chocolate praline with a fat based filling. Thus, oil migration in stored chocolate confectionery systems is the main reason for the loss of quality. The cocoa butter TAGs in chocolate differ from those of the fillings. As described earlier, cocoa butter mainly consists of the TAGs POP, POSt and StOSt[2]. Hazelnut oil, which is commonly used in chocolate confectionery fillings mainly consists of the TAG triolein (OOO) together with other TAGs based on oleic and linolenic acid (LOO, LLO, LLL). The differences in TAG composition between filling and chocolate layer in contact leads to migration of the TAGs until equilibrium in TAG concentration is reached between filling and chocolate. However, with time liquid fractions from the cocoa butter in the chocolate will also migrate into the filling. This will result in a chocolate shell that becomes softer and a filling that becomes harder[36, 44]. Thus, the solid fat content (SFC) of chocolate does not only depend on temperature but also on the presence of other fats. The fat phase in a chocolate system may be considered as a two phase system, with one migrating liquid phase and one solid resident, crystalline phase. The filling fat usually has a lower SFC than the shell fat phase due to the containment of liquid TAGs, such as triolein. A high level of hazelnut oil TAGs have low melting points that can dissolve cocoa butter crystals that subsequently migrate to the surface where they re-crystallise into the most stable polymorph[45]. This migration has been clearly coupled to the development of fat bloom at the chocolate surface, as will be discussed further in section 4. Oil migration also enhances fat bloom development through the mechanism of Ostwald ripening, i.e. dissolution of small crystals and growth of big ones[28, 46].

Smith *et al.*[43] showed that even small additions of nut oil to chocolate, i.e. 1%, can have a significant impact on the rate of transformation from

polymorph $\beta_2 V$ to polymorph $\beta_1 VI$. They observed that the degree of migration of nut oil from filling to chocolate shell is linked to the polymorphic transformation. Rousseau and Smith[47] demonstrated that fat bloom kinetics and morphology strongly differ depending on whether a filling fat is present or not.

3 Methods for evaluation of oil migration and fat bloom development

There are several publications regarding oil migration and fat bloom development in chocolate where various analytical techniques have been used. The polymorphic development of cocoa butter TAGs has mainly been analysed using differential scanning calorimetry (DSC)[48-53, Paper III-IV] and X-ray diffraction[37-38, 43, 54-56]. The main physical techniques that have been used to monitor and analyse microstructure and fat bloom development at the surface of chocolate are atomic force microscopy (AFM)[38, 54-59] and scanning electron microscopy (SEM)[40, 47, Paper I-IV]. Surface roughness has also been connected to fat bloom on chocolate by using AFM[38], laser scanning microscopy (LSM)[60-61] and optical profilometry[51, Paper I, III-IV]. Oil migration in chocolate confectionery systems has mainly been studied by using magnetic resonance imaging (MRI)[49, 62-71] and high pressure liquid chromatography (HPLC)[48, 53-54, 72].

The main techniques used in this thesis will be described in the following sections, focusing on their application to this work. Novel methods to the field that were developed during the work of this thesis are presented in more depth. Figure 5 illustrates typical results from the different techniques and their correlation to a chocolate confectionery product. For a more detailed description of the applied methods the reader is referred to respective paper[Paper I-IV].
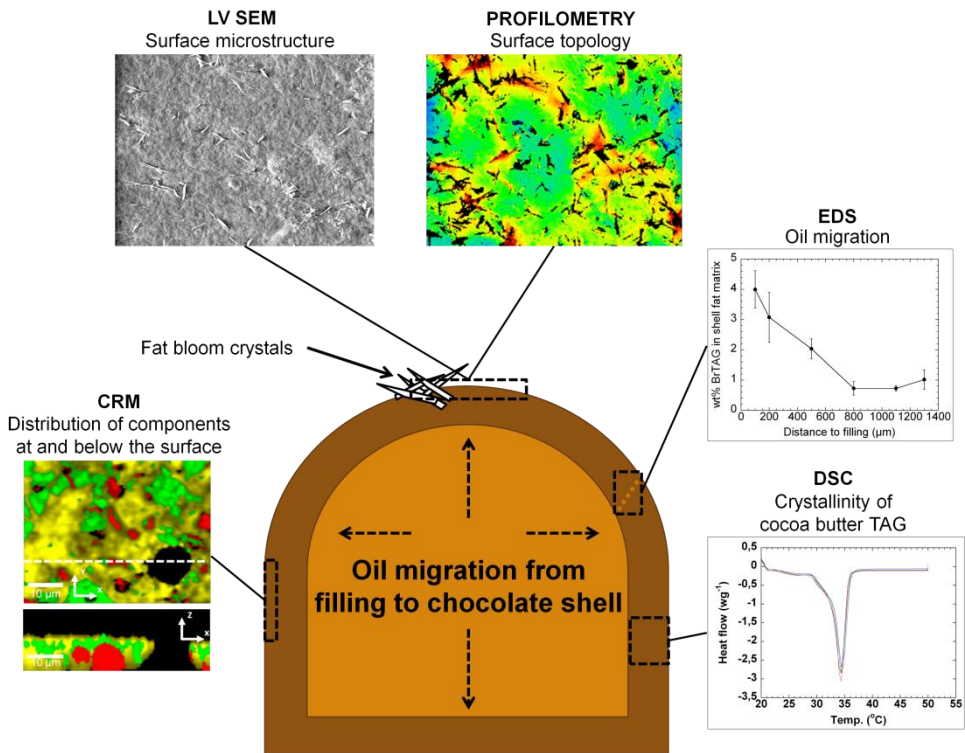
Figure 5. Illustration of how the different techniques are used to examine chocolate samples including some typical results.

3.1 Established methods

3.1.1 Differential scanning calorimetry

Differential scanning calorimetry (DSC) measures heat capacity as a function of temperature. The technique is widely used across a range of applications since many chemical reactions and physical transitions are connected to heat, either by consumption or generation of heat. Food components are suitable for analysis with DSC in order to obtain information about the thermal and thermodynamic stability of various phases[73].

The principle of DSC is to measure the difference between the heat flow (J/s or W) required to maintain a sample and a reference at the same

temperature as a function of temperature or time while exposed to a controlled temperature-time programme. During scanning, peaks or inflection points can be observed and these reflect the thermally induced transitions of the material[73-74]. Depending on the direction of the peak, the nature of the transition is either endothermic (heat absorbing) or exothermic (heat releasing), solid material that melts display endothermic behaviour while crystallisation displays exothermic behaviour.

DSC is often used to investigate the melting and crystallisation behaviour of cocoa butter in chocolate products. DSC can provide melting points and enthalpies for the correct determination of the polymorphic forms of cocoa butter TAGs. Figure 6 shows an example of DSC melting curves for a freshly produced seeded cocoa butter sample and a cocoa butter sample that has developed fat bloom. The temperature at the different peaks gives the melting temperature of the major part of the fat crystals within the sample. The areas between the vertical lines can be correlated to different polymorphic forms. Care must be taken during sample preparation in order not to melt the cocoa butter crystals.
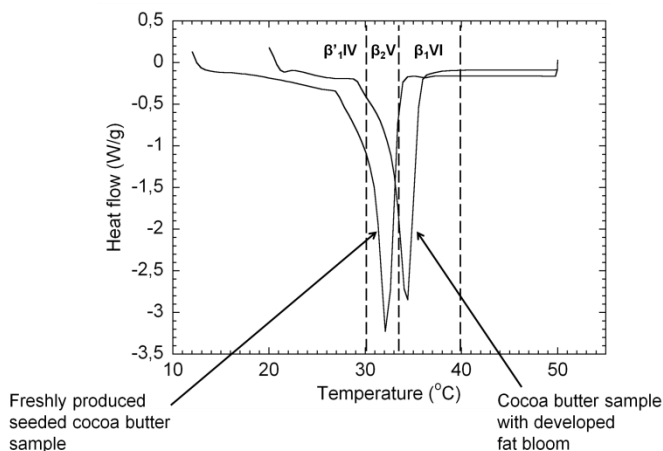

Figure 6. DSC melting curves for a freshly produced seeded cocoa butter sample and a cocoa butter sample that has developed fat bloom. The areas between the vertical dashed lines can be correlated to different polymorphic forms of the cocoa butter TAGs.

3.1.2 Low vacuum scanning electron microscopy

A scanning electron microscope (SEM) uses a beam of electrons at vacuum (10^{-6} torr) to create an image of the sample surface. Topographic images can be obtained in the magnification range 10-10 000×[75]. The electron beam is swept, line by line across the sample surface, and as the electrons

17

penetrate the sample they release energy. This energy is partly carried away from the sample by ejected or scattered electrons that are collected by a detector system where the signals are converted into an image. Low vacuum SEM (LV SEM) can operate while the specimen chamber contains a gas at a pressure of 0.1 – 20 torr and while the electron column is still under high vacuum. This makes it possible to observe images of samples with poor conductivity without coating them with a conducting metal layer. Analysing an uncoated chocolate sample requires a sacrifice in magnification and resolution, since the chocolate surface might melt when irradiated with the electron beam. However, by analysing the samples without a coating, the native surface can be studied[76]. Thus, LV SEM is a suitable technique for investigation of chocolate surfaces and for characterisation of topological changes over time. Figure 7 shows typical LV SEM images of a fresh chocolate surface (A), chocolate that has developed a low frequency of fat bloom crystals that are not yet visible to the eye (B), and a heavily fat bloomed chocolate sample (C).
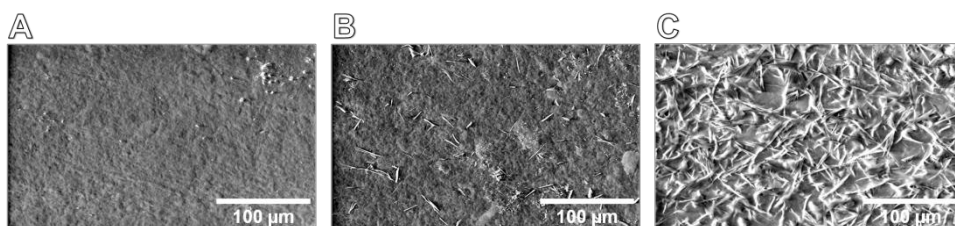

Figure 7. Typical LV SEM images of chocolate surfaces representing: A: Fresh chocolate surface, B: Chocolate surface with low frequency of fat bloom crystals, C: Chocolate surface with high frequency of fat bloom crystals. Scale bars represent 100 μm.

3.2 Novel methods

3.2.1 Optical profilometry

Profilometry is a microscope-based method used to measure surface profiles, in order to quantify its roughness. Optical profilometry is a non-contact method which is advantageous when analysing chocolate or other soft food materials since no surface damage will occur. This technique provides images and quantitative data of surface roughness, which can be associated with fat bloom development at chocolate surfaces.

Optical profilometry is based on white light interferometry where the sample surface is scanned by a light beam. Movement of the sample stage along two axes (x, y) and measurement of the light beam (z) movement allows 3D measurement of the topography. Light from the microscope divides within the interferometric objective; one portion reflects from the sample surface and another portion reflects from an internal, high quality reference surface in the objective. Both portions are then directed onto a solid-state camera (CCD). Interference between the two light waves results in an image indicating the surface structure of the sample. The sample is scanned by vertically moving the objective with a piezoelectric transducer[77]. As the objective scans, a video system captures intensities at each camera pixel. These intensities are converted into images by a software application. The results are displayed on a colour display as images and plots. There is access to several roughness parameters in order to quantify the surface topology. The data can be analysed using different applications in the analysis and control software.

The roughness parameter, Rq (μm) is the root-mean-square (rms) roughness and the waviness parameter, Wq (μm), is the root-mean-square (rms) waviness. They are defined as the average of the measured height deviations taken within the evaluation length or area and measured from the mean linear surface (Eq.1):

$$rms = \sqrt{\frac{1}{L}\int_0^L z^2(x)dx} \qquad\qquad 1$$

z(x) represents the height elements along the profile and *L* is the number of discrete elements[78]. By digital filtering (cut-off filter), the input data for the sample can be separated into waviness and roughness (Figure 8). This filter includes a high filter wavelength which defines the noise threshold; all shorter spatial wavelengths are considered noise. It also includes a low filter wavelength which defines the form threshold where all longer spatial wavelengths are considered form (waviness). Everything between these two wavelengths is assigned to roughness[77].
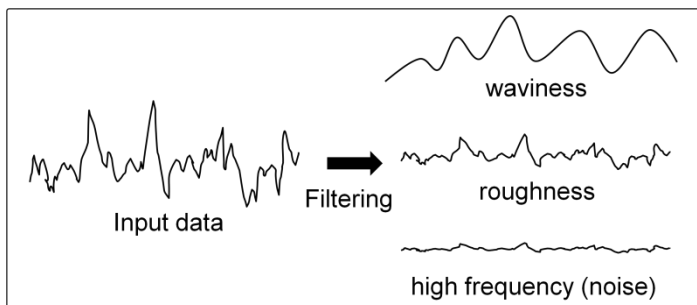
Figure 8. Illustration of the separation of input data into waviness, roughness and noise by digital filtering (cut-off filter).

The vertical resolution is usually in the nanometre level, and the spatial resolution depends on scanning speed and the adjustable step length. Limitations to consider are that the sample reflectivity must be high enough (better than 0.1%), the roughness (peak-to-valley) should be <100 μm and the local inclination of the topological features should not be too steep. The dimension of this inclination depends on the objective and magnification used.

In this present work, a positive correlation of profilometry data to chocolate surface characteristics and early fat bloom development has been established[Paper I]. Furthermore, relating profilometry results to LV SEM images provided complementary topological information and hence this can be used as a toolkit for the study of chocolate surfaces prior and post fat bloom formation[Paper I, III-IV]. In addition, a method has been developed providing the possibility to return to the same sample area on each analysis occasion (±20 μm)[Paper I]. This gives an opportunity to follow and compare topological surface changes over time in that specific area of interest. As a result of this, noise (normally observed due to the use of different areas for data collection) can be reduced.

3.2.2 Confocal Raman microscopy

Confocal Raman microscopy (CRM) can be used to analyse the distribution of different components within a sample. This technique offers the possibility to acquire a Raman spectrum and hence chemical information of a sample, with a resolution down to the optical diffraction limit (typically half the wave length of the light). The analysis can be performed at ambient conditions, without requiring any special sample preparation or addition of

dyes. Confocal Raman microscopy combines the two different techniques confocal microscopy and Raman spectrometry.

In confocal microscopy, a light source is focused with a lens or an objective onto a sample. A small pinhole, aligned to the focus of the objective, allows only the light coming from the focal plane to pass into the detector. Therefore, image contrast is strongly enhanced. The focal plane can be moved several micrometers into the sample, which gives the opportunity of gaining 3D information[79].

Raman spectroscopy uses the effect of inelastic scattering of photons when a sample is irradiated with a monochromatic light source[80]. Upon interaction with light, molecules in the sample will absorb photons to a virtual level which in most cases are instantly scattered elastically back to the initial energy level. This is called Rayleigh scattering. However, a small fraction of the photons absorbed will return to a different energy level and a wavelength shift is created. This inelastic scattering is called Stokes-Raman or Anti-Stokes Raman depending on if the scattered photons have lower or higher energy and frequency than the photons absorbed, respectively[79, 81]. The wavelength shift from the scattered photons provides information about the vibrational transitions in the molecules, which are unique for each type of molecule. Thus, a chemical fingerprint of a sample can be obtained. Peaks in a Raman spectrum correspond to the different Raman excitations.

Performing confocal Raman microscopy, a Raman spectrum is recorded at every image pixel. When analysing specific peaks of the spectra, a variety of images can be generated using only a single set of data. To obtain a full set of data, the sample needs to be mapped. A surface scan provides a 2D image by mapping a layer at the sample surface, i.e. in the x-y direction. Information from a samples' 2D cross-section can be obtained by mapping in the z-y direction. Figure 9 illustrates a surface scan (A) and a depth scan (B) of white chocolate surface, where the distribution of the different compounds can be observed. Some of the areas show their recorded Raman spectrum. The lateral resolution depends on the laser wavelength and the numerical aperture and can at its best be ~200 nm, and the resolution in vertical direction is ~500 nm[79, 82].
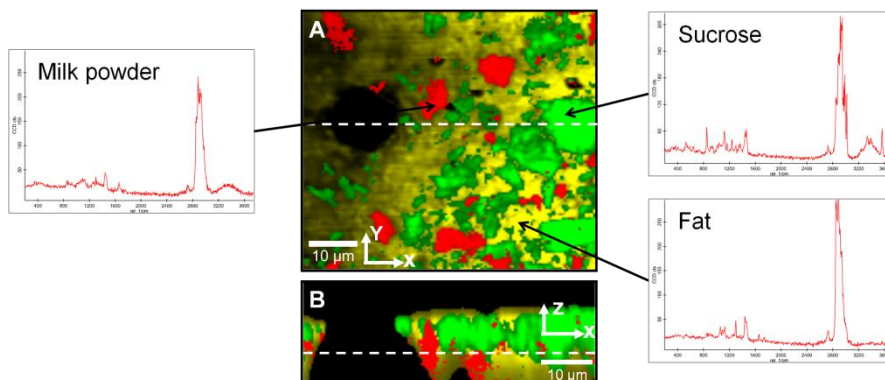
Figure 9. A: Surface scan and B: depth scan of white chocolate praline surface. The dashed line in A represents where the depth scan, B, was recorded. The dashed line in B represents where the surface scan, A, was recorded. Yellow colour represents fat, green colour represents sucrose, red colour represents milk powder and black colour represents air. Recorded Raman spectra are shown for some of the areas. The figures are modified after Paper II.

Sampling limitations are components without covalent bonds (e.g. metals), dark or rough samples, and temperature sensitive samples. For analysing delicate samples, like chocolate, the microscope can be equipped with a cold stage, preventing the sample from melting. Due to fluorescence when analysing milk- and dark chocolate (probably due to the dark cocoa solids), only white chocolate or cocoa butter samples can be analysed with this technique. The scan range for an image can vary, and a larger scan range leads to a longer scan time. In order to be able to determine the distribution of the components, reference spectra have to be recorded for each component in the sample. The data can be evaluated using a software program, which together with the reference spectra will generate images showing the distribution of the different components in the sample.

3.2.3 Energy dispersive X-ray spectroscopy

Energy dispersive X-ray spectroscopy (EDS) is a powerful micro analytical tool used for elemental analysis and chemical characterisation of a sample. EDS can give quantitative as well as qualitative results. Almost all elements in the periodic table, from Na to Pu, can be detected. Chemical analysis is performed by measuring the energy and intensity distribution of the X-ray signal generated by a focused electron beam[75]. The generation of the electron beam is the same for EDS as for SEM. As the electron beam interacts with the atoms in a sample, the inner shell electrons can be ejected, and the atom is then left in an excited state. X-ray photons will be

emitted as the atom relaxes back to its low energy ground state. This energy difference is specific for each element, and the different elements in the sample therefore generate X-ray photons with energies specific for only these elements. By measuring the emitted X-rays it is thus possible to determine the elemental composition of the sample. Not all beam electrons interact with sample atoms and eject electrons; some undergo deceleration in the Coulombic field of the sample atoms[75]. During deceleration the electron will lose energy, which is emitted as a photon. This radiation is called Bremsstrahlung ("breaking radiation"), and can be observed in the EDS spectrum as the continuum background, preventing fully quantitative determination of the atomic species. The shape and depth profile of the detection is related to the energy of the electron beam and to the probed material, e.g. a carbon sample irradiated by 15 keV would give a depth and width profile of approximately 2.7 and 2.8 µm, respectively. When performing analyses under low vacuum, electrons are scattered due to collisions with the gas atoms and thus, there is a skirt effect of the beam spread over the size of the electron beam diameter[75, 83].

Through this work EDS has been proven to be a useful method to quantify oil migration from a filling into a chocolate shell. The elements that will appear when analysing both chocolate and filling are C and O (H will not appear due to the weak signal). Therefore a TAG labelled with bromine added to the filling can be detected when migrating into the chocolate shell. In order to follow the migration of the labelled TAG, the surface of an intersection of the sample is analysed. From each measuring spot, relative intensities are obtained (Figure 10) that are converted into atomic percent (At%) and weight percent (wt%) of each element by a software. By plotting the concentration of the labelled TAGs as a function of the distance from the filling, a migration profile can be achieved. Due to the presence of non-fat particles in chocolate, noise is inevitable.
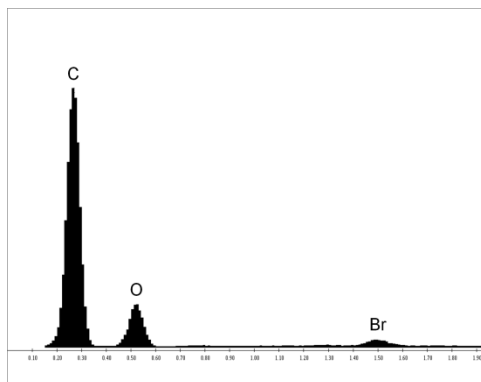
Figure 10. Schematic EDS spectrum showing the relative intensities of C, O and Br.

The choice of using brominated triacylglycerol (BrTAG) as a probe for oil migration from filling into shell was based on several conditions[*]. Primarily, due to the presence of bromine the BrTAG is easy to detect by using EDS, and further, it is liquid at room temperature similar to e.g. triolein. The BrTAG used within this work consists of soybean oil that has been subjected to partial bromination, where 2 bromine atoms have been added to a double bond (on average there are 1.34 bromine atoms per TAG). Soybean oil TAGs mainly consist of linoleic, oleic, palmitic, linolenic and stearic fatty acids (iodine value~130), and thus, soybean oil is expected to behave similar to other TAGs in the model filling, such as triolein (iodine value~86). Larsson[84-87] used the possibilities of replacing atoms in long-chained compounds with heavy atoms, such as replacing the terminating methyl group in lauric acid with a bromine atom. Five crystal forms of brominated lauric acid were found of which two were isomorphous with lauric acid, indicating that the bromine atom behaves similar to a methyl group when replacing it in long-chained compounds. In contrast to this, for the BrTAG used within the work of this thesis, bromine atoms have been added at the centre of the fatty acid chain. Thus, the BrTAG might interact somewhat differently with the solid cocoa butter compared to e.g. triolein. However, compared to other available labelled molecules that are used as probes for oil migration within confectionery products, such as dyes, the BrTAG is expected to behave more similar to migrating filling oil.

---

[*] The purpose of using BrTAGs in chocolate products is solely for the use of analytical investigations and thus, not for use as a food additive.

4 Causes for oil migration-induced fat bloom development

The main causes related to oil migration-induced fat bloom development in chocolate confectionery systems are processing, composition and storage conditions[66]. This section gives an overview to the state of the art related to these main causes together with findings from the work of this thesis.

4.1 Pre-crystallisation during processing

The final quality of a chocolate product is highly dependent on the polymorphic forms of the TAGs in the fat phase. If a product is not optimally crystallised during production there will most probably be consequences like early fat bloom development. The rate of oil migration in chocolate confectioneries has been suggested to be influenced by shell microstructure properties such as the distribution and homogeneity of the fat crystal network, where the migration rate is increased due to improper crystallisation of the cocoa butter[9, 36, 41, 88]. This hypothesis will be reviewed and discussed in this section.

Marangoni and McGauley[89] characterised the microstructure and the polymorphic development over time of cocoa butter that had been crystallised statically from the melt at different temperatures. Their results demonstrated that the microstructure of the cocoa butter is a direct consequence of the crystallisation kinetics of the system. It has been shown that pre-crystallisation under controlled shear is of great importance for ensuring a product with the desired crystal form ($\beta_2 V$), smaller fat crystals and thus, a more homogeneous crystal network, leading to less oil migration[63, 88, 90-95].

De Graef *et al.*[50] observed that under-tempered chocolate bloomed quicker than well-tempered, while fat bloom was delayed on over-tempered chocolate samples. Kinta and Hartel[96] investigated the fat bloom development on chocolate that had been pre-crystallised by the addition of

various amounts of cocoa butter seeds of form β_2V. When subjected to under-seeding the formation of β'_1IV crystals was substantial compared to the optimal-seeded samples that developed mainly β_2V crystals. Further, the under-seeded chocolate samples developed fat bloom at an early stage.

Miquel *et al.*[62] observed a higher concentration of migrated oil into under-tempered chocolate compared to tempered chocolate. Still, no difference could be observed for the speed of migration. Motwani *et al.*[97] observed that migration of peanut oil into a layer of cocoa butter was significantly reduced when the cocoa butter was tempered compared to when it was under-tempered. However, the solid fat content and the counter-diffusion of cocoa butter were not influenced. In recent studies, the pre-crystallisation process developed by Zeng *et al.* has been shown to create chocolate products with increased fat bloom stability[31-32, 52-53, 98]. By using this method of pre-crystallisation Svanberg *et al.*[98] demonstrated that optimal seeded and over-seeded chocolate samples exhibited the highest resistance against fat migration followed by well-tempered chocolate, while under-tempered chocolate samples showed significantly higher levels of migrating oil. In further studies by Svanberg *et al.*[52-53] results from confocal laser scanning microscopy (CLSM) indicated that the crystallisation of cocoa butter samples varies dependent on different pre-crystallisation techniques. Seeded samples formed multiple nucleation sites which induced a rapid growth of fat crystals and resulted in a more homogeneous microstructure, whereas non-seeded samples showed a more random structure, where some areas developed large spherical crystals while other parts developed a more heterogeneous microstructure with large domains of liquid fat.

In agreement with earlier studies, results from the work of this thesis show that that microstructural changes, induced by means of variations in pre-crystallisation, can be used to influence migration behaviour and thus, the development of fat bloom[Paper III]. This was realised by following the migration of BrTAGs from a model filling into cocoa butter shells that had been subjected to different pre-crystallisation procedures, i.e. non-seeded, under-seeded, seeded and over-seeded, where the non-seeded samples were produced in a hand-tempered-like manner. Filling- and shell compositions as well as seeding amounts are presented in Table 2 (page 33). As can be seen in Table 2, the model filling fat phase was saturated by cocoa butter TAGs. The migration results obtained from EDS could be correlated to surface microstructure results from LV SEM and to roughness values from profilometry as well as to polymorphic development by using DSC. This is demonstrated in Figure 11 and Figure 12, where Figure 11 shows LV SEM images, roughness results and polymorphic development

for samples that were stored at 23°C for 6 and 8 weeks, and Figure 12 shows migration profiles for samples stored at 23°C. The migration of BrTAGs into the shells and the fat bloom development is highly correlated to the pre-crystallisation procedures of the shells. The shell microstructure of a hand-tempered-like cocoa butter shell (non-seeded) induced the highest initial migration rate of filling oil into the shell together with the highest frequency of developed fat bloom crystals and the highest rate of roughness development. When applying seeding to the cocoa butter shells a lower initial migration rate, lower frequency of fat bloom crystals and lower rate of roughness development could be observed. The most obvious difference between the seeded samples was shown by the over-seeded samples where the roughness values stayed approximately at the same level during the storage period. Furthermore, these samples showed the lowest frequency of developed fat bloom crystals at the surface.

The observed differences in migration rate and fat bloom formation could be explained by the formation of an ordered fat crystal network when applying seeding where the cocoa butter contracts upon solidification. This would give a more homogeneous crystal network compared to non- or under-seeded samples, which in contrast would create a more heterogeneous crystal network upon solidification with larger inter-crystalline spaces increasing the rate of migration and thus, fat bloom development. After 6 weeks storage, the over-seeded samples indicate a fat crystal network consisting of a larger amount of $\beta_2 V$ crystals compared to the non-seeded samples that indicate a larger amount of $\beta_1 VI$ crystals (Figure 11). These differences contributed to differences in the microstructure, where cocoa butter shells consisting of a large amount of $\beta_1 VI$ crystals give a heterogeneous microstructure with liquid domains, while the over-seeded samples possess a more homogenous structure.
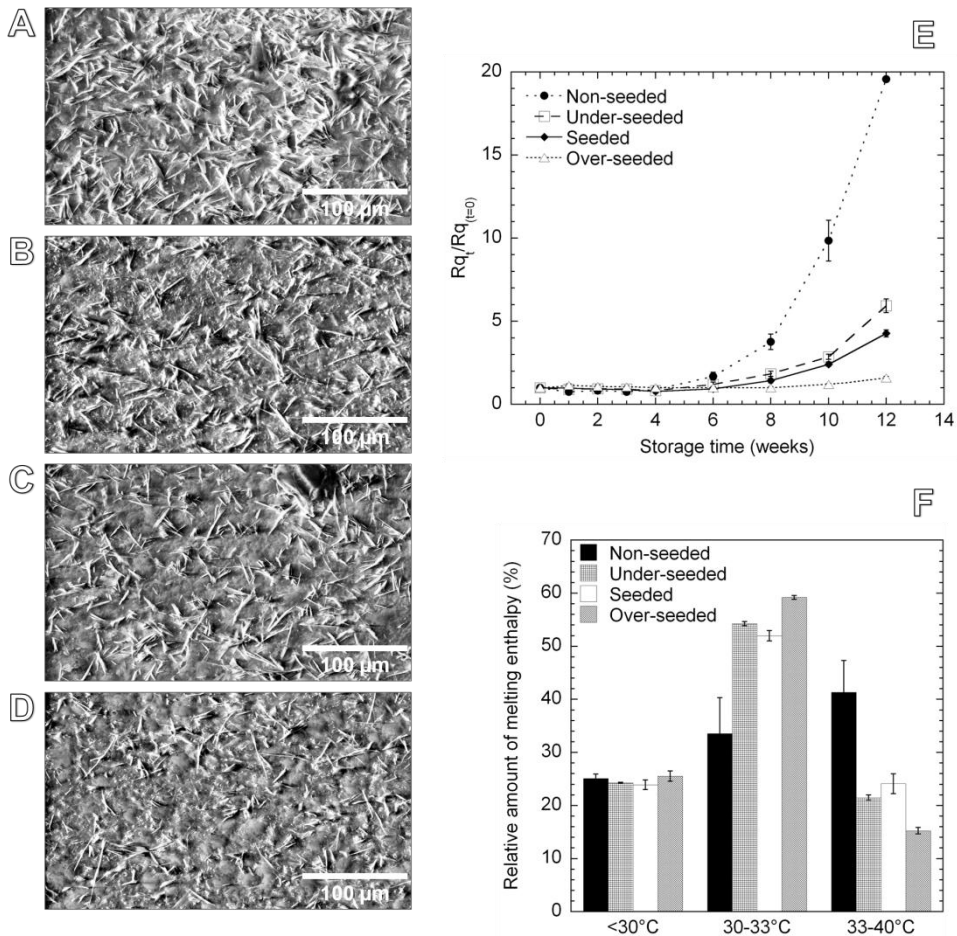
Figure 11. Results of model pralines stored at 23°C. A-D: LV SEM images of model pralines stored for 8 weeks (scale bars represent 100 μm). A: Non-seeded CB shells, B: Under-seeded CB shells, C: Seeded CB shells, D: Over-seeded CB shells. E: Normalised roughness values as a function of storage time. F: Relative amount of melting enthalpy at the temperature intervals <30°C, 30-33°C and 33-40°C for the shells of model pralines stored for 6 weeks. The figures are modified after Paper III.
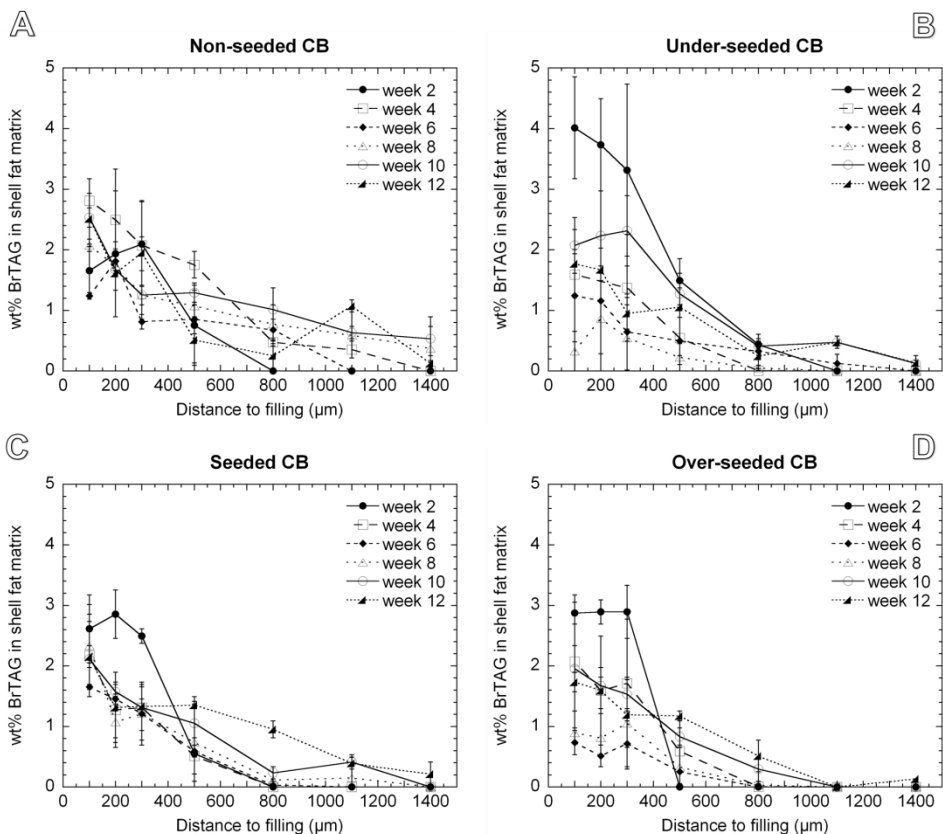
Figure 12. Migration profiles of model pralines stored at 23°C. A: Non-seeded CB shells, B: Under-seeded CB shells, C: Seeded CB shells, D: Over-seeded CB shells. The figures are modified after Paper III.

4.2 Composition

An additional way to affect the microstructure of the surrounding chocolate shell in a chocolate confectionery product is by adding other vegetable fats, emulsifiers or by varying the amount and size of the non-fat particles. There have been several reported studies regarding these microstructural changes including their influence on oil migration and fat bloom development. Some of these studies together with findings from the work of this thesis will be reviewed and discussed in this section.

It has been shown that the presence of milk fat lowers the final SFC due to thermodynamic incompatibility between the TAGs of cocoa butter and milk fat, leading to an eutectic mixture (i.e. a combination of fats that solidifies at a lower temperature than either one of the fats by itself)[99]. When certain amounts of milk fat are added to chocolate systems an anti-fat bloom effect has been observed[2, 56, 59, 69, 99-100]. Despite different theories and extensive research, the mechanism behind this effect is still not totally understood. However, small amounts of milk fat (~5%) are occasionally added to dark chocolate in order to delay fat bloom development[1]. Garti *et al.*[101] investigated the polymorphic behaviour of cocoa butter in the presence of several food emulsifiers. They observed that solid emulsifiers were the most efficient in delaying the transition of form β_2V to form β_1VI. Additional research has been performed regarding the effect of different emulsifiers on crystallisation behaviour and on development of fat bloom in chocolate products[101-107]. However, due to regulations in many countries only a few emulsifiers are approved to be used in chocolate and thus, the effect of other emulsifiers will be of limited interest for the industry in many parts of the world. According to the current EU regulations lecithin may be used according to the principle of *quantum satis*, i.e. no maximum level is specified. Still it must be used within The Good Manufacturing Practise directive and at levels no higher than needed for the intended purpose[1].

By using AFM and X-ray diffraction, Rousseau and Sonwai[55] observed that the microstructure and crystallisation behaviour of the fat phase in chocolate were strongly altered by the presence of non-fat particles. The chocolate samples showed micron-sized amorphous mounds appearing on the chocolate surface after cooling. These features gradually increased in size and number, and eventually they developed into disordered crystal agglomerates. These surface imperfections were not observed on the pure cocoa butter samples. Thus, the authors suggested that a heterogeneously distributed particulate network in chocolate has a substantial impact on the morphology and crystallisation pathway of the fat phase.

Bricknell and Hartell[37] found that chocolate produced with amorphous sugar instead of crystalline sugar was more resistant to visual fat bloom, even though polymorph β_1VI could be observed experimentally. It was hypothesised that oil migration was reduced due to closer packing of the spherical shaped amorphous sugar, and that the smooth sugar surfaces inhibited fat re-crystallisation at the surface due to hindering nucleation of fat crystals. Dhonsi and Stapley[91] observed reduced induction times for crystallisation when sugar was added to cocoa butter compared to pure cocoa butter systems, and suggested that the surfaces of the sugar particles

provide sites for heterogeneous nucleation. However, upon addition of emulsifier to the cocoa butter-sugar system, the crystallisation was slightly delayed. The authors suggested that the presence of emulsifier coating the sugar particles led to a less favourable environment for the occurrence of heterogeneous nucleation. Even though the crystallisation took place at a higher rate when sugar particles were added this proved to generate polymorphs with lower melting points, indicating on a formation of less stable polymorphs. Further studies have indicated that the crystallisation kinetics of chocolate samples accelerate as solid particles (cocoa particles and sugar) are added, thus acting as nucleating agents[52-53, 108-109]. Smaller particle size has also been suggested to increase the crystallisation kinetics, due to a greater nuclei density[108]. However, the above mentioned studies regarding non-fat particles acting as nucleation sites were produced during static crystallisation temperatures or under-tempering regimes. For seeded cocoa butter systems no significant difference relating to the induction time for crystallisation could be observed upon the addition of non-fat particles[52-53].

Regarding the impact of non-fat particles on oil migration rate, Motwani *et al.*[97] investigated migration of peanut oil into samples composed of cocoa butter with or without the addition of cocoa particles, and observed that oil migration was enhanced when cocoa particles were present, at the same time as the counter-diffusion of cocoa butter decreased. It was suggested that the enhanced migration rate was a consequence of cocoa particles reducing the strength of the fat crystal network, resulting in higher migration. Choi *et al.*[66, 69] and McCarthy and McCarthy[67] observed that the migration rate of oil was higher when the non-fat particle size in the chocolate was larger (60 μm compared to 45 μm). However, the observed difference in migration rate was not that pronounced, where the 95% confidence intervals of the 45 and 60 μm formulations overlapped. Furthermore, these results were contradicted when Altimiras *et al.*[110] could show that cocoa butter samples containing sand particles of a smaller size (~5 μm) showed a higher oil migration rate than for samples containing larger particles as well as the biggest whiteness index change. It was suggested that the particles create disturbances in the fat crystal network and that the particle surfaces could influence the fat crystallisation process.

In order to elucidate the impact of non-fat particles on oil migration and its connection to fat bloom development, addition of such particles to cocoa butter model shells that were stored against a model filling was studied in this present work[Paper III]. All systems were subjected to seeding in order to keep a controlled production. The model systems were compared with a reference model system where the shell consisted of seeded pure cocoa

butter. The non-fat particles added to the cocoa butter shells were powdered sugar, cocoa particles (CP) and defatted cocoa particles (dCP). The compositions of the model samples (filling and shell) as well as the particle size distribution (PSD) of the non-fat particles are presented in Table 2. Here it can be seen that the filling fat phase is saturated by cocoa butter TAGs. Analysis of filling oil migration into the model shells was realised by following the migration of BrTAGs from the filling into the shells using EDS. The addition of non-fat particles showed a noticeably higher migration rate compared to the pure cocoa butter samples. In Figure 13, migration profiles for the different model samples stored at 23°C are presented. The migration results could further be correlated to surface microstructure results from LV SEM and to roughness results from profilometry, where a higher frequency of fat bloom crystals and a higher rate of surface roughness development could be observed for the samples containing non-fat particles, as can be seen in Figure 14. This was especially evident for the samples containing cocoa particles. Due to the difference in specific surface area between the added particles, this indicates that especially smaller particles enhance the migration rate of filling oil into the shell. Thus, it may be suggested that the volume next to the surface of the particles represents a heterogeneity in the structure and that the fat crystal density is lower in the vicinity of the particles than on average. This would result in increased possibility for oil migration close to the particle surfaces, and hence an accelerated development of fat bloom.

Table 2. Filling and shell compositions for the different model systems[Paper III-IV]. Where non-fat particles are incorporated to the cocoa butter matrix PSD is represented by 90% of the volume fraction (D(v, 0.9)), Sauter mean diameter (D[3.2]) and specific surface area. The fat content of the cocoa particles (CP) is 10%.

| Model system	CB (wt%)	CB seeds (wt%)	Sugar (wt%)	CP (wt%)	dCP (wt%)	Lecithin (wt%)	Triolein (wt%)	BrTAG (wt%)	Fat content (Wt%)	D(v, 0.9) (µm)	D[3.2] (µm)	Specific surface area (m²/g)
Non-seeded CB	100								100			
Under-seeded CB	99.5	0.5							100			
Seeded CB	96.4	3.6							100			
Over-seeded CB	90	10							100			
Sugar + CB	72.4	2.6	25						75	99.8	12.4	0.5
CP + CB	69.6	2.6		27.8					75	24.6	5.5	1.1
dCP + CB	72.4	2.6			25				75	29.0	4.1	1.5
15 µm	30.4	1.2	50	18		0.4			32	14.5	3.0	2.0
22 µm	30.4	1.2	50	18		0.4			32	22.4	3.6	1.7
40 µm	30.4	1.2	50	18		0.4			32	40.3	4.1	1.5
Filling	69.4	3.6					22	5	100			
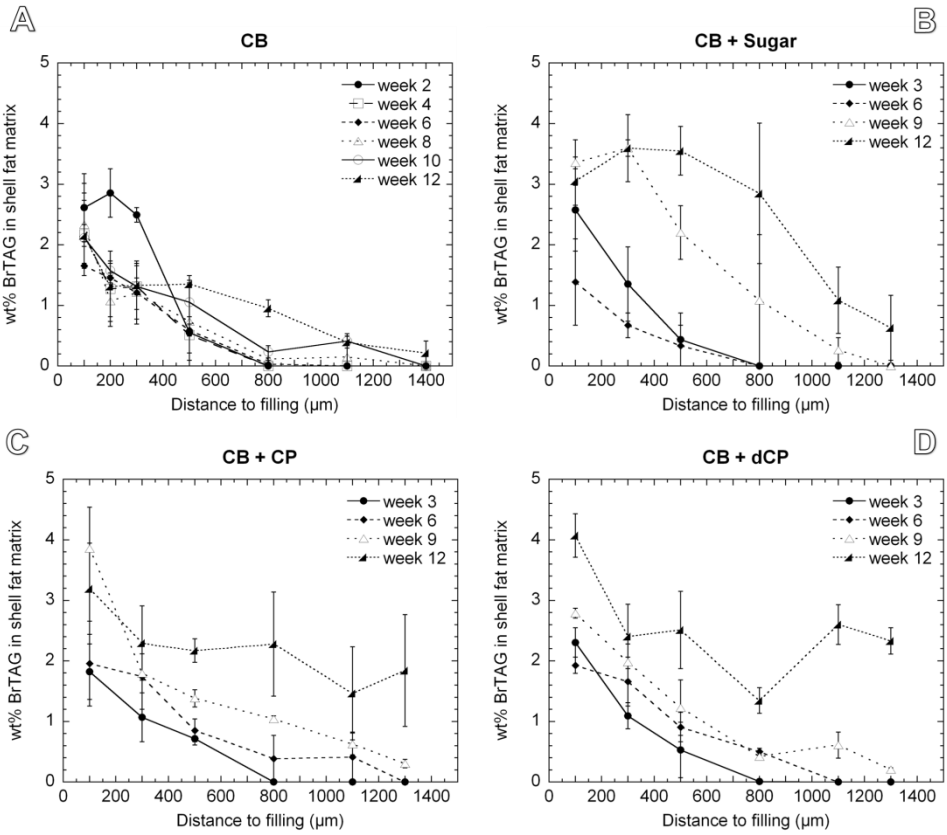
Figure 13. Migration profiles of model pralines stored at 23°C. Seeded shells consisting of A: CB, B: CB and sugar, C: CB and CP, D: CB and dCP. The figures are modified after Paper III.
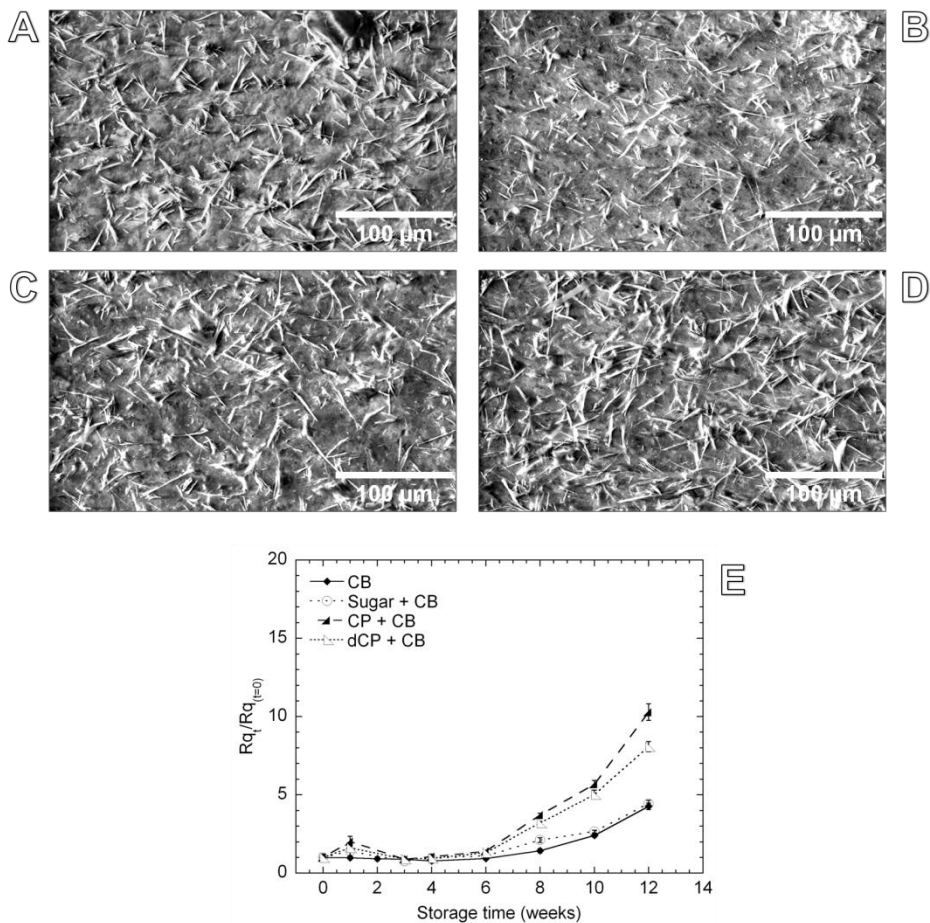
Figure 14. Surface microstructure and roughness results for model pralines stored at 23°C. A-D: LV SEM images of model pralines with seeded shells stored for 8 weeks consisting of A: CB, B: CB and sugar, C: CB and CP, D: CB and dCP (scale bars represent 100 μm). E: Normalised roughness values as a function of storage time. The figures are modified after Paper III.

To further investigate the effect of particle size on oil migration and the connected fat bloom development, chocolate samples with varied particle size (15, 22 and 40 μm) stored against a model filling were investigated within the work of this thesis[Paper IV]. As for the previous study all samples were subjected to seeding in order to keep a controlled production, and the filling fat phase was saturated by cocoa butter TAGs. The migration of filling oil into the model shells was observed by following the migration of BrTAGs from the filling into the shells using EDS. The compositions of the

35

chocolate model shells and the filling as well as the PSD of the non-fat particles can be seen in Table 2 (page 33). The results confirmed the hypothesis of a higher migration rate when smaller particles, and thus, with a larger specific surface area are used in a model chocolate confectionery product. By combining migration results with surface microstructure and topology results, clear differences could be observed between the samples. At 23°C storage, the samples with a particle size of 15 µm indicated a higher rate of oil migration and the strongest development of fat bloom at the surface, as can be seen in Figure 15. This could be observed both macroscopically and microscopically. Thus, it appears that larger specific surface area of the non-fat particles facilitates migration of filling oil, possibly due to a more heterogeneous and coarser crystal network with higher permeability. Smaller particle size contributes to a larger surface area and thus, more passages for migration.

Additionally, a subsequent study was initiated with similar composition of shell and filling as in the study presented above, but where the chocolate confectionery had the shape of a praline instead of two connected discs. The objective of this was to investigate if the behaviour of migration and fat bloom development is comparable when the filling is enclosed by a chocolate shell and when the filling and shell are connected by simply laying on top of each other. Early results indicated a higher migration rate when smaller non-fat particles were present in the chocolate shell. However, this study must be further investigated in order to provide useful and reliable results.
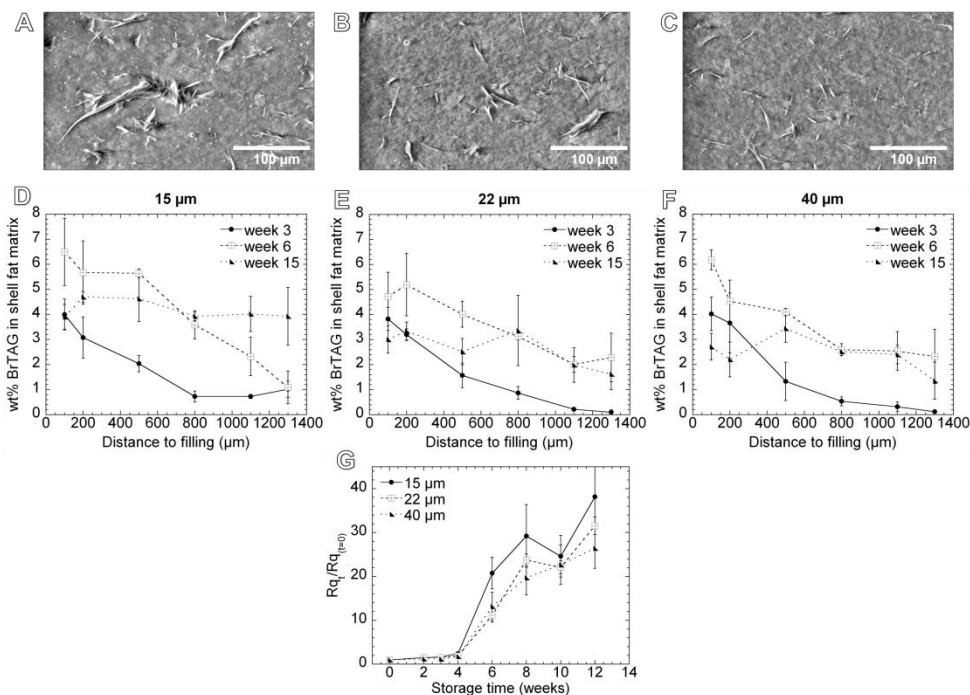
Figure 15. Results of seeded chocolate shells stored against a model filling at 23°C. A-C: LV SEM images of model samples stored for 6 weeks where the non-fat particle size is A: 15 µm, B: 22 µm, C: 40 µm (scale bars represent 100 µm). D-F: Migration profiles where the non-fat particle size is D: 15 µm, E: 22 µm, F: 40 µm. G: Normalised roughness values as a function of storage time. The figures are modified after Paper IV.

4.3 Storage temperature

After chocolate production the storage conditions for the products are of great importance since structural changes take place in cocoa butter after production and during storage. This is due to the proceeding fat crystallisation which may include nucleation of new crystals or crystal growth, Ostwald ripening (dissolution of small crystals and growth of big ones), polymorphic transformation, migration of small crystals, and sintering (bridging of existing fat crystals by solid fat)[39, 111].

The influence of storage temperature has been shown to have substantial impact on fat bloom development and oil migration. Several authors have found that the oil migration rate increases at higher storage temperatures[48-49, 54, 62, 64-65, 67, 69]. A higher rate of oil migration has further

been connected to polymorphic changes[48-49, 54] and to development of fat bloom at the surface[48, 54]. Depypere *et al.*[72] demonstrated that freezing and chilling pre-treatment of freshly produced samples consisting of milk chocolate surrounding a hazelnut filling resulted in lower oil migration rate and subsequent fat bloom development.

During the research of this thesis, distinct differences in surface structure development was observed between samples stored at different temperatures in terms of macroscopic and microscopic information and supporting qualitative and quantitative data[Paper I, III-IV]. White chocolate pralines were stored at two temperature-controlled conditions (at 18°C, and cycled between 15 and 25°C). Surface properties were then investigated during storage. The surface images and the roughness parameters indicated distinct development of surface characteristics for the two storage conditions, as can be seen in Figure 21 (page 50).

Other studies within this thesis revealed that an increase in temperature from 20 to 23°C had a substantial impact on oil migration and fat bloom development as can be seen in Figure 16. The impact due to the difference in storage temperature could be explained by a higher liquid fat fraction in the shell and the filling at a higher storage temperature. Since the migration of TAGs takes place via the liquid fat portions, permeability increases and therefore migration-induced fat bloom development is enhanced when the storage temperature is increased. The observed effect of higher rate of migration during higher storage temperature agrees with the results from earlier studies[48-49, 54, 62, 64-65, 67, 69]. Thus, the storage temperature is of great importance to ensure a product with increased shelf life.
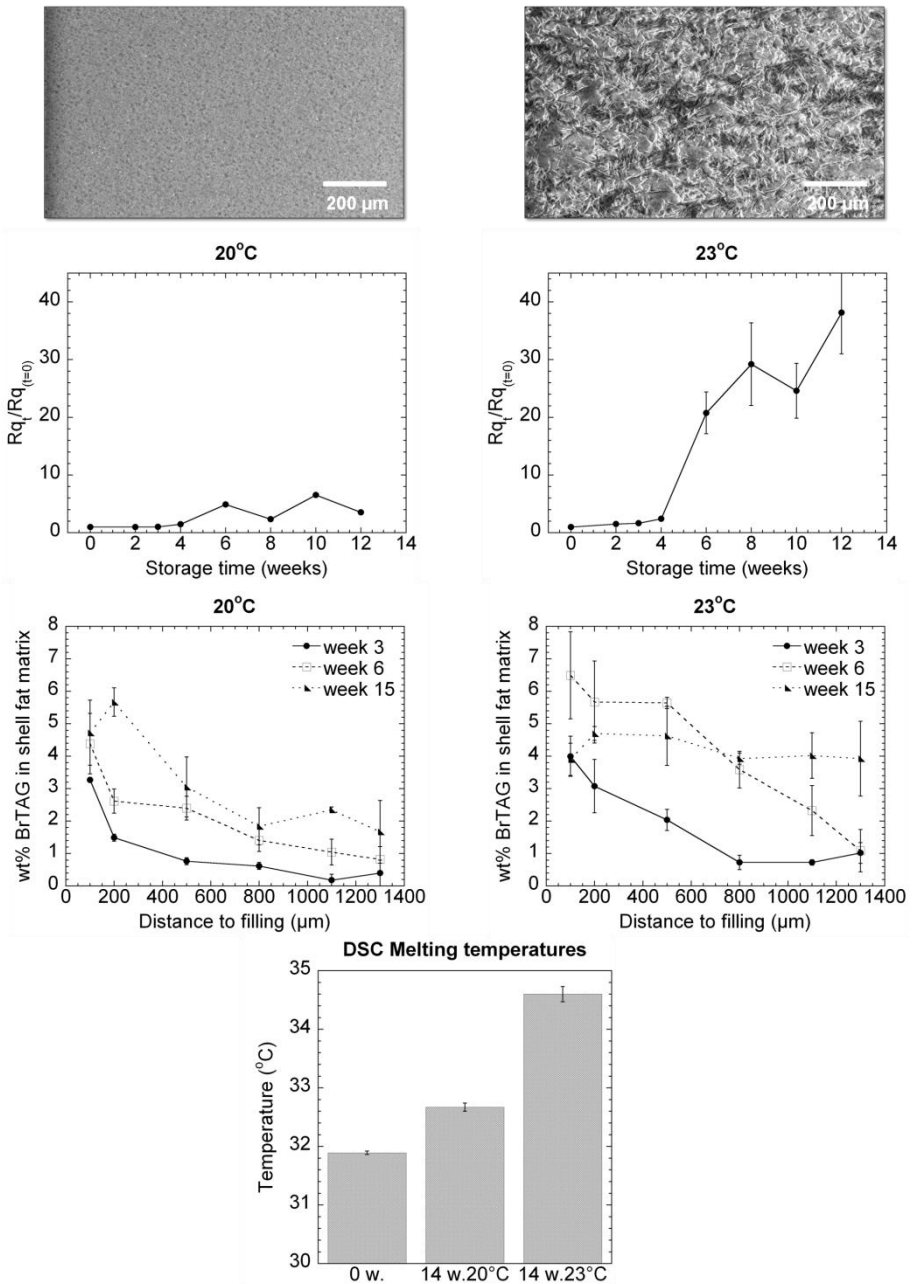
Figure 16. LV SEM images, surface roughness development, migration profiles and DSC-melting temperatures (peak maxima) for samples with equal compositions stored at different temperatures (scale bars represent 200 μm). Left: stored at 20°C. Right: stored at 23°C. Centered: stored at 20 and 23°C. The figures are modified after Paper IV.

39

5 Mechanisms for oil migration

As described earlier, the fat phase of a chocolate shell may be considered as a two-phase system with a solid phase and a liquid phase, through which the majority of TAG migration takes place. Oil migration in chocolate confectionery systems has been explained by several hypotheses and mechanisms. The most cited mechanisms are based on molecular diffusion[62-63, 67-68, 71, 112-114], where the driving force for migration is due to mixing entropy between the migrating TAGs in filling and chocolate. However, a concern while using the diffusion models is their lack of sensitivity toward aspects of microstructure. Chocolate products contain micro fractures such as cracks or pores, where movement of oil can take place. Thus, capillary flow has also been suggested to play a significant role during oil migration and has been proposed as an alternative mechanism[47, 61, 65-66, 69, 115-116]. Furthermore, migration connected to a pressure driven convective flow has been discussed in literature[110, 117, Paper I-IV]. This has mainly been explained by an increase in volume upon melting and re-crystallisation of cocoa butter which forces oil to the surface through the crystal network and through micro fractures and pores formed during crystallisation. Still, it is often suggested that a combination of different mechanisms leads to the migration of oil, with one of the above mentioned dominating. These mechanisms together with novel results from this thesis will be described and discussed in this section.

5.1 Molecular diffusion

Diffusion is a process where matter is transported from one part of a system to another as a result of random motion of molecules and small particles. This occurs whenever there is a concentration gradient between two points, and the molecules or particles will migrate from a higher concentration to a lower concentration until the system has reached thermodynamic equilibrium[118-119]. Molecular diffusion can be described mathematically using Fick´s laws of diffusion.

Fick´s first law (Eq.2) states that, within a continuous medium and under the presence of a concentration gradient, the net migration of solute molecules due to random movement occurs from a region of high concentration to one of lower concentration, i.e. the driving force for diffusion is a concentration gradient[116]:

$$J = -D\frac{\partial c}{\partial x} \qquad\qquad 2$$

J refers to the diffusion flux, c to the concentration of diffusing substance, x to the space coordinate measured normal to the section, and D is the diffusion coefficient. Since diffusion occurs in the direction opposite to that of increasing concentration, the sign in the equation is negative.

Fick´s second law (Eq.3), for transport in one dimension, states that the rate at which diffusion proceeds at a point in space, where one solute is present in a large portion of solvent, is proportional to the variation of the slope of the concentration gradient. In this equation, t refers to time:

$$\frac{\partial c}{\partial t} = D\frac{\partial^2 c}{\partial x^2} \qquad\qquad 3$$

The transport of oil in food systems is normally characterised as a diffusion process described by Fick´s laws. For 1-dimensional mass transfer of oil into chocolate, with a constant diffusion coefficient, models of these equations have frequently been used[44, 54, 62, 112-114]. Ziegleder *et al.*[112-114] proposed an approximation of the solution of Fick´s second law, describing oil migration in filled chocolate products (Eq.4):

$$\frac{c_t}{c_0} = \frac{2\cdot K\cdot A\sqrt{D\cdot t}}{V\sqrt{\pi}} \qquad\qquad 4$$

In this approximation, c_t and c_o is the amount of incoming and outgoing oil within the chocolate after time t and 0, respectively. A is the contact area between the layers, t is the time for migration, V is the volume of the chocolate sample, and D is the diffusion coefficient. The authors refer to K as a constant describing the contact between the layers. For an ideal system $K=1$, for insufficient contact $K<1$ and for structural changes due to swelling or eutectic effects $K>1$, in fact, describing effects beyond diffusion[112, 114]. When using this model the following assumptions are made: the concentration at the interface reaches equilibrium directly, the time required for thermal equilibrium of the chocolate is negligible compared with the time for equilibrium sorption, and changes in chocolate dimension

due to swelling are negligible during the solvent exposure time. Thus, this model does not take into account structural parameters of chocolate such as fat crystal structure, polymorphic form, tortuosity and phase volume[54].

Ziegleder *et al.*[112-114] proposed an additional equation describing the speed of oil migration in chocolate (Eq.5):

$$\frac{m_t}{m_s} = \frac{\sqrt{D \cdot t}}{d}$$

5

where m_t and m_s is the amount of migrated oil at time t and at infinity, respectively. D is the diffusion coefficient for oil in chocolate, d is the thickness of the chocolate layer and t is the storage time. The ideal case is assumed ($K=1$) and thus, microstructural parameters mentioned above are not taken into account. During the early stages of migration, when $m_t \ll m_s$, m_t increases linearly with $\sqrt{t}$, while in the later stages, when $m_t \approx m_s$, m_t asymptotically approaches saturation, i.e. equilibrium[112-114]. This means that according to this equation, relatively large amounts of oil are migrating during the very first part of the timeframe, and this process slows down over time. Figure 17 shows a schematic illustration of a typical migration profile by molecular diffusion, where the migrated amount is presented as a function of distance to the interface.
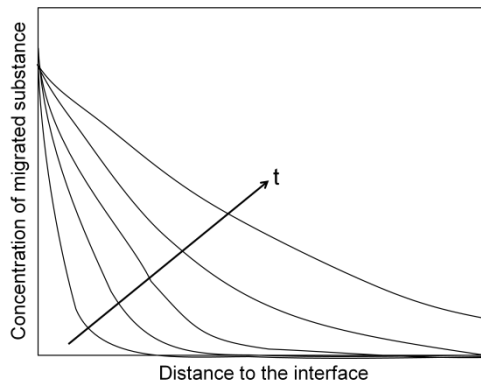

Figure 17. Schematic illustration of a typical migration profile by molecular diffusion.

Eq. 5 has been frequently used to describe oil migration through chocolate[44, 62]. However, in order to take microstructural parameters into account this equation has been further adapted[45, 54]. Based on molecular diffusion, Galdamez *et al.*[45] proposed a new model, where they accounted for structural parameters such as fat crystal microstructure, tortuosity and swelling of the chocolate.

5.2 Capillary flow

Fat migration can be thought of as the movement of liquid fat through interparticle passages and connected pores under capillary flow. In a porous medium, fluid can be drawn into the pore by an interfacial pressure gradient. This phenomenon is widely observed in many physical situations including printing of coated paper, capillary flow of water in soils, and wetting and dying of fibres. Capillary flow can be described mathematically by Lucas-Washburn equation (Eq.6), where the movement of a fluid in a porous space is due to the balance of surface tension, gravity, and viscosity[116, 120]:

$$\frac{2}{r}\gamma cos\theta = \frac{8}{r^2}\mu h \frac{dh}{dt} + \rho gh \qquad\qquad 6$$

In this equation r is the capillary radius, h is the distance the fluid is drawn into the capillary, γ is the surface tension of the fluid, Θ is the contact angle between the fluid and the capillary wall, μ is the viscosity of the fluid, ρ is the density of the fluid and g is the acceleration due to gravity. This equation can further be expressed as short and long time solutions (Eq.7 and Eq.8):

$$h = \sqrt{\frac{r\gamma cos\theta t}{2\mu}} \qquad when\ t \rightarrow 0 \qquad\qquad 7$$

$$h = h_\infty \left[1 - exp\left(-\frac{\rho gr^2}{8\mu h_\infty}\right)t\right] \qquad when\ t \rightarrow \infty \qquad\qquad 8$$

where h_∞ is the fluid height within the capillary which is reached when the interfacial pressure difference is balanced by the hydrostatic pressure at long times, i.e. at equilibrium (Eq.9)[121]:

$$h_\infty = \frac{2\gamma cos\theta}{\rho gr} \qquad\qquad 9$$

Figure 18 shows a schematic illustration of a typical migration profile by capillary flow, where the migrated amount is presented as a function of distance to the interface. The capacity of the migration mechanism in a medium with low porosity is reflected in the profile.
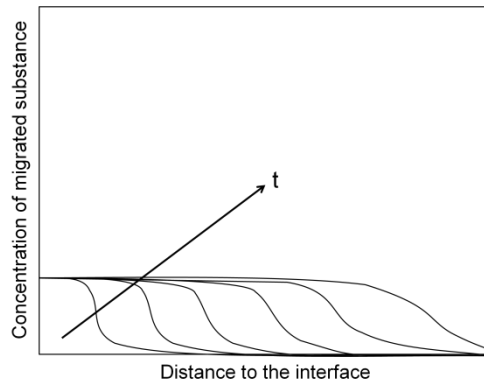
Figure 18. Schematic illustration of a typical migration profile by capillary flow in a medium with low porosity.

According to calculations performed by Altimiras *et al.*[110] capillary flow is an extremely fast process, where only a few seconds are enough for liquid cocoa butter to reach the maximum height within capillaries. This was compared to the experimentally determined times which were days. Even when the tortuosity was taken into account, which would delay capillary flow, the predicted times were still too short compared to the experimentally determined times. Deka *et al.*[71] measured the density of both the solid and liquid fat simultaneously in chocolate during migration of hazelnut oil. Their conclusion was that the migration process is complex and includes both a rapid mechanism and a slower mechanism which they attributed to diffusion.

Choi *et al.*[66] concluded that a Fickian-based model with a constant diffusivity is not capable of accurately predicting the spatial distribution of liquid oil in chocolate as a function of time for peanut oil migration in chocolate. The model accurately predicted the oil content near the interface between filling and chocolate, but under-predicted the oil concentration throughout the majority of the chocolate region. At long times the Fickian model slightly over-predicted the oil content in the chocolate region. When applying calculations for capillary flow the authors could state that both the Fickian diffusion and the capillary flow predicted quantitatively similar behaviour as a function of time for the amount of material that had migrated. Thus, they suggested that additional microstructural data was needed to differentiate between the two phenomena.

5.3 Pressure driven convective flow

When subjecting cocoa butter to higher temperatures the amount of liquid phase increases, e.g. the amount of liquid phase in a cocoa butter originating from West Africa is approximately 15% at 20°C compared to 40% at 30°C[6]. Since the density of liquid cocoa butter is lower than for solid cocoa butter this means that a liquid fraction occupies a larger volume than a solid fraction of cocoa butter. Thus, when part of the cocoa butter in a chocolate product dissolves due to eutectic effects or Ostwald ripening, or melts due to a temperature rise, an increase in volume takes place. This forces the liquid through the network and through pores and cracks towards the surface and also towards the interface of the filling and chocolate. It has been suggested that the density difference is the key driving force in fat migration and hence in fat bloom development[110, 117]. Figure 19 shows a schematic illustration of a typical migration profile by a pressure driven convective flow, where the migrated amount is presented as a function of distance to the interface.
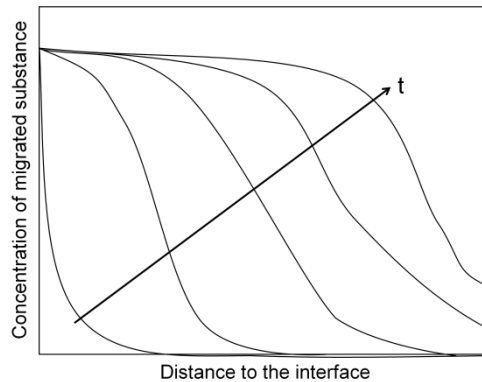

Figure 19. Schematic illustration of a typical migration profile by a pressure driven convective flow.

5.4 Oil migration related to microstructure

Investigations of chocolate surface microstructure have shown the presence of imperfections in the form of pores and protrusions. It has been hypothesised that these imperfections could be related to fat bloom development, mainly through connected channels leading through the body of the chocolate where fat migration could take place[47, 56-59].

Smith and Dahlman[57] suggested that fat bloom growth in pralines is a two-phase process, with drops initially forming at the surface and subsequently, fat bloom crystals nucleating and growing from them. They observed channels leading into the centre of the chocolate through which the migration of filling oil could preferentially take place. In agreement with this study, Sonwai and Rousseau[56, 59] observed cone-like structures on chocolate surfaces and suggested that these may have formed by welling and deposition of liquid-state fat pushed from within the matrix onto the surface during contraction. These cones hardened with age and crystal outcroppings protruded from them, suggesting that these features acted as loci for fat bloom crystals. In addition, Rousseau[58] observed microscopic pores at the surface of milk chocolate randomly distributed over the surface, and suggested that these were not directly involved in fat bloom development or oil transport since fat bloom crystals also could be observed in the absence of these imperfections. However, this observation rather speaks for a combination of different mechanisms taking place in parallel for the development of fat bloom.

Loisel *et al.*[117] have shown the presence of a porous matrix, partly filled with liquid cocoa butter fractions, in dark chocolate by using mercury porosimetry. It was suggested that the porous matrix is a network of cavities closed by multiple walls of fat crystals impregnated with liquid fat. Due to the difference in dilation coefficients between solid and liquid fat and further due to polymorphic evolution, the liquid phase leaves spaces and air fills pores close to the surface or yields empty cavities. During temperature variations the difference in dilation of air and liquid fat could push the liquid fat fraction to the surface and thus contribute to fat bloom formation. The authors reported that chocolate (~32% cocoa butter) had a porosity of 1-4% of the total chocolate volume which is a rather small void volume. However, the pressures used with mercury porosimetry might have collapsed any voids or channels present as chocolate is soft compared to metals and polymers that are usually tested with this technique.

In the work of this thesis, Confocal Raman microscopy was used to elucidate the connection between a porous matrix and the observed imperfections at chocolate surfaces[Paper II]. Combined with LV SEM images, the presence of protrusions and pores at white chocolate praline surfaces could be confirmed, having a base mean diameter of 20±1.5 µm, and an inner pore mean diameter of 9.7±1.2 µm (Figure 20). Raman horizontal and depth scans showed that the protrusions and pores continue at least 10 µm into the chocolate shell and that some protrusions and channels mainly consist of fat (Figure 20B), while some consisted of a fat layer, leaving a hollow space underneath (Figure 20A). The pores and their continuing

channels consisted of nothing but air (Figure 20C). If the observed channels continue even further into the chocolate shell, liquid fat from the filling and the chocolate matrix could be transported through these and up to the surface. It can be assumed that the liquid fat might move through the channels, depending on pressure gradients caused by temperature changes, crystallise on the edge at the surface and then the liquid fat may return, leaving a hollow protrusion with a fat shell, which in some cases could collapse, leaving a pore at the surface. These findings support the idea that the pores and protrusions could be connected to oil migration in filled chocolate products and, thus, to fat bloom development. The mechanism of oil migration was interpreted as a pressure driven convective flow through the chocolate network and through pores and cracks in two directions, i.e. up to the surface and back into the shell.

Additionally, a subsequent study was initiated where white chocolate pralines surrounding a filling consisting of cocoa butter, triolein and hexyl benzoate were investigated by confocal Raman microscopy. The results indicated the presence of hexyl benzoate connected to the observed pores and protrusions, thus, providing even stronger evidence for the connection of pores and protrusions to migration from the filling. Nevertheless, further analyses would need to be realised in order to substantiate the significance of these results.
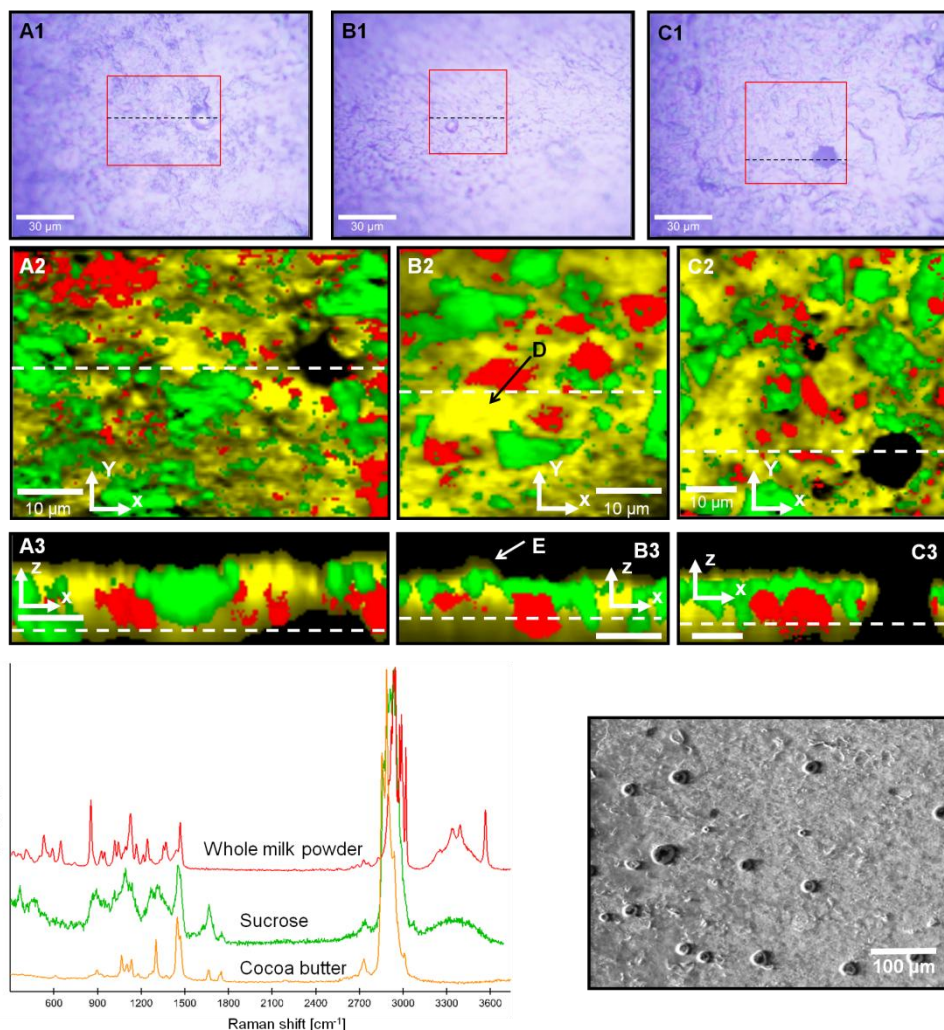
Figure 20. A1-C1: Light microscopy images of white chocolate praline surfaces, containing a hazelnut filling (scale bars represent 30 μm). The red squares represent the area where horizontal scans have been recorded and the dashed lines where the depth scans have been recorded. A2-C2 represent horizontal scans connected to A1-C1 and to the depth scans in A3-C3. The dashed lines in A2-C2 show where the depth scans have been recorded, and the dashed lines in A3-C3 show where the horisontal scans have been recorded (scale bars represent 10 μm). D, E: Indicating a protrusion covered by a region enriched by fat. The colors in the scans are connected to the colors in the reference spectra (lower left). Lower right: LV SEM image of the chocolate surface where pores and protrusions can be observed (scale bar represents 100 μm). The figures are modified after Paper II.

48

Recent studies have focused on the relationship between surface topology and fat migration, where AFM, LSM, SEM and optical profilometry have been used as main techniques[38, 47, 55-60, 122]. Rousseau and Smith[47] argued that transport of TAGs in plain and filled chocolate is a combination of both diffusive and capillary forces where liquid TAG redistribution is caused by specific micro- and nanoscale pores and diffusive mixing. They observed that a number of pores present at the surface of filled chocolate had disappeared after short time of storage, suggesting that liquid-state fat had reached the surface of the chocolate. After the disappearance of the pores fat crystals began to appear at the surface.

Within the work of this thesis, protrusions were observed at the surface of white chocolate pralines enclosing a hazelnut filling by using optical profilometry[Paper I] (Figure 21). For samples stored at 18°C some of the protrusions disappeared and some reappeared over time (Figure 21A), and some changed their appearance (Figure 21B), at the same time as new topological features arose at the surface. For samples that were stored at a cycled temperature (15-25°C) some topological features disappeared completely (Figure 21C), while others remained throughout the storage period and became enhanced with time (Figure 21D). These observations were possible since the same area of interest (±20 µm) was analysed at each analysis occasion. The smooth nature of some of the protrusions suggests that these topological features consist of oil (i.e. not crystallised), from the filling and the chocolate matrix, that has been transported to the surface of the chocolate. Samples stored at a cycled temperature showed initially large protrusions at the surface, and after 2 weeks storage the surfaces became smoother. Few structures were observed by optical profilometry although there was an increase in small peaks, indicating fat crystal growth. According to macroscopic measured shape, the filling shrunk and the shell expanded (~40 volume%) (Figure 22). Thus there might have been a flux of oil from the filling into the shell but to a lesser extent to the surface.

Results from this study suggest once again that some imperfections, in form of pores or protrusions, could play a role in the development of fat bloom, and further, that there may be different mechanisms of fat migration taking place depending on the storage conditions. Considering the samples stored at constant temperature a convective flow as a main mechanism is suggested, where a two-step process could take place, with oil protrusions initially forming at the surface and then crystals nucleating and growing from them. In the case of storage at cycled temperature there is a decrease of the filling volume, probably caused by migration of liquid fat from the filling into the expanding shell. In addition these observations

show an effect which can be interpreted as a convective flow through the network and through pores and cracks in two directions, i.e. up to the surface and back into the shell. The driving internal pressure fluctuations can be due to changes in the liquid to solid ratio in the fat at the surface and internally when the temperature is cycled. Part of the liquid fat could be pressed out at the surface, spreading out, allowing movement of the solid components, while part of the liquid fat could be reabsorbed into the chocolate shell, where re-crystallisation could occur. Since the migrating oil is welling out at the surface, it may be concluded that capillary flow is not the mechanism connected to the protrusions in these studies. In the case of capillary flow the oil would stop at the surface level. However, capillary flow could be an additional mechanism present, contributing to the absorption of oil into the shell. The appearance of protrusions at the surface was supported by LV SEM images as can be seen in Figure 21.
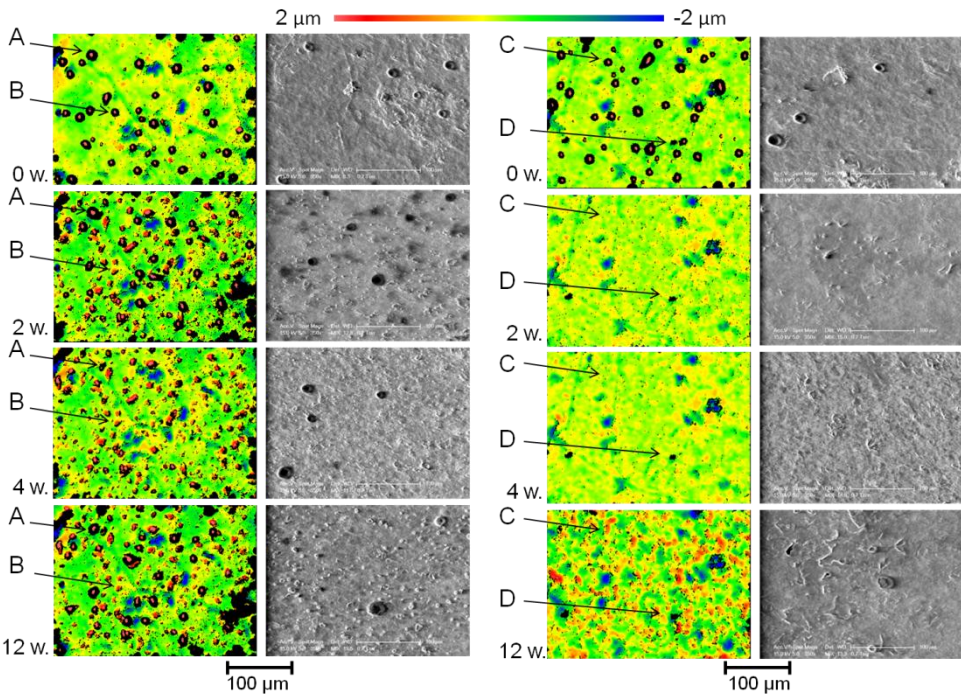

Figure 21. Optical profilometry images (color) and LV SEM images (black&white) of the top surfaces of white chocolate pralines stored at two different temperature environments for 0, 2, 4 and 12 weeks. Left: Stored at 18°C. Right: Cycled between 15 and 25°C. Topological features that A: disappear and re-appear, B: change their appearance, C: disappear completely, D: remain and become enhanced. Scale bars represent 100 μm. The figures are modified after Paper I.

In several studies where oil migration in chocolate confectionery systems has been analysed, a swelling of the shells has been observed[45, 65, 71, 123]. These observations have also been seen during the work of this thesis. White chocolate pralines with a hazelnut filling stored at cycled temperatures developed a soft shell and a visually observable hardened filling after 36 weeks of storage[Paper I]. These samples also expanded approximately 2 mm in diameter and height compared to the fresh samples and the samples stored at constant temperature, which corresponds to a total shell volume increase of approximately 40%. At the same time, the volume of the filling decreased markedly and the bottom of the praline cracked and moved towards the centre of the praline (Figure 22).
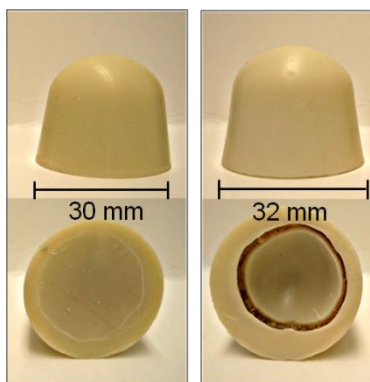

Figure 22. White chocolate pralines containing a hazelnut filling, from the front and from underneath. The sample to the right show an increase in volume during storage. The figures are modified after Paper I.

In the studies of oil migration and fat bloom development connected to pre-crystallisation, presence of non-fat particles and effect of particle size, a swelling of the shells was observed when stored at 23°C[Paper III-IV]. However, the relative volumes of the shells and the fillings were not characterised. Since both filling and shell fat phases in these studies were saturated by cocoa butter TAGs, dissolution of cocoa butter crystals in the shell is not expected to occur to any substantial extent. Thus, a possible reason for the observed swelling could be crystal growth in the cocoa butter matrix of the shell due to Ostwald ripening and re-crystallisation into more stable polymorphs. If the number of crystals is constant while they are growing in size the network will become coarser and absorb an increasing amount of liquid fat. This effect can be further strengthened by presence of non fat particles that may enhance the impact of a coarsening fat crystal network.

The migration behaviour that was shown in Figure 12, Figure 13 and Figure 15 indicate that molecular diffusion is not the dominating migration mechanism for these model systems. A diffusion process following Fick´s second law should lead to a reduced slope of the concentration profile and a constant or falling concentration close to the interface. Additionally, the highest increase should be at the position were the second derivate of the concentration curve reaches its maximum. Furthermore, the pore volumes reported by Loisel *et al.*[117] are too small in order to explain the high levels of migrated BrTAGs in these studies. Thus, a likely scenario could be that there is an initial phase of molecular diffusion followed by a re-crystallisation processes and crystal growth, as mentioned above, leading to a coarsening network and a convective oil migration into the expanding shell. Thus, a pressure driven convective flow is suggested as an important contribution in addition to molecular diffusion and capillary flow.

6 Concluding remarks and future perspectives

The aim of this work was primarily to provide a deeper understanding of fat bloom development and oil migration in chocolate confectionery products. In this section the main conclusions will be highlighted together with future perspectives.

It has been demonstrated that the surface topology development over time can be conveniently followed in a specific area (±20 µm) by using optical profilometry, both quantitatively and qualitatively. The combined information from profilometry and LV SEM results provide an analytical toolkit for the early recognition of surface changes and early fat bloom development. Since the surface topology development can be followed in the same area of interest, changes of specific topological features over time can be monitored and thus, together with statistical surface roughness parameters, give useful information to possible mechanisms of fat migration.

Confocal Raman microscopy (CRM) has been shown to be a useful technique for the investigation of white chocolate surfaces. The appearance of protrusions and pores at the chocolate surface could be confirmed and characterised. Raman horizontal and depth scans have shown that the protrusions and pores continue at least 10 µm into the chocolate shell. Results obtained through CRM, optical profilometry and LV SEM suggest that some imperfections, in form of pores or protrusions, play a role in the development of fat bloom, where a temperature connected pressure driven convective flow of liquid fat is suggested as main mechanism.

EDS has been shown to be a useful method to achieve migration profiles for migration from a filling into a chocolate shell, where BrTAGs can be used as a probe for migrating filling oil.

Microstructural changes, induced by means of different tempering or seeding, addition of non-fat particles, addition of non-fat particles with varied particle size and storage conditions can be used to influence

migration behaviour and thus, fat bloom development. By applying seeding to cocoa butter shells, reduced oil migration rate and thus, a reduced development of fat bloom could be observed compared to poorly tempered cocoa butter shells. Addition of particles to seeded cocoa butter shells increased the migration rate noticeably compared to pure cocoa butter samples. Additionally, the development of fat bloom was accelerated. The effects of particle size regarding oil migration and fat bloom development on chocolate model pralines indicate that a smaller particle size leads to a higher rate of oil migration from filling to shell and thus an accelerated fat bloom development. Thus, the specific surface area of the non-fat particles seems to be an important parameter for oil migration and fat bloom development in chocolate pralines. The particle size in a chocolate product is an accessible parameter for the industry. Thus, the study of the influence of particle size on oil migration and fat bloom development is of relevant interest.

The storage temperature was shown to have a substantial impact on oil migration and fat bloom development. Thus, the importance of controlled storage environments for chocolate confectionery products cannot be emphasised enough.

Convective flow is suggested to be an important contribution to the migration in addition to molecular diffusion and capillary flow.

For future perspectives, it would be interesting to investigate if the presence of filling fat can be connected to the observed pores and protrusions by using CRM, confirming the connection of the surface imperfections to oil migration from the filling. Furthermore, the influence of particles on oil migration and fat bloom development could be further developed by investigating the addition of particles and substances such as milk solids and emulsifiers. In addition, one approach to further investigate the correlation between particle size and oil migration could be by adjusting the amount of emulsifier relative to the specific surface area of the non-fat particles. Furthermore, by relating the migration of BrTAGs from filling to shell with quantitative data of chocolate shell swelling this interaction could be further investigated.

There are still many questions left to be answered regarding oil migration and fat bloom development in chocolate confectionery systems. However, my hope is that through results achieved during the work of this thesis, new ideas and interesting studies can be realised in order to further elucidate the remaining questions in this area of research.

Acknowledgements

During the work that has resulted in this thesis, many people have contributed and been involved in different ways. I am very grateful to all of you and would like to thank everybody for your time and support. There are some in particular that I would like to take the opportunity to express my gratitude to.

First of all, I would like to thank my supervisor, Professor Björn Bergenståhl, for sharing your knowledge and for guiding me throughout this work. Thank you for always taking the time to discuss the work, even when you had none. My co-supervisor, Dr. Anna Millqvist-Fureby deserves all considerable credit for always being around to help me and for sharing your knowledge. Thank you to my initial co-supervisor, Dr. Daniel Kalnin, for your encouragement and enthusiasm during my first months as a PhD student. Furthermore, I would like to thank Prof. Mark Rutland and Dr. Paul Smith for introducing me to surface chemistry and the science of chocolate in the very beginning.

The EU commission, grant 218423 under FP7-SME-2007-2, is gratefully acknowledged for financial support. The partners of the EU project *ProPraline* are thanked for valuable input, and special thanks goes to my PhD student partners Claudia Delbaere, Daniel Ehlers and Lina Svanberg for great cooperation and for good times together when exploring the European chocolate world. Annika Altskär is acknowledged for her kindness and for introducing me to chocolate tempering.

Thank you to the department of product development at Mondelez, Upplands Väsby, for helping me with experimental work. A special thanks goes to Soili Vehmas and Veronica Harrison.

I would also like to thank all former and present colleagues at YKI and SP for contributing to my work and for creating a nice working atmosphere. I have really enjoyed my time working with you. Through these years I have had the privilege of having a manager with a truly positive spirit and who always showed that he believed in me – Fredrik Johansson, thank you. Kerstin Linsten, thank you for being a great listener when I went through

possibility to read this I want to thank you for everything that you taught me about life and for all the time that we spent together. I miss you so much. Ludde, there are no words possible to describe how grateful I am for your patience, support and love during these past years. You are amazing. And our little Jack – ever since you joined us, life is always fun and meaningful. Now that this thesis is finished, I really look forward being able to spend more time with my wonderful family and friends.

Photo: Dick Gillberg.

Rosenlundsgatan, Stockholm 2014

Populärvetenskaplig sammanfattning

Utvecklingen av nya innovativa chokladprodukter har tagit fart under de senaste åren i takt med att konsumenterna ställer allt högre krav på chokladkvaliteten. Eftersom produktionsprocessen är komplicerad och hållbarhetstiden begränsad uppskattas att man slänger drygt 100 000 ton chokladprodukter varje år i Europa till ett värde av 1.2 miljarder Euro. Att optimera produkternas egenskaper är därför en viktig parameter för chokladindustrin.

Choklad har en mycket unik egenskap. I rumstemperatur är en chokladbit hård men så fort man stoppar den i munnen smälter den. Orsaken till detta är att kakaosmörets fettkristaller smälter vid 32-34°C, strax under kroppstemperatur. Detta är dock endast fallet om chokladen tillverkats under speciella, kontrollerade förhållanden. Kakaosmör är ett polymorft fett, vilket betyder att det kan anta flera olika kristallformer, alla med olika stabilitet och smältpunkt. Vid chokladproduktion tempererar man chokladen, vilket betyder att man med hjälp av en temperaturcykel styr in kakaosmöret till den kristallform som smälter vid just 32-34°C. Genom naturlagarna kommer denna kristallform med tiden att omvandlas till den mest stabila formen som har en högre smältpunkt och större, nålformade kristaller (Figur 1). Chokladen förlorar då sin initiala glans och får en matt, grå-vit yta. Framför allt leder detta till estetiska förändringar men det påverkar även de sensoriska egenskaperna vilket gör chokladen mindre aptitlig. Fenomenet kallas fettblom och har kommit att utgöra grunden till min avhandling.

Fettblom utvecklas snabbare om något gått fel i produktionen eller om man förvarat chokladen under felaktiga temperaturförhållanden. Produkter som består av en fet fyllning med ett omgivande chokladskal, exv. chokladpraliner tenderar att utveckla fettblom mycket tidigare än en vanlig chokladkaka. Detta beror på att fettmolekylerna från fyllningen förflyttar sig eller migrerar in i chokladskalet och påskyndar processen. Fettmigrering ger också upphov till att chokladskalet blir mjukt medan fyllningen blir hård vilket inte är önskvärt hos konsumenterna. Genom att

fördröja fettmigreringshastigheten i chokladpraliner kan man alltså få produkter med längre hållbarhet. Men för att kunna göra detta måste man veta vilka mekanismer som ligger bakom migreringen samt vilka egenskaper hos produkten som påverkar den. Under den senaste 10-årsperioden har en hel del forskning inom området bedrivits och man diskuterar framförallt tre olika fettmigreringsmekanismer; diffusion, kapillära flöden och konvektiva flöden.

Syftet med avhandlingen har varit att bidra till denna pågående forskning genom att utveckla nya metoder för att studera fettmigrering och fettblomutveckling, samt att undersöka chokladskalets mikrostrukturella inverkan. Genom att använda en nyutvecklad metod (EDS) kan man se hur snabbt märkta fettmolekyler från fyllningen rör sig in i chokladskalet under olika förhållanden. Detta kan vidare kopplas till resultat från elektronmikroskopibilder och ytråhetsdata vilket ger en verktygslåda där man kan relatera fettmigreringshastighet till utveckling av fettblomkristaller på chokladytan. Ytterligare en ny teknik som använts för analys av choklad är konfokalt Raman mikroskopi. Med hjälp av detta har vi identifierat bubblor på chokladytan som fortsätter in i chokladskalet i form av kanaler. Dessa kanaler och bubblor kan vara en möjlig väg för fyllningsfettet att vandra genom chokladen och bidra till fettblomutveckling.

Chokladskalets mikrostruktur har visats ha en betydlig påverkan på fettmigreringshastigheten. En kristallstruktur bestående av fler små fettkristaller som packats tätt ledde till långsammare fettmigrering och därigenom långsammare utveckling av fettblom. Även partikelstorleken visade sig påverka hastigheten av fettmigrationen, då mindre partikelstorlek i chokladen ledde till en snabbare migrering och snabbare utveckling av fettblom. Förvaringstemperaturen visade sig ha en mycket stor påverkan på fettmigreringshastigheten och fettblomsutvecklingen. En förvaringstemperatur på 23°C gjorde att det gick betydligt snabbare än en förvaringstemperatur på 20°C. Med stöd av ovannämnda resultat diskuteras tänkbara fettmigreringsmekanismer avslutningsvis i avhandlingen. Förhoppningen är att genererade resultat kan leda till en djupare förståelse för mekanismer bakom fettmigrering och fettblomutveckling i chokladpraliner, och därigenom skapa förutsättningar för vidare produktutveckling inom industrin.
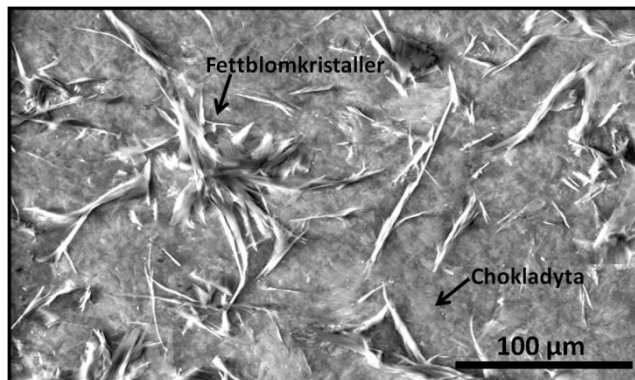
Figur 1. Elektronmikroskopibild som visar fettblomkristaller på ytan av en chokladpralin.

References

1.   Becket ST (2008) *The Science of Chocolate*. 2nd edition, RSC Publishing, 240 pp.
2.   Timms RE (2003) *Confectionery Fats Handbook: Properties, Production and Application*. The Oily Press, 441 pp.
3.   Rajah KK (ed) (2002) *Fats in Food Technology*. CRC Press, 379 pp.
4.   Larsson K (1994) *Lipids - Molecular Organization, Physical Functions and Technical Applications*. The Oily Press LTD, 290 pp.
5.   Minifie BW (1980) *Cocolate, Cocoa and Confectionery: Science and Technology*. 2nd edition, AVI Publishimg Company, INC, 735 pp.
6.   Lidefelt J-O (ed) (2007) *Vegetable oils and fats, Handbook AAK*. 2nd edition, AAK AB, 252 pp.
7.   Timms RE (1984) *Phase behaviour of fats and their mixtures*. Progress in Lipid Research 1, 1-38
8.   Foubert I, Vanrolleghem P, Thas O, Dewettinck K (2004) *Influence of chemical composition on the isothermal cocoa butter crystallization*. Journal of Food Science 69, 478-487
9.   Marty S, Marangoni AG (2009) *Effects of Cocoa Butter Origin, Tempering Procedure, and Structure on Oil Migration Kinetics*. Crystal Growth & Design 9, 4415-4423
10. Larsson K, Quinn P, Sato K, Tiberg F (2006) *Lipids: Structure, Physical Properties and Functionality*. The Oily Press, 267 pp.
11. Timms RE (2002) *Oil and Fat Interactions. Theory, Problems and Solutions*. The Manufacturing Confectioner 50-64
12. Larsson K (1966) *Classification of glyceride crystal forms*. Acta Chemica Scandinavica 20, 2255-2260
13. Wille R, Lutton E (1966) *Polymorphism of cocoa butter*. Journal of the American Oil Chemists Society 43, 491-496
14. van Malssen K, van Langevelde A, Peschar R, Schenk H (1999) *Phase behavior and extended phase scheme of static cocoa butter investigated with real-time X-ray powder diffraction*. Journal of the American Oil Chemists Society 76, 669-676
15. Chapman GM, Akehurst EE, Wright WB (1971) *Cocoa Butter and Confectionery Fats - Studies Using Programmed Temperature X-Ray Diffraction and Differential Scanning Calorimetry*. Journal of the American Oil Chemists Society 48, 824-830
16. Dewettinck K, Foubert I, Basiura M, Goderis B (2004) *Phase Behavior of Cocoa Butter in a Two-Step Isothermal Crystallization*. Crystal Growth and Design 4, 1295-1302

17. Dimick PS, Davis TR (1986) *Solidification of Cocoa Butter*. The Manufacturing Confectioner 123-128

18. Dimick PS, Manning DM (1987) *Thermal and Compositional Properties of Cocoa Butter During Static Crystallization*. Journal of the American Oil Chemists Society 64, 1663-1669

19. Fessas D, Signorelli M, Schiraldi A (2005) *Polymorphous transitions in cocoa butter - A quantitative DSC study*. Journal of Thermal Analysis and Calorimetry 82, 691-702

20. Loisel C, Keller G, Lecq G, Bourgaux C, Ollivon M (1998) *Phase transitions and polymorphism of cocoa butter*. Journal of the American Oil Chemists Society 75, 425-439

21. Lovegren NV, Gray MS, Feuge RO (1976) *Effect of Liquid Fat on Melting-Point and Polymorphic Behavior of Cocoa Butter and a Cocoa Butter Fraction*. Journal of the American Oil Chemists Society 53, 108-112

22. Vaeck S (1960) *Cacao butter and fat bloom*. The Manufacturing Confectioner 35-74

23. Gunstone FD, Harwood JL, Padley FB (1994) *The Lipid Handbook*. 2nd edition, Chapman & Hall, 551 pp.

24. Widlak N, Hartel R, Narine S (ed) (2001) *Crystallization and Solidification Properties of Lipids*. AOCS Press, 246 pp.

25. Hartel RW (2013) *Advances in Food Crystallization* in *Annual Review of Food Science and Technology, Vol 4*. M. Doyle and T. Klaenhammer (ed) 277-292

26. Marangoni AG, Narine SS (ed) (2002) *Physical Properties of Lipids*. Marcel Dekker, Inc., 589 pp.

27. Marangoni AG (2005) *Fat Crystal Networks*. Marcel Dekker, 854 pp.

28. Garti N, Sato K (ed) (2001) *Crystallization Processes in Fats and Lipid Systems*. Marcel Dekker, Inc., 533 pp.

29. Hachiya I, Koyano T, Sato K (1989) *Seeding Effects on Solidification Behavior of Cocoa Butter and Dark Chocolate 1.Kinetics of Solidification*. Journal of the American Oil Chemists Society 66, 1757-1762

30. Hachiya I, Koyano T, Sato K (1989) *Seeding Effects on Solidification Behavior of Cocoa Butter and Dark Chocolate 2.Physical-Properties of Dark Chocolate*. Journal of the American Oil Chemists Society 66, 1763-1770

31. Windhab EJ (1999) *New developments in crystallization processing*. Journal of Thermal Analysis and Calorimetry 57, 171-180

32. Zeng Y (2000) *Impf- und Scherkristallisation von Schokladen*. Doctoral thesis, ETH, Zürich.

33. Zeng Y, Braun P, Windhab EJ (2002) *Tempering: Continous precrystallization of chocolate with seed cocoa butter crystal suspension*. The Manufacturing Confectioner 71-80

34. Hartell RW (1999) *Chocolate: Fat bloom during storage*. The Manufacturing Confectioner 89-99

35. Kinta Y, Hatta T (2005) *Morphology of fat bloom in chocolate*. Journal of the American Oil Chemists Society 82, 685-685

36. Lonchampt P, Hartel RW (2004) *Fat bloom in chocolate and compound coatings*. European Journal of Lipid Science and Technology 106, 241-274

37. Bricknell J, Hartel RW (1998) *Relation of fat bloom in chocolate to polymorphic transition of cocoa butter.* Journal of the American Oil Chemists Society 75, 1609-1615

38. Hodge SM, Rousseau D (2002) *Fat bloom formation and characterization in milk chocolate observed by atomic force microscopy.* Journal of the American Oil Chemists Society 79, 1115-1121

39. Sonwai S, Rousseau D (2006) *Structure evolution and bloom formation in tempered cocoa butter during long-term storage.* European Journal of Lipid Science and Technology 108, 735-745

40. James BJ, Smith BG (2009) *Surface structure and composition of fresh and bloomed chocolate analysed using X-ray photoelectron spectroscopy, cryo-scanning electron microscopy and environmental scanning electron microscopy.* Food Science and Technology 42, 929-937

41. Kinta Y, Hatta T (2007) *Composition, structure, and color of fat bloom due to the partial liquefaction of fat in dark chocolate.* Journal of the American Oil Chemists Society 84, 107-115

42. Talbot G (1995) *Chocolate fatbloom - The cause and the cure.* International Food Ingredients 40-45

43. Smith KW, Cain FW, Talbot G (2007) *Effect of nut oil migration on polymorphic transformation in a model system.* Food Chemistry 102, 656-663

44. Ghosh V, Ziegler GR, Anantheswaran RC (2002) *Fat, Moisture, and Ethanol Migration through Chocolates and Confectionary Coatings* Critical Reviews in Food Science and Nutrition 42, 583 – 626

45. Galdamez JR, Szlachetka K, Duda JL, Ziegler GR (2009) *Oil migration in chocolate: A case of non-Fickian diffusion.* Journal of Food Engineering 92, 261-268

46. Ziegler GR, Shetty A, Anantheswaran RC (2004) *Nut Oil Migration Through Chocolate.* The Manufacturing Confectioner

47. Rousseau D, Smith P (2008) *Microstructure of fat bloom development in plain and filled chocolate confections.* Soft Matter 4, 1706-1712

48. Ali A, Selamat J, Man YBC, Suria AM (2001) *Effect of storage temperature on texture, polymorphic structure, bloom formation and sensory attributes of filled dark chocolate.* Food Chemistry 72, 491-497

49. Walter P, Cornillon P (2002) *Lipid migration in two-phase chocolate systems investigated by NMR and DSC.* Food Research International 35, 761-767

50. De Graef V, Foubert I, Agache E, Bernaert H, Landuyt A, Vanrolleghem PA, Dewettinck K (2005) *Prediction of migration fat bloom on chocolate.* European Journal of Lipid Science and Technology 107, 297-306

51. Rousseau D, Sonwai S, Khan R (2010) *Microscale Surface Roughening of Chocolate Viewed with Optical Profilometry.* Journal of the American Oil Chemists Society 87, 1127-1136

52. Svanberg L, Ahrne L, Loren N, Windhab E (2011) *Effect of sugar, cocoa particles and lecithin on cocoa butter crystallisation in seeded and non-seeded chocolate model systems.* Journal of Food Engineering 104, 70-80

53. Svanberg L, Ahrne L, Loren N, Windhab E (2011) *Effect of pre-crystallization process and solid particle addition on microstructure in chocolate model systems.* Food Research International 44, 1339-1350

54. Khan RS, Rousseau D (2006) *Hazelnut oil migration in dark chocolate - kinetic, thermodynamic and structural considerations.* European Journal of Lipid Science and Technology 108, 434-443

55. Rousseau D, Sonwai S (2008) *Influence of the dispersed particulate in chocolate on cocoa butter microstructure and fat crystal growth during storage.* Food Biophysics 3, 273-278

56. Sonwai S, Rousseau D (2008) *Fat crystal growth and microstructural evolution in industrial milk chocolate.* Crystal Growth & Design 8, 3165-3174

57. Smith PR, Dahlman A (2005) *The use of atomic force microscopy to measure the formation and development of chocolate bloom in pralines.* Journal of the American Oil Chemists Society 82, 165-168

58. Rousseau D (2006) *On the porous mesostructure of milk chocolate viewed with atomic force microscopy.* Food Science and Technology 39, 852-860

59. Sonwai S, Rousseau D (2010) *Controlling fat bloom formation in chocolate - Impact of milk fat on microstructure and fat phase crystallisation.* Food Chemistry 119, 286-297

60. Briones V (2006) *Scale-sensitive fractal analysis of the surface roughness of bloomed chocolate.* Journal of the American Oil Chemists Society 83, 193-199

61. Quevedo R, Brown C, Bouchon P, Aguilera JM (2005) *Surface roughness during storage of chocolate: Fractal analysis and possible mechanisms.* Journal of the American Oil Chemists Society 82, 457-462

62. Miquel ME, Carli S, Couzens PJ, Wille HJ, Hall LD (2001) *Kinetics of the migration of lipids in composite chocolate measured by magnetic resonance imaging.* Food Research International 34, 773-781

63. Maleky F, McCarthy KL, McCarthy MJ, Marangoni AG (2012) *Effect of Cocoa Butter Structure on Oil Migration.* Journal of Food Science 77, 74-79

64. Altan A, Lavenson DM, McCarthy MJ, McCarthy KL (2011) *Oil Migration in Chocolate and Almond Product Confectionery Systems.* Journal of Food Science 76, 489-494

65. Guiheneuf TM, Couzens PJ, Wille H-J, Hall LD (1997) *Visualisation of Liquid Triacylglycerol Migration in Chocolate by Magnetic Resonance Imaging.* Journal of the Science of Food and Agriculture 73, 265-273

66. Choi YJ, McCarthy KL, McCarthy MJ, Kim MH (2007) *Oil migration in chocolate.* Applied Magnetic Resonance 32, 205-220

67. McCarthy KL, McCarthy MJ (2008) *Oil migration in chocolate-peanut butter paste confectionery as a function of chocolate formulation.* Journal of Food Science 73, 266-273

68. Lee WL, J.Mccarthy M, L.Mccarthy K (2010) *Oil Migration in 2-Component Confectionery Systems.* Journal of Food Science 75, 83-87

69. Choi YJ, McCarthy KL, McCarthy MJ (2005) *Oil migration in a chocolate confectionery system evaluated by magnetic resonance imaging.* Journal of Food Science 70, 312-317

70. Miquel ME, Hall LD (2002) *Measurement by MRI of storage changes in commercial chocolate confectionery products.* Food Research International 35, 993-998

71. Deka K, MacMillan B, Ziegler GR, Marangoni AG, Newling B, Balcom BJ (2006) *Spatial mapping of solid and liquid lipid in confectionery products using a ID centric SPRITE MRI technique.* Food Research International 39, 365-371

72. Depypere F, De Clercq N, Segers M, Lewille B, Dewettinck K (2009) *Triacylglycerol migration and bloom in filled chocolates: Effects of low-temperature storage.* European Journal of Lipid Science and Technology 111, 280-289

73. Kaletunc G (ed) (2009) *Calorimetry in Food Processing: Analysis and Design of Food Systems.* Wiley-Blackwell and IFT Press, 392 pp.

74. Höhne G, Hemminger W, Flammersheim H-J (1996) *Differential Scanning Calorimetry: An Introduction for Practitioners.* Springer Verlag, 222 pp.

75. Goldstein JI, Newbury DE, Echlin P, Joy DC, Lyman CE, Lifshin E, Sawyer L, Michael JR (2003) *Scanning Electron Microscopy and X-Ray Microanalysis.* 3rd edition, Springer Science & Buissnes Media, Inc., 690 pp.

76. Stokes DJ (2003) *Low Vacuum Scanning Electron Microscopy: A rewiev of Progress & Applications.* Microscopy and Microanalysis 9, 972-973

77. ZygoCorporation (1998) *MetroPro reference guide.*

78. Thomas TR (1999) *Rough surfaces.* 2nd edition, Imperial College Press, 278 pp.

79. Dieing T, Hollricher O, Toporski J (ed) (2010) *Confocal Raman Microscopy.* Springer Verlag, 289 pp.

80. Larkin P (2011) *Infrared and Raman Spectroscopy: Principles and Spectral Interpretation.* Elsevier, 230 pp.

81. Schmitt M, Popp J (2006) *Raman spectroscopy at the beginning of the twenty-first century.* Journal of Raman Spectroscopy 37, 20-28

82. Tabaksblat R, Meier RJ, Kip BJ (1992) *Confocal Raman Microspectroscopy - Theory and Application to Thin Polymer Samples.* Applied Spectroscopy 46, 60-68

83. Zoukel A, Khouchaf L, Arnoult C, Di Martino J, Ruch D (2013) *A new approach to reach the best resolution of X-ray microanalysis in the variable pressure SEM.* Micron 46, 12-21

84. Larsson K (1962) *On the Structure of the Crystal form C of 11-Bromoundecanioc Acid.* Acta Chemica Scandinavica 16, 1751-1756

85. Larsson K (1963) *The Crystal Structure of the D-form of 11-Bromoundecanoic Acid.* Acta Chemica Scandinavica 17, 199-207

86. Larsson K (1963) *On the Structure of the Crystal form E of 11-Bromoundecanoic Acid.* Acta Chemica Scandinavica 17, 215-220

87. Larsson K (1963) *Polymorphism of 11-Bromoundecanoic Acid.* Acta Chemica Scandinavica 17, 221-226

88.   Maleky F, Marangoni A (2011) *Nanoscale effects on oil migration through triacylglycerol polycrystalline colloidal networks.* Soft Matter 7, 6012-6024

89.   Marangoni AG, McGauley SE (2003) *Relationship between crystallization behavior and structure in cocoa butter.* Crystal Growth & Design 3, 95-108

90.   Ziegleder G (1985) *Verbesserte Kristallisation von Kakaobutter Unter dem einfluss eines scherge falles* Int. Z. Lebensm. Tech. Verfahrenst 36, 412-418

91.   Dhonsi D, Stapley AGF (2006) *The effect of shear rate, temperature, sugar and emulsifier on the tempering of cocoa butter.* Journal of Food Engineering 77, 936-942

92.   Maleky F, Marangoni A (2011) *Thermal and Mechanical Properties of Cocoa Butter Crystallized under an External Laminar Shear Field.* Crystal Growth & Design 11, 2429-2437

93.   MacMillan SD, Roberts KJ, Rossi A, Wells MA, Polgreen MC, Smith IH (2002) *In Situ Small Angle X-ray Scattering (SAXS) Studies of Polymorphism with the Associated Crystallization of Cocoa Butter Fat Using Shearing Conditions.* Crystal Growth and Design 2, 221-226

94.   Maleky F, Marangoni AG (2008) *Process development for continuous crystallization of fat under laminar shear.* Journal of Food Engineering 89, 399-407

95.   Stapley AGF, Tewkesbury, Heather, Fryer, Peter J. (1999) *The effects of shear and temperature history on the crystallization of chocolate* Journal of the American Oil Chemists Society 76, 677-685

96.   Kinta Y, Hartel RW (2010) *Bloom Formation on Poorly-Tempered Chocolate and Effects of Seed Addition.* Journal of the American Oil Chemists Society 87, 19-27

97.   Motwani T, Hanselmann W, Anantheswaran RC (2011) *Diffusion, counter-diffusion and lipid phase changes occurring during oil migration in model confectionery systems.* Journal of Food Engineering 104, 186-195

98.   Svanberg L, Ahrne L, Loren N, Windhab E (2013) *Impact of pre-crystallization process on structure and product properties in dark chocolate.* Journal of Food Engineering 114, 90-98

99.   Lohman MH, Hartel RW (1994) *Effect of Milk-Fat Fractions on Fat Bloom in Dark Chocolate.* Journal of the American Oil Chemists Society 71, 267-276

100.   Liang B, Hartel RW (2004) *Effects of milk powders in milk chocolate.* Journal of Dairy Science 87, 20-31

101.   Garti N, Schlichter J, Sarig S (1986) *Effect of Food Emulsifiers on Polymorphic Transitions of Cocoa Butter.* Journal of the American Oil Chemists Society 63, 230-236

102.   Easton NR, Kelly DJ, Bartron LR, Cross ST, Griffin WC (1952) *The Use of Modifiers in Chocolate to Retard Fat Bloom.* Food Technology 6, 21-25

103.   Savage CM, Dimick, P.S. (1995) *Influence of phospholipids during crystallization of hard and soft cocoa butters.* The Manufacturing Confectioner 127-132

104. Johansson D, Bergenstahl B (1992) *The Influence of Food Emulsifiers on Fat And Sugar Dispersions in Oils 1.Adsorption, Sedimentation.* Journal of the American Oil Chemists Society 69, 705-717

105. Johansson D, Bergenstahl B (1992) *The Influence of Food Emulsifiers on Fat And Sugar Dispersions in Oils 2.Rheology, Colloidal Forces.* Journal of the American Oil Chemists Society 69, 718-727

106. Siew WL, Ng WL (1996) *Effect of diglycerides on the crystallisation of palm oleins.* Journal of the Science of Food and Agriculture 71, 496-500

107. Smith PR, Povey MJW (1997) *The effect of partial glycerides on trilaurin crystallization.* Journal of the American Oil Chemists Society 74, 169-171

108. Fernandes VA, Muller AJ, Sandoval AJ (2013) *Thermal, structural and rheological characteristics of dark chocolate with different compositions.* Journal of Food Engineering 116, 97-108

109. Bowser A (2006) *Crystallisation of Cocoa Butter.* The Manufacturing Confectioner 115-118

110. Altimiras P, Pyle L, Bouchon P (2007) *Structure-fat migration relationships during storage of cocoa butter model bars: Bloom development and possible mechanisms.* Journal of Food Engineering 80, 600-610

111. Johansson D (1994) *Colloids in Fats.* Doctoral thesis, Lund University, Lund. Department of Food Technology.

112. Ziegleder G, Moser, C., Geiger-Greguska, J. (1996) *Kinetics of fat migration in chocolate products part I: Principles and analythical aspects.* Fett/Lipid 98, 196-199

113. Ziegleder G, Moser, C., Geiger-Greguska, J. (1996) *Kinetics of fat migration in chocolate products part II: Influence of storage temperature, diffusion coefficient, solid fat content.* Fett/Lipid 98, 253-256

114. Ziegleder G, Schwingshandl I (1998) *Kinetics of fat migration within chocolate products. Part III: fat bloom.* Fett/Lipid 100, 411-415

115. Marty S, Baker K, Dibildox-Alvarado E, Rodrigues JN, Marangoni AG (2005) *Monitoring and quantifying of oil migration in cocoa butter using a flatbed scanner and fluorescence light microscopy.* Food Research International 38, 1189-1197

116. Aguilera JM, Michel M, Mayor G (2004) *Fat migration in chocolate: Diffusion or capillary flow in a particulate solid? A hypothesis paper.* Journal of Food Science 69, 167-174

117. Loisel C, Lecq G, Ponchel G, Keller G, Ollivon M (1997) *Fat bloom and chocolate structure studied by mercury porosimetry.* Journal of Food Science 62, 781-788

118. Crank J (1975) *The Mathemathics of Diffusion.* 2nd edition, Oxford University Press, 414 pp.

119. Walstra P (2003) *Physical Chemistry of Foods.* Marcel Dekker, Inc., 807 pp.

120. Krotov V, Rusanov A (1999) *Physicochemical hydrodynamics of capillary systems.* Imperial College Press, 492 pp.

121. Zhmud BV, Tiberg F, Hallstensson K (2000) *Dynamics of capillary rise.* Journal of Colloid and Interface Science 228, 263-269

122.   Briones V, Aguilera JM, Brown C (2006) *Effect of surface topography on color and gloss of chocolate samples.* Journal of Food Engineering 77, 776-783

123.   Svanberg L, Loren N, Ahrne L (2012) *Chocolate Swelling during Storage Caused by Fat or Moisture Migration.* Journal of Food Science 77, 328-334

ORIGINAL PAPER

Investigation of Chocolate Surfaces Using Profilometry and Low Vacuum Scanning Electron Microscopy

Hanna Dahlenborg · Anna Millqvist-Fureby ·
Björn Bergenståhl · Daniel J. E. Kalnin

Abstract In this study we establish the use of optical non-contact profilometry combined with low vacuum scanning electron microscopy (LV SEM) for the investigation of lipid surfaces. We illustrate, by using profilometry, a methodology for investigation of chocolate surface topology as a function of time, in the same area of interest. Both qualitative and quantitative data analysis has been performed for profilometry data. Further, relating these results to LV SEM images provides complementary topological information and hence a useful toolkit for the study of the chocolate surface prior and post fat bloom formation. For the demonstration of the successful combination of these two analytical techniques, white chocolate pralines were stored at two temperature-controlled conditions (at 18 °C, and cycled between 15 and 25 °C). Surface properties were then investigated during 36 weeks of storage. The surface images and the roughness parameters indicated distinct development of surface characteristics for the two storage conditions. From the results it is suggested that some imperfections, in the form of pores or protrusions, could play a role in fat bloom development and that there may be different main mechanisms of fat migration taking place for the different storage environments. In the present work, a positive correlation of profilometry data to chocolate surface characteristics and early bloom development has been established. There are indications that early prediction of fat bloom can be possible, however further work needs to be done to quantify prediction of fat bloom.

Introduction

Chocolate is a confection defined by its raw materials: sugar, cocoa mass, cocoa butter (CB), and milk solids in the case of milk or white chocolate. However, from a material science perspective, chocolate is a composite material consisting of solid particles (i.e. cocoa powder, sugar and in some cases milk powder) in a lipid continuous matrix, where the final quality of the product is highly dependent on the polymorphic forms of the triacylglycerols (TAG) in the fat phase and the distribution and size of the solid particles therein.

Chocolate is unique in that it is solid at room temperature and at the same time melts easily in the mouth. This property of chocolate is due to the lipid matrix, consisting mainly of CB, which has a relatively simple TAG composition that is responsible for a specific polymorphism (formation of different crystalline structures with the same composition) [1, 2]. CB TAG can crystallize into six different polymorphs which can be named as form I–VI [3] or as γ, α, β'_2, β'_1, β_2 and β_1 [4], with respect to increasing stability and increasing melting points from approximately 17–36 °C. However, more recent research by Van Malssen et al. [5] found only five polymorphic forms, where β' existed as a phase range rather than two distinct separate phases. Further recent studies have advanced the

H. Dahlenborg · A. Millqvist-Fureby · D. J. E. Kalnin (✉)
YKI, Institute for Surface Chemistry, Box 5607,
114 86 Stockholm, Sweden
e-mail: daniel.kalnin@yki.se

H. Dahlenborg · B. Bergenståhl
Department of Food Technology, Engineering and Nutrition,
Lund University, P.O. Box 124, 221 00 Lund, Sweden

understanding of the CB structure and its individual TAG [6–8]. Still, the former mentioned nomenclatures are often used in the field of chocolate research and chocolate industry. Form V is the desired form for TAG in chocolate, achieved when it is well tempered (controlled crystallization) during production, while form VI is a thermodynamically stable polymorph, normally associated with fat bloom.

Chocolate that has developed fat bloom is normally characterized by loss of its initial gloss and the greyish/whitish haze formed at the surface. This dulling appearance of fat bloom is generally explained by the scattering of light of the needle-like fat crystals that are formed at the chocolate surface [9]. However, fat bloom can also take various other forms, from surface to internal structures, depending on the product and the storage conditions [1, 10–13]. Fat bloom makes the chocolate appear unappetizing and is thereby a major issue that leads to rejection and to reduced shelf-life in chocolate, particularly in filled chocolate products such as pralines.

Fat bloom on center-filled chocolate products is mostly thought to consist of diluted or melted CB that migrates to the chocolate surface, where it re-crystallizes into the most stable polymorphic form, VI [14, 15]. Still, the mechanism of fat migration in chocolate pralines is not yet fully understood, and hence the detailed development of fat bloom remains unclear. However, the most cited mechanism by which CB migrates to the surface of filled chocolate has been fat diffusion, where a diffusion equation derived from Fick's second law normally is used to model the migration [16, 17]. The diffusive mobility in the mainly crystalline matrix can be expected to depend on the exchange rate at the liquid crystal interfaces as suggested by Löfborg et al. [18]. Lately, also capillary flow has been claimed to play a major role [19–21]. In a hypothesis paper by Aguilera et al. [21] it is proposed that within the chocolate matrix, formed by an assembly of fat-coated particles, the liquid fraction of CB (which increases with temperature) is likely to move under capillary flow through interparticle passages and connected pores.

The relationship between surface topology and fat migration has been investigated by some researchers, where atomic force microscopy, scanning electron microscopy and laser scanning microscopy have been used as the main techniques [13, 22–28]. Some of these studies have reported chocolate surfaces featuring imperfections in form of pores and protrusions, which could be related to fat migration and fat bloom formation. Smith and Dahlman [27] suggested that bloom growth in pralines is a two-step process, with drops initially forming at the surface and then bloom crystals nucleating and growing from them. In agreement with this study, Sonwai and Rousseau [28] found that cone-like structures at the surface of milk chocolate might have formed

by welling and deposition of liquid-state fat pushed from within the matrix onto the surface during contraction. These cones hardened with age, and crystal outcroppings protruded from the cones. In addition, the presence of a porous structure within chocolate has been shown by mercury porosimetry, and formation of fat bloom was related to these pores [29].

Optical profilometry, a white light interferometry technique, has been used in various fields in order to characterize surface topology of materials [30–32]. However, it is a technique not widely used in the field of food technology. Based on a certain set of statistical parameters, derived from a surface profile or a surface map, the surface topology can be quantified. Since these analyses can be performed using a non-contact mode, surface damage will be avoided. Although some research has been devoted to studying the development of surface topology on fresh and bloomed chocolate, rather less attention has been paid to studying the change of these topological features in a specific area over time.

The aim of this study is to follow the development and kinetics of surface topology in a specific area as a function of time and storage temperature. This will be realized by employing optical profilometry. Further, by combining this technique with low vacuum scanning electron microscopy (LV SEM), we can gain insight in the mechanisms taking place during migration of oil from the filling to the chocolate surface. Understanding the role of chocolate surface topology development over time can lead to deeper understanding of the mechanism of fat migration and thus, also an extended understanding of the early stages of fat bloom on chocolate. Different ways of detecting, preventing and controlling the growth of fat bloom can then be further envisaged.

Materials and Methods

Materials

White chocolate pralines with a hazelnut filling were manufactured by Ganache AB (Lilla Edet, Gothenburg, Sweden). The composition of the white chocolate and the hazelnut filling is listed in Table 1. The hazelnut mass consisted of caramelized and mixed hazelnuts, the milk chocolate had a cocoa level of 40% and contained whole milk powder, and the cream in the filling contained 40% fat. The white chocolate was tempered in a tempering unit (LCM 25 Twin), with temperatures set to 43.0 and 28.5 °C.

The selection of white chocolate for analysis was based on a parallel study where Confocal Raman Microscopy was used as the main technique. Because of interfering fluorescence when analyzing milk- and dark chocolate (probably due to the cocoa solids) white chocolate was the most

Table 1 Composition of white chocolate and hazelnut filling

	White chocolate	Hazelnut filling
Cocoa butter (%)	35	
Sugar (%)	43	
Whole milk powder (%)	21.5	
Emulsifier and vanilla (%)	0.5	
Hazelnut mass (%)		54
Cream (%)		27
Milk chocolate (%)		19
Total fat (%)	41.1	36.1
Sugar (%)	43	31.4
Water (%)	<1	15

suitable option. Still, the methods used in this study are applicable to the same extent for dark chocolate.

Storage Conditions

Five days after production, the samples were stored at two different temperature-controlled environments. The samples were stored in heating cabinets (temperature accuracy ±0.5 °C) where the temperature was kept at either 18 °C or cycled between 15 and 25 °C, with a temperature ramp of 0.1 °C/min and a residence time at each temperature of 12 h (±2 h). The actual temperature was additionally controlled by a k-type thermocouple using a Picco Tc-08 interface for continuous measurement. The samples were stored for 36 weeks in these temperature-controlled environments, with the exception that the cycled samples were transferred to 18 °C after the 12th week. This was due to the initial intention of ending the study after 12 weeks storage.

Profilometry

Instrumentation

The surface topology of the chocolate was analyzed using Profilometry Zygo New View 5010 (Middlefield, CT, USA), which is a non-contact profilometry method based on white light interferometry. Light from the microscope is divided within the interferometric objective: one portion is reflected from the sample surface and another portion reflects from an internal, high quality reference surface in the objective. Both portions are then directed into a CCD camera. Interference between the two light beams results in an image of light and dark bands, fringes, which characterize the surface structure of the sample observed. The surface is scanned by vertically moving the objective with a piezoelectric transducer. As the objective scans, a video system captures intensities at each camera pixel. These

intensities are converted into images by a software application. The results are displayed on a color display as images, plots, and numeric representations of the surface. Since profilometry uses reflective light, the degree of light absorption to the analyzed sample has no impact on the results. Therefore, this technique is also applicable to dark chocolate and other light absorbing surfaces.

Limitations for this technique are that the sample reflectivity must be high enough (better than 0.1%), the roughness (peak-to-valley) should be <100 μm and the local inclination of the topological features should not be too steep, in this case the inclination should be <15°. The *number of points* displays the number of valid data points in the data set, i.e. the number of camera pixels used in the analysis. Without data drop out the value will be 307×10^3 points. Thus, due to topological surface features with high inclinations (>15°), some profilometry data might not be interpretable and will then be illustrated with black color in the result images [33, 34].

In order to quantify the surface topology, there is access to several surface topological parameters, and in order to obtain reliable results it is essential to choose appropriate ones. *Peak number* (peaks per observation area) is the peak count or the number of peaks included in the analysis. A peak is defined as a data point whose height is above an operator-selected bandwidth. The band is centered around the mean plane of the data, where the upper edge of the band is the reference value for finding peaks. Thus, it is of importance that the choice of reference values is well considered. *Peak height* (μm) is the height for each peak included in the peak analysis and *peak area* (μm^2) is the area of each peak included in the peak analysis. The roughness parameter, R_q (μm) is the root-mean-square (rms) roughness and the waviness parameter, W_q (μm), is the root-mean-square (rms) waviness. Thus, they are defined as the average of the measured height deviations taken within the evaluation length or area and measured from the mean linear surface (Eq. 1). $Z(x)$ represents the height elements along the profile and L is the number of discrete elements.

$$\text{rms} = \sqrt{\frac{1}{L} \int_0^1 z^2(x) \, dx} \quad (\mu m) \tag{1}$$

Through a digital filtering (cutoff filter) of the data, the surface characteristics of the investigated surface can be broken down into waviness and roughness results. This filter includes a high filter wavelength which defines the noise threshold; all shorter spatial wavelengths are considered noise. It also includes a low filter wavelength which defines the form threshold where all longer spatial wavelengths are considered form (waviness). Everything

between these two wavelengths is assigned to roughness. Also in this case it is essential that the choice of reference values is well considered.

Experimental Setup, Sampling and Data Analysis

Each sample was fixed to a microscope slide, which was fitted into a 90° angle on a rectangular plate. This plate was mounted on the profilometry stage with screws and was thereby fixed in the same position on each occasion. The different analysis points had known x- and y-coordinates, and by means of these coordinates the different analysis points could be retrieved. In this study a 20× Mirau interference objective (Zygo) with a 1× zoom was used, which provide an image of 350 × 263 μm, with a theoretical lateral resolution of 0.88 μm. By using the lab-made mounting we were able to analyze the same area (±20 μm) on each analysis occasion. This enabled us to follow and compare surface changes in that specific area of interest. As a result, we were able to reduce noise, normally observed due to the use of different spots for data collection.

Sampling was performed when the samples were received, i.e. week 0, and then after storage of 2, 4, 12 and 36 weeks, respectively. Three samples from the cycled temperature conditions were monitored, and measurements were carried out at three different spots for each sample. Since the constant temperature was set as a reference temperature, one sample from this environment was analyzed. Also here measurements were carried out at three different spots. The analyses were performed on the top of the pralines, at room temperature (20 °C approximately). After each measurement the samples were put back into their temperature-controlled environment for continued storage.

The data was analyzed using the advanced texture application in MetroPro™ (Middlefield, CT, USA) analysis and control software. Roughness (R_q), waviness (W_q), peak number, peak height and peak area were investigated in this study. The reference band for peak definition was set at 2 μm. The cutoff filter, defining roughness and waviness, were set at 1.5 and 100 μm, respectively, which give a high filter frequency of 0.67 μm^{-1} and a low filter frequency of 0.01 μm^{-1}.

Low Vacuum Scanning Electron Microscopy

Scanning electron microscopy (SEM) is a technique producing high resolution images of a sample surfaces. Due to the way in which the image is created, SEM images have a characteristic three-dimensional appearance and are useful for judging the surface structure of a sample. A Philips XL30 environmental scanning electron microscope, equipped with a cold stage set to 5 °C was used with mixed detectors [biased gaseous detector (GSE) 75% and back-scattered electron detector (BSE) 25%], at 15 keV and in the low vacuum mode with 0.7–0.9 Torr, which gives an RH of 13% approximately. These parameters were chosen considering that they cause minimal damage of the chocolate surface, and for optimizing the imaging quality. In this study, analyses of the samples were performed without sample preparation, i.e. without coating the sample surface. This leads to a sacrifice in magnification and resolution; however, by analyzing without a coating, the true surface can be monitored.

Sampling was performed parallel to profilometry, meaning when the samples were received, i.e. week 0, and then after storage of 2, 4, 12 and 36 weeks, respectively. Two samples from each environment were monitored on each analysis occasion, and the analysis was performed on the top of the pralines, as for profilometry. After each analysis the monitored samples were sacrificed due to the possible impact from the microscope such as electron beam, temperature, humidity and pressure.

Results and Discussion

Macroscopic Observations

The samples stored at a cycled temperature developed a soft shell and a visually observed hardened filling, after 36 weeks of storage. These shells also expanded by 2 mm in diameter (7%) compared to the fresh samples and the samples stored at a constant temperature. At the same time, the volume of the filling decreased markedly and the bottom of the praline cracked and moved towards the center of the praline (Fig. 1). The temperature fluctuations in the cycled environment probably led to liquid TAG moving from the filling into the shell of the praline, giving an expansion of the shell and shrinkage of the filling. As a consequence of the change in composition we expect the shell to become softer and the filling to become harder. Further, the water activity in the filling was measured to a value of 0.77. Therefore, it could be suggested that diffusion of moisture from the filling into the shell led to swelling of milk particles, which simultaneously to the fat migration caused swelling of the shell and a decrease in filling volume [20, 35]. In addition, the glossiness of the cycled samples disappeared and its color turned to white compared to creamy white for the fresh samples, which could be described as visible bloom development. Further, the presence of moisture in the filling could lead to sugar bloom development in addition to fat bloom development.
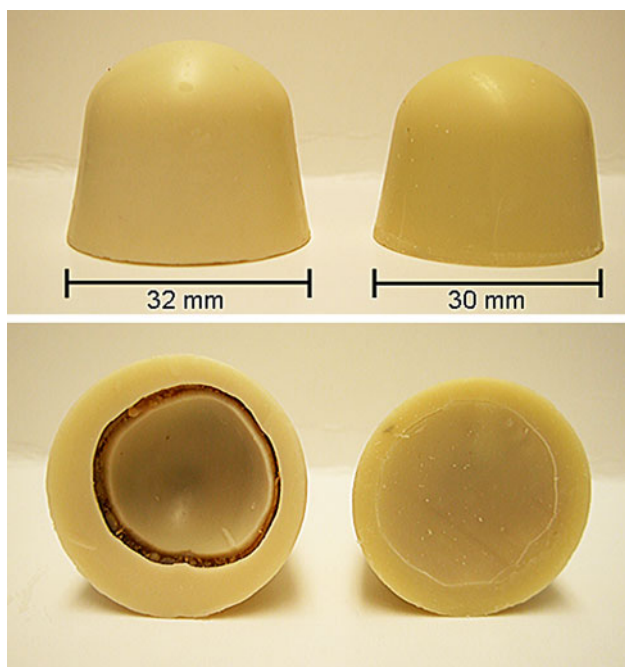
Fig. 1 White chocolate praline from the front and from underneath. *Left* sample stored at a cycled temperature, after 36 weeks. *Right* sample stored at a constant temperature, after 36 weeks

Microscopic Observations

Samples Stored at a Constant Temperature of 18 °C

The profilometry and LV SEM results in Fig. 2 demonstrates how the surface topology and the topological features change over time, i.e. from week 0 to week 36, when stored at a constant temperature. The surface images to the left represent 2D profilometry images (350 × 263 μm), and to the right LV SEM images are displayed in the same size range as the profilometry images. It should be noted that the profilometry images are produced from the same spot on the same samples, while all the LV SEM images represent different samples, and hence larger surface variability is to be expected from the latter method. However, the result images from both profilometry and LV SEM are representative.

Some profilometry data are not interpretable due to the method's detection limit, with regards to topological features with high inclinations (>15°). This is illustrated by a black color in the images. Table 2 shows the mean number of points per observation area at each analysis occasion, which displays values that give the information of data drop out. Further, the number of points for samples stored at a constant temperature at week 36 is too low ($113 \times 10^3 \pm 8.7$ points per observation area) to be able to use for interpretation of the data, this probably due to high inclinations of the topological features.
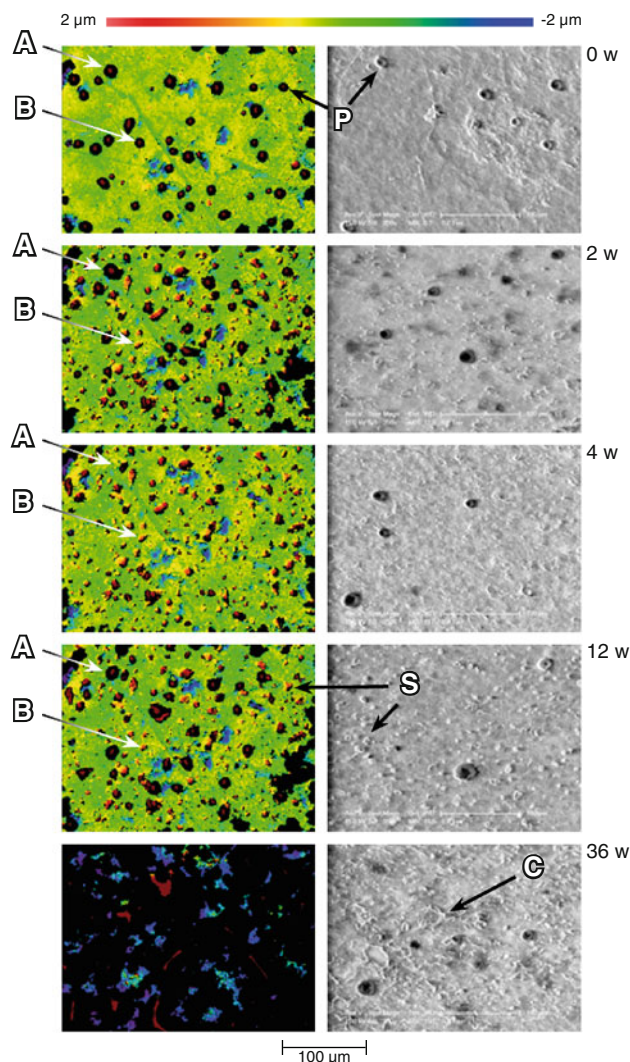

Fig. 2 Surface images of white chocolate pralines stored at a constant temperature (18 °C). *Left* 2D profilometry images (350 × 263 μm), produced from the same spot on the same sample, weeks 0, 2, 4, 12, 36. Some of the protrusions disappear and then re-appear (*A*), while some change their appearance over time (*B*). *Right* LV SEM images, from different samples, weeks 0, 2, 4, 12, 36, including protrusions (*P*), ridge-like topological features (*S*) and needle-shaped crystals (*C*)

As can be concluded from these images, the changes of the surface topology show similar appearance over time by using both profilometry and LV SEM. At week 0 both methods indicate a surface with a fine roughness, including protrusions (mountain-like topological features) with sharp inclinations heterogeneously spread over the surface, and with a size range of a few microns to around 20 μ in diameter. After 2 weeks of storage only few of these protrusions remain. Further, the images from both techniques illustrate additional ridge-like topological features with a wide size range, of different shapes and less sharp inclinations. After 4 weeks of storage, the surface is

Table 2 Number of points per observation area (350 × 263 μm) and standard error of mean for each profilometer analyze occasion of white chocolate pralines stored at 18 °C and at 15–25 °C, respectively (maximum number of points = 307 × 10^3)

Week	Cycled temperature (%)	Sem[a] cycled temperature (%)	Constant temperature (%)	Sem[a] constant temperature (%)
0	87	1.2	85	2.4
2	95	1.1	71	4.2
4	96	0.8	85	1.6
12	90	1.4	76	2.4
36	83	1.7	37	2.8

[a] Standard error of mean

homogeneously covered by these new ridge-like topological features, and after 12 weeks of storage both types of topological features mentioned are present. Further, the LV SEM images show a surface with more distinct topological features at week 12 compared to week 2 and 4. Since it is always the same area that is analyzed by the profilometer, it can be noted that some of the protrusions disappear and some reappear over time (point A and B in Fig. 2), at the same time as new topological features arise at the surface. After 36 weeks of storage, LV SEM images show that the surface is completely dominated by different topological features, some of them observed as needle-like shapes. The profilometry images show a large number of lost data, most likely due to a very rough surface.

In order to ensure that the surface topological features resembling protrusions actually are protrusions, sample surfaces were monitored by LV SEM from a tilted angle. These results, which are represented in Fig. 3, show that the surface displays protrusions of various sizes.

The result parameter peak height (μm), for samples stored at a constant temperature, is illustrated in Fig. 4. These results indicate that the low frequency of peaks present at week 0 is in the height range of 1–6 μm. Further, between week 0 and 2, the frequency of smaller peaks (<3 μm) has increased markedly in number, after which the number remains nearly constant. In addition, the frequency of larger peaks is higher by week 2 and 12. In Fig. 5 the parameter peak area (μm^2) is shown for samples stored at a constant temperature. At week 0 the results indicate that there is a small number of peaks, and that these peaks are spread over a wide size range. Between week 0 and 2, an increase in the number of peaks can be observed, and these peaks show an even wider size distribution. These results correlate with the profilometry images and the LV SEM images in Fig. 2, where new shapes of surface imperfections, with a wide size distribution appear by week 2 and stay until week 12. In addition to these topological features, larger mountain-like protrusions are present at week 2 and 12.
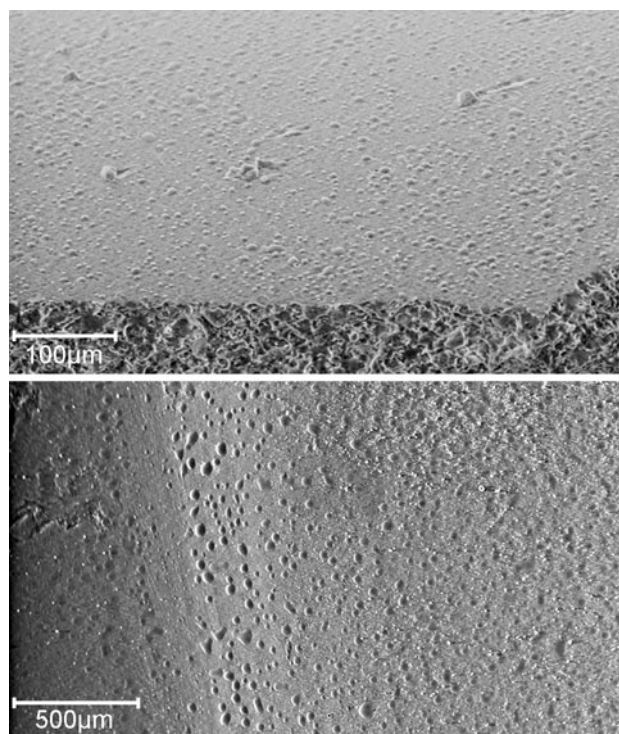
Fig. 3 LV SEM images of tilted chocolate samples

Fig. 4 Number of peaks per observation area (350 × 263 μm) as a function of peak height for samples stored at a constant temperature (18 °C). The number is calculated as a mean of $n = 3$. The standard error of mean is ±0.9

Samples Stored at a Cycled Temperature, 15–25 °C

Development of the topological surface features of samples stored at a cycled temperature (15–25 °C), investigated using profilometry and LV-SEM, is shown in Fig. 6. At week 0 the results show protrusions with sharp inclinations heterogeneously spread over the surface, and with a size
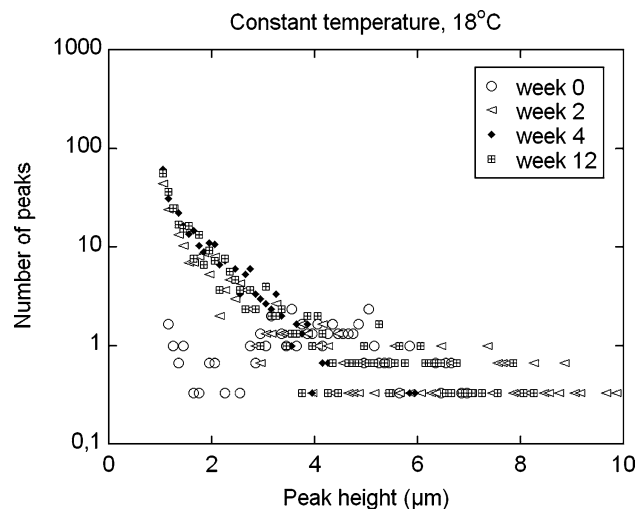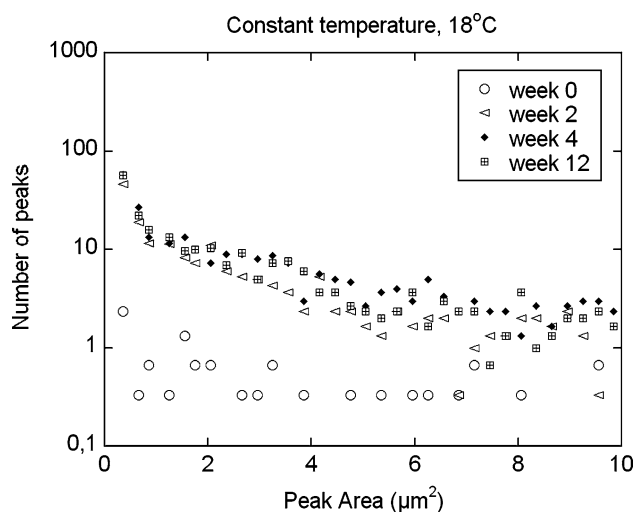
Fig. 5 Number of peaks per observation area (350 × 263 μm) as a function of peak area for samples stored at a constant temperature (18 °C). The number is calculated as a mean of $n = 3$. The standard error of mean is ±1.2

range of a few microns up to around 20 μ in diameter. After 2 weeks of storage the surface appears relatively smooth, and the protrusions from week 0 have generally disappeared. The surface remains almost similar after 4 weeks of storage, and after 12 weeks a homogeneously rough surface is observed that evolves to be even rougher after 36 weeks of storage (note that between week 12 and 36, the samples were stored at 18 °C), although with less height variation compared to the constant temperature samples. As indicated by point A in Fig. 6, some topological features disappear completely, while others remain throughout the storage period and become enhanced with time (point B in Fig. 6). The roughness is created by comparable smooth ridges, particularly visible in the LV SEM images, at week 12 and 36. A comparable morphology is not observable in the samples stored at a constant temperature.

Figure 7 shows the frequency as a function of peak height (μm) for samples stored at a cycled temperature. These results show that the larger peaks (2–6 μm) almost disappear from week 0 to week 2, reach a minimum week 2–4, and increase again between week 12 and 36 (2–4 μm). The sharp peaks between 4 and 6 μm do not return. Further, from week 4 to week 12 and 36 a sharp increase in frequency of smaller peaks (<2 μm) can be observed. The development of the frequency as a function of peak area (μm^2) is shown in Fig. 8. The results show that over time the sample surfaces develop many small peaks, in the size range of 1–2 μm^2, and with a dominant peak area of <1 μm^2. After 2 and 4 weeks a decrease in the frequency of larger peaks with an area between 2 and 8 μm^2 can be observed. At longer times, 12–36 weeks, an increase in all
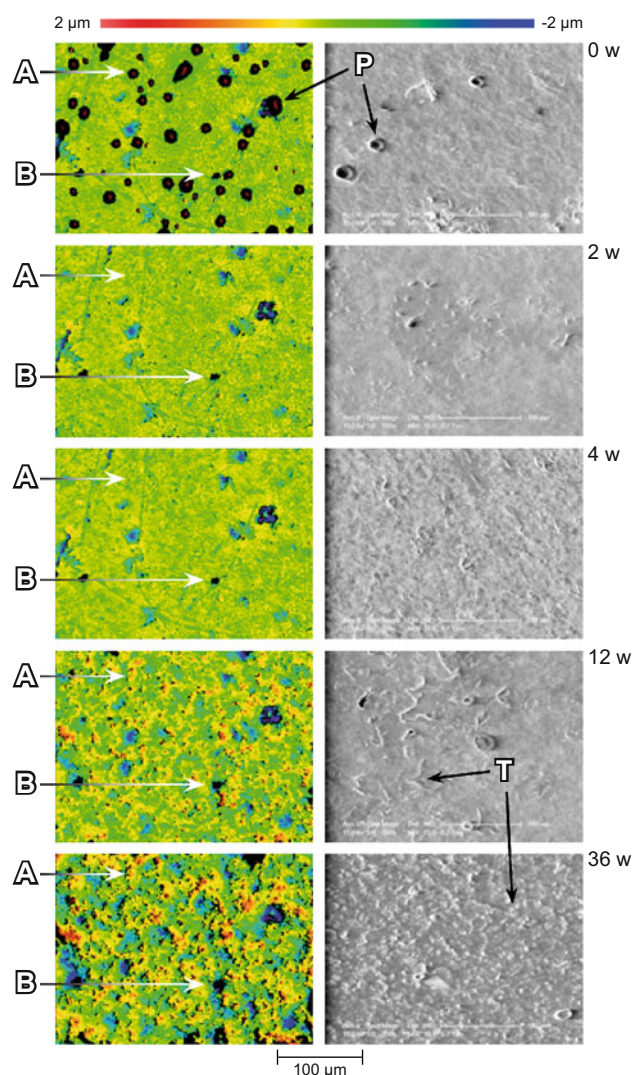
Fig. 6 Surface images of white chocolate pralines stored at a cycled temperature (15–25 °C). *Left* 2D profilometry images (350 × 263 μm), produced from the same spot on the same sample, week 0, 2, 4, 12, 36. Some surface topological features disappear completely over time (*A*), while some remain and become enhanced with time (*B*). *Right* LV SEM images, from different samples, week 0, 2, 4, 12, 36, including protrusions (*P*) and other topological features (*T*)

size ranges is observed. These results are consistent with the images in Fig. 6, which show a presence of relatively large protrusions at week 0, and then a development of topological features of various sizes from week 2 to 36.

Quantitative Analysis by Peak Number (Peaks per Observation Area)

The mean peak number per observation area (350 × 263 μm) as a function of time for samples stored at constant and at cycled temperature, respectively, is shown in Fig. 9. The results of the samples stored at 18 °C show a

Fig. 7 Number of peaks per observation area (350 × 263 μm) as a function of peak height for samples stored at a cycled temperature (15–25 °C). The number is calculated as a mean of $n = 9$. The standard error of mean is ±1.0
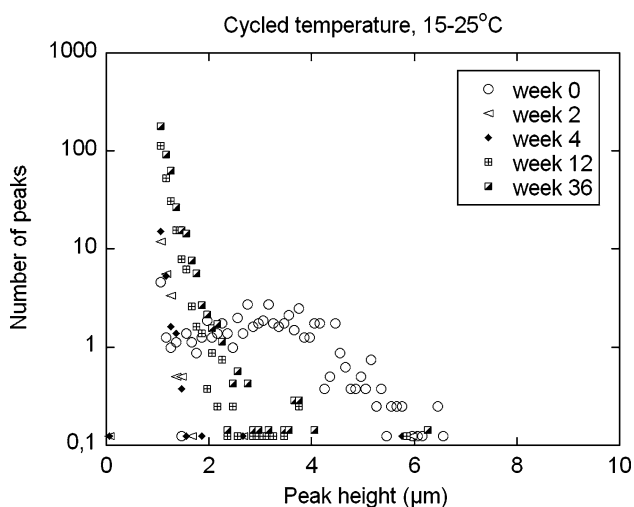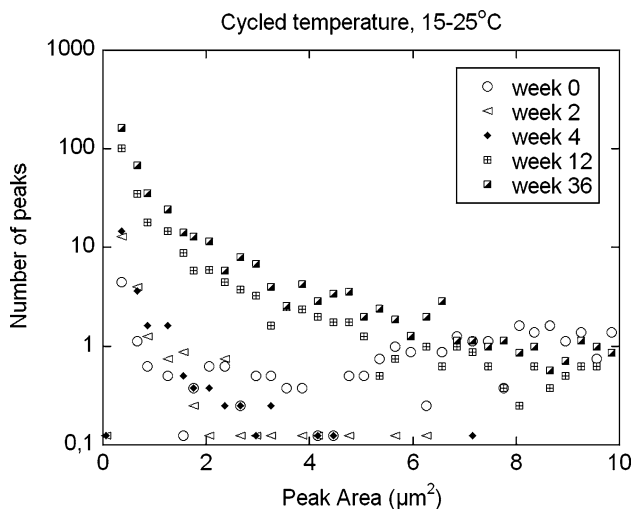

Fig. 8 Number of peaks per observation area (350 × 263 μm) as a function of peak area for samples stored at a cycled temperature (15–25 °C). The number is calculated as a mean of $n = 9$. The standard error of mean is ±0.9

sharp rise in peak number from week 0 to week 2 and 4 (From 49 to 290 peaks per observation area), which then remains steady until week 12. The sharp increase from week 0 to week 2 also agrees with the impression in Fig. 2, where new topological features have developed after 2 weeks. In contrast to the samples stored at a constant temperature, the peak number for the cycled samples decreases from week 0 to week 2 (from 62 to 25 peaks per observation area) and then remains stable until week 4. Further on, between week 4 and 12, a sharp increase in peak number can be observed (from 24 to 270 peaks per observation area), which continues until week 36 (420
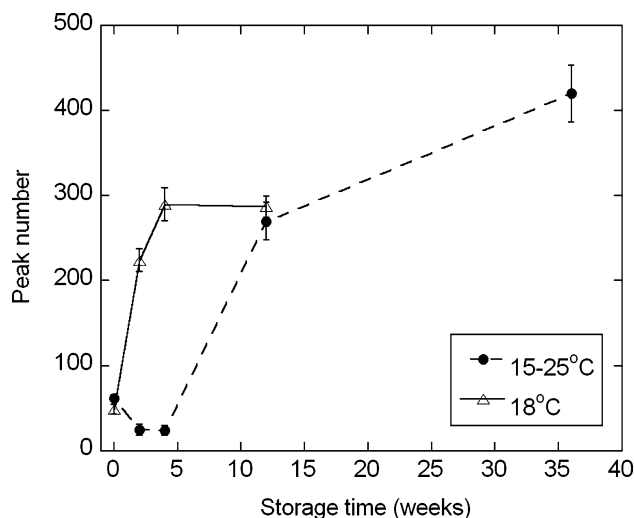

Fig. 9 Number of peaks (1–10 μm) per observation area (350 × 263 μm) as a function of time for samples stored at 18 °C (*open triangles*) and at 15–25 °C (*filled circles*), respectively. The *error bars* show the standard error of mean

peaks per observation area). Also these results can be correlated to the images in Fig. 6, where the surface appears relatively smooth at week 2 and 4, and then an increase in irregularities at the surface during week 12 and 36 can be observed. In addition, the peak number is within the same order of magnitude (approximately 50 peaks per observation area) at week 0 for all samples, which suggests that the samples possessed a similar surface appearance prior to storage at different temperature conditions.

Quantitative Analysis by Roughness, R_q (μm), and Waviness, W_q (μm)

The roughness, R_q, is presented as a function of time in Fig. 10. For the samples stored at a constant temperature, the roughness increases from week 0 to week 2 (from 0.5 to 0.8 μm) and then decreases to a value (0.5 μm) close to the starting value. After week 4 the roughness increases again (to a value of 0.7 μm). These roughness results can further be connected to the surface images in Fig. 2, where an increase in quantity of surface imperfections can be observed at week 2. Then, at week 4, the protrusions observed at week 0, disappear which would give a decrease in roughness. Some of these protrusions then reappear at week 12, where we also see an increase in roughness. On the other hand, R_q values for samples stored at a cycled temperature behave similar to the peak number, where we at first can observe a decrease in roughness, and then after week 4 an increase. This similar behavior is probably due to the fact that there are no protrusions observed after week 0. Thus, also R_q for the cycled samples can be connected to the images in Fig. 6. Further, the R_q values lie within the
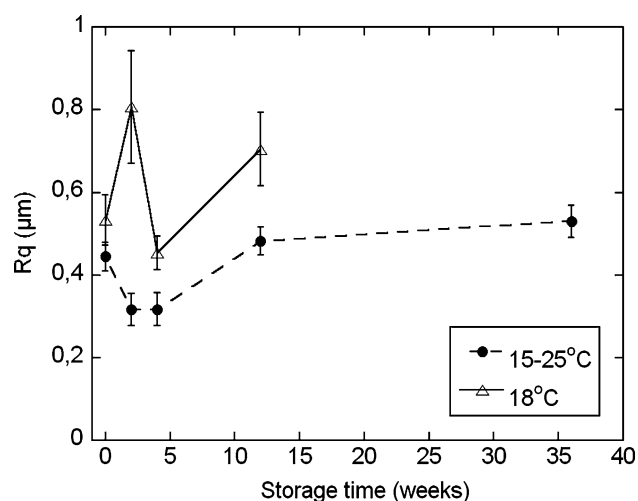
Fig. 10 R_q as a function of time for samples stored at 18 °C (*open triangles*) and at 15–25 °C (*filled circles*), respectively, including standard error of mean

Fig. 11 W_q as a function of time for samples stored at 18 °C (*open triangles*) and at 15–25 °C (*filled circles*), respectively, including standard error of mean

same order of magnitude (around 0.5 μm) at week 0 for all samples. Thus, the samples displayed a similar roughness prior to the distribution into different storage conditions.

Figure 11 presents the waviness, W_q, as a function of time for samples stored at a constant and a cycled temperature, respectively. Both results indicate an increase from week 0. Still, for the cycled samples the inclination is steeper between week 4 and 12 than for the samples stored at a constant temperature (ΔW_q cycled = 0.12 μm and ΔW_q constant = 0.03 μm). This can be connected to the profilometry images in Fig. 6, where there is a distinct difference between week 4 and 12 in means of large irregularities. In contrary, the overall waviness does not seem to vary to any great extent in the images in Fig. 2.

Discussion

The results presented in Fig. 2 show that the pralines stored at a constant temperature for 2 weeks display large protrusions (as evident in Fig. 3) that are gradually changing into ridge-like structures. The smooth nature of the protrusions suggests that these topological features consist of oil (i.e. are not crystallized), from the filling and the chocolate matrix, that has been transported to the surface of the chocolate. A convective flow of this type, spreading at the surface, is probably caused by a pressure gradient. In the case of samples stored at a constant temperature (18 °C), the chocolate contracts due to crystallization. As there is more liquid fat in the filling than in the shell, the shell contracts more than the filling. This would lead to a higher internal pressure that may press liquid fat to the surface. Further, we suggest that the bloom development is a two-step process (pores to oil-filled protrusions to
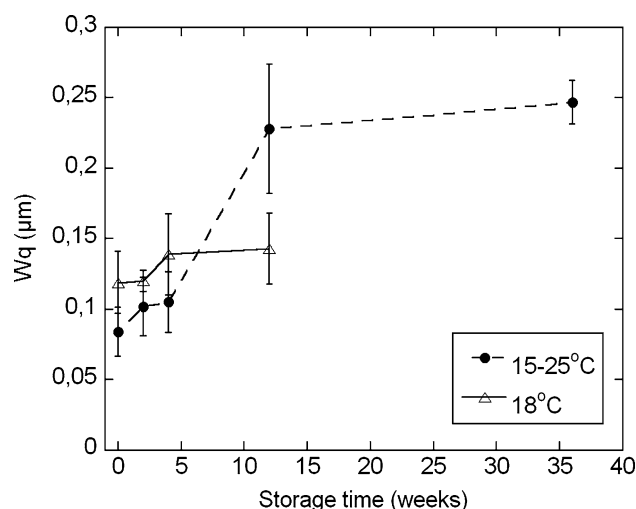
crystals), with the mentioned protrusions initially forming at the surface and then crystals nucleating and growing from them. Thus, the developed ridge-like features are most likely to be interpreted as an early sign of crystallization, and hence indicative for future bloom development. These suggestions are supported by the quantitative data, where the number of small peaks (Fig. 4) increases with time rapidly in the first 2 weeks and the number of larger peaks increases more gradually (Fig. 5). Further there is a wide size distribution of the peaks (Fig. 5). These observations and suggestions agree well with earlier studies observing conical protrusions acting as sites for crystal growth and chocolate bloom [27, 28].

The possibility of sugar bloom formation is also to be considered. However, since some of the ridge-like features seem to be connected to the original protrusions we suggest that these features consist of fat.

The results presented in Fig. 6 show that the pralines stored at a cycled temperature after 2 weeks become smoother, in contrast to the samples at the constant temperature. Very few structures are observed in the microscope although an increase in very small peaks is observed (Figs. 7, 8). After a longer time, more shallow waves are observed, an increased number of smaller peaks with a large area and increased waviness (Fig. 11). The filling shrinks and the shell expands according to the measured macroscopic shape. Thus, we may assume that we might have a flux of oil from the filling into the shell but to a lesser extent to the surface. The early observations of protrusions are most likely caused by a convective flow, due to a pressure gradient originating from the shrinking when the praline was formed. In this case of samples stored at a cycled temperature, the temperature fluctuations should lead to periodic changes in solid fat content (SFC).

Further, temperature gradients arise within the chocolate sample, a warmer surface when the temperature is increased and a warmer interior when the temperature is decreased. This would lead to an overpressure in the filling during cooling and an under pressure during heating. Thus, protrusions formed in the cooling cycle can be sucked into the structure in the heating cycle. Therefore, volume changes and pressure fluctuations would occur. Thus, it may be concluded that the main mechanism taking place in this case could be due to the fluctuation of the internal pressure (which is due to the change in SFC), where liquid fat is moving in two directions, i.e. pushed through the chocolate shell and up to the surface and also reabsorbed back into the chocolate shell [1, 11, 13]. However, as can be seen in Fig. 1, the bottom of the praline eventually cracked and moved towards the center of the praline. This is probably an effect of the pressure differential, and as the cracks appear the pressure differences should be equalized.

Some of the liquid fat that has been transported to the surface may spread out over the surface and give rise to a smoothening effect. Over time this liquid fat at the surface could allow movement of the solid components (solid fat crystals, sugar, milk solids, etc.) [12, 13], giving rise to the surface topology that can be observed at week 12 and 36 in Fig. 6. This can further be supported by the development of peak number and R_q, and also by the peak height and peak area results, which indicate an increase in amount of small peaks, but also larger, shallow peaks over time.

The developed waviness, which has increased markedly by week 12, may be interpreted as an effect of internal crystal changes in the chocolate shell. As the composition of the shell matrix changes, as a consequence of absorption of filling fat, it will be more susceptible to re-crystallization. Further support for this crystal growth within the matrix comes from the observations of the nature of the surface topology in the images after 12 and 36 weeks (Fig. 6).

The roughness and the number of peaks were consistently higher for the samples stored at a constant temperature than for the samples stored in a cycled environment, while the waviness developed higher values for the cycled samples. The LV SEM images from the samples stored at a constant temperature showed, among other topological structures, some needle-like crystals at the surface after 36 weeks of storage. This was not the case for the samples stored in a cycled environment, but instead other types of topological structures were observed. The lack of needle-like fat bloom crystals on the cycled samples could be due to the high temperature during cycling. Thus, the fat bloom crystal development could be connected to the higher values of roughness and peak number, while the swelling and reorganization of the chocolate matrix could be connected to the higher waviness values. Since the samples were white, the development of visual bloom was impossible to determine.

Still, after 36 weeks the cycled samples appeared whiter than the samples stored at a constant temperature. Thus, this color change would not be due to developed fat bloom crystals, but rather to other surface changes which are reflecting changes within the chocolate matrix.

Since the migrating oil wells out at the surface, it may be concluded that capillary flow is not the mechanism connected to the protrusions in these studies. In the case of capillary flow [19–21] the oil would stop at the surface level. Still, capillary flow could be an additional mechanism present, contributing to the absorption of oil into the shell.

Conclusion

This study demonstrates that the surface topology development over time can be conveniently followed in a specific area, by using profilometry, both quantitatively and qualitatively. Further, the combined information from profilometry and LV SEM can after validation provide an analytical toolkit for the early recognition of surface changes and hence early bloom development in the process of chocolate manufacture and storage. Further, distinct differences in surface topology development could be observed between samples stored in two different environments regarding macroscopic and microscopic information, and regarding qualitative and quantitative data, which all support each other. The statistical quantification of the images shows that the degree of surface roughness increases with time in terms of peak number, roughness, waviness, peak height and peak area for both storage environments, still with diverse magnitude and velocity. Since the surface development was followed in the same area of interest, the change of specific topological features over time could be monitored and thus, together with the statistical parameters, give more information to possible mechanisms of fat migration. The results suggest that some imperfections, in form of pores or protrusions, could play a role in the development of fat bloom, and that there may be different main mechanisms of fat migration taking place depending on the storage conditions. Regarding the samples stored at a constant temperature we suggest a convective flow as a main mechanism, where a two-step process could take place, with oil protrusions initially forming at the surface and then crystals nucleating and growing from them. In the case of storage at a cycled temperature there is a decrease in the filling volume, probably caused by a migration of liquid fat from the filling into the expanding shell. In addition our observations show an effect which can be interpreted as a convective flow through pores and cracks in two directions, i.e. up to the surface and back into the shell. The driving internal pressure fluctuations may be due to changes in the liquid to

solid ratio in the fat at the surface and internally when the temperature is cycled. Part of the liquid fat could be pressed out at the surface, spreading out, allowing movement of the solid components, while part of the liquid fat could be reabsorbed into the chocolate shell, where re-crystallization could occur.

Through this study a positive correlation of profilometry data to early chocolate bloom development has been established on white chocolate samples. Further work needs to be undertaken, and is in progress, for the early prediction of visible fat bloom and not only the monitoring of early fat bloom development.

References

1. Lonchampt P, Hartel RW (2004) Fat bloom in chocolate and compound coatings. Eur J Lipid Sci Technol 106:241–274
2. Padar S, Jeelani SAK, Windhab EJ (2008) Crystallization kinetics of cocoa fat systems: experiments and modeling. J Am Oil Chem Soc 85:1115–1126
3. Wille R, Lutton E (1966) Polymorphism of cocoa butter. J Am Oil Chem Soc 43:491–496
4. Larsson K (1966) Classification of glyceride crystal forms. Acta Chem Scand 20:2255–2260
5. van Malssen K, van Langevelde A, Peschar R, Schenk H (1999) Phase behavior and extended phase scheme of static cocoa butter investigated with real-time X-ray powder diffraction. J Am Oil Chem Soc 76:669–676
6. Schenk H, Peschar R (2004) Understanding the structure of chocolate. Radiat Phys chem 71:829–835
7. Yano J, Ueno S, Sato K, Arishima T, Sagi N, Kaneko F, Kobayashi M (1993) FT-IR study of polymorphic transformations in SOS, POP, and POP. J Phys Chem 97:12967–12973
8. van Mechelen Jan B, Goubitz K, Pop M, Peschar R, Schenk H (2008) Structures of mono-unsaturated triacylglycerols. V. The $\beta'1$–2, β'-3 and β2–3 polymorphs of 1, 3-dilauroyl-2-oleoylglycerol (LaOLa) from synchrotron and laboratory powder diffraction data. Acta Crystallogr Sect B Struct Sci 64:771–779
9. Lohman MH, Hartel RW (1994) Effect of milk fat fractions on fat bloom in dark chocolate. J Am Oil Chem Soc 71:267–276
10. Kinta Y, Hatta T (2007) Composition, structure, and color of fat bloom due to the partial liquefaction of fat in dark chocolate. J Am Oil Chem Soc 84:107–115
11. Hartell RW (1999) Chocolate: fat bloom during storage. Manuf Confect 79(5):89–99
12. James BJ, Smith BG (2009) Surface structure and composition of fresh and bloomed chocolate analysed using X-ray photoelectron spectroscopy, cryo-scanning electron microscopy and environmental scanning electron microscopy. LWT Food Sci Technol 42:929–937
13. Hodge SM, Rousseau D (2002) Fat bloom formation and characterization in milk chocolate observed by atomic force microscopy. J Am Oil Chem Soc 79:1115–1121
14. Smith KW, Cain FW, Talbot G (2007) Effect of nut oil migration on polymorphic transformation in a model system. Food Chem 102:656–663
15. Depypere F, De Clercq N, Segers M, Lewille B, Dewettinck K (2009) Triacylglycerol migration and bloom in filled chocolates: effects of low-temperature storage. Eur J Lipid Sci Technol 111:280–289
16. Miquel ME, Carli S, Couzens PJ, Wille HJ, Hall LD (2001) Kinetics of the migration of lipids in composite chocolate measured by magnetic resonance imaging. Food Res Int 34:773–781
17. Ghosh V, Ziegler GR, Anantheswaran RC (2002) Fat, moisture, and ethanol migration through chocolates and confectionary coatings. Crit Rev Food Sci Nutr 42:583–626
18. Löfborg N, Smith P, Furó I, Bergenståhl B (2003) Molecular exchange in thermal equilibrium between dissolved and crystalline tripalmitin by NMR. J Am Oil Chem Soc 80:1187–1192
19. Marty S, Baker K, Dibildox-Alvarado E, Rodrigues JN, Marangoni AG (2005) Monitoring and quantifying of oil migration in cocoa butter using a flatbed scanner and fluorescence light microscopy. Food Res Int 38:1189–1197
20. Choi YJ, McCarthy KL, McCarthy MJ, Kim MH (2007) Oil migration in chocolate. Appl Magn Reson 32:205–220
21. Aguilera JM, Michel M, Mayor G (2004) Fat migration in chocolate: diffusion or capillary flow in a particulate solid? A hypothesis paper. J Food Sci 69:R167–R174
22. Briones V (2006) Scale-sensitive fractal analysis of the surface roughness of bloomed chocolate. J Am Oil Chem Soc 83:193–199
23. Briones V, Aguilera JM, Brown C (2006) Effect of surface topography on color and gloss of chocolate samples. J Food Eng 77:776–783
24. Rousseau D (2006) On the porous mesostructure of milk chocolate viewed with atomic force microscopy. Food Sci Technol 39:852–860
25. Rousseau D, Smith P (2008) Microstructure of fat bloom development in plain and filled chocolate confections. Soft Matter 4:1706–1712
26. Rousseau D, Sonwai S (2008) Influence of the dispersed particulate in chocolate on cocoa butter microstructure and fat crystal growth during storage. Food Biophys 3:273–278
27. Smith PR, Dahlman A (2005) The use of atomic force microscopy to measure the formation and development of chocolate bloom in pralines. J Am Oil Chem Soc 82:165–168
28. Sonwai S, Rousseau D (2008) Fat crystal growth and microstructural evolution in industrial milk chocolate. Cryst Growth Des 8:3165–3174
29. Loisel C, Lecq G, Ponchel G, Keller G, Ollivon M (1997) Fat bloom and chocolate structure studied by mercury porosimetry. J Food Sci 62:781–788
30. Grove GL, Grove MJ, Leyden JJ (1989) Optical profilometry: an objective method for quantification of facial wrinkles. J Am Acad Dermatol 21:631–637
31. Cross SE, Kreth J, Wali RP, Sullivan R, Shi W, Gimzewski JK (2009) Evaluation of bacteria-induced enamel demineralization using optical profilometry. Dent Mater 25:1517–1526
32. Visscher M, Hendriks CP, Struik KG (1994) Optical profilometry and its application to mechanically inaccessible surfaces. Part II. Application to elastomer/glass contacts. Precis Eng 16:199–204
33. Thomas TR (1999) Rough surfaces, 2nd edn. Imperial College Press, London
34. ZygoCorporation (1998) MetroPro reference guide, Middlefield, Connecticut
35. Ghosh V, Ziegler GR, Anantheswaran RC (2005) Moisture migration through chocolate-flavored confectionery coatings. J Food Eng 66:177–186

II

Research Article

Study of the porous structure of white chocolate by confocal Raman microscopy[†]

Hanna Dahlenborg[1,2]**, Anna Millqvist-Fureby**[1]**, Birgit D. Brandner**[1] **and Bjorn Bergenstahl**[2]

[1] YKI, Institute for Surface Chemistry, Stockholm, Sweden
[2] Department of Food Technology, Engineering and Nutrition, Lund University, Lund, Sweden

Confocal Raman microscopy has been shown to be a useful technique for investigation of white chocolate surfaces. The appearance of protrusions and pores, and the distribution of fat, sucrose, and milk powder at and below the surface of white chocolate pralines were investigated using confocal Raman microscopy. Raman horizontal and depth scans showed that the protrusions and pores continue at least 10 μm into the chocolate shell and that some protrusions and channels mainly consist of fat, while some consisted of a fat layer, leaving a hollow space underneath. Further, the pores and their continuing channels consisted of nothing but air. These findings indicate that the protrusions might be connected to channels where we suggest a pressure driven convective flow of liquid fat from within the chocolate matrix that, depending on temperature, moves up to the surface or goes back into the matrix, leaving an empty pore with a shell of fat at the surface, which in some cases collapse and leaves a hollow pore and channel. Therefore, these findings support that the protrusions could be connected to oil migration in chocolate and, thus, further to fat bloom development.

Practical applications: Confocal Raman microscopy can be used to investigate the local distribution of different components in white chocolate. This technique offers the possibility to acquire the local distribution of different components within the sample, with a resolution down to the optical diffraction limit. Further, the analysis can be performed at ambient conditions, without requiring any special sample preparation or marker molecules. The results obtained by using this technique suggest that specific surface imperfections on chocolate could be part of a network of pore structures at and beneath the chocolate surface, which could be related to oil migration and thus, to fat bloom formation.

1 Introduction

Fat migration in chocolate products, often leading to fat bloom development, is a major issue for the confectionery industry, since it negatively affects both the visual and textural quality of the products. Chocolate that has developed fat bloom is normally characterized by loss of its initial gloss and a whitish haze at the surface. This dulling appearance is generally explained by the scattering of light due to needle-like fat crystals, larger than 5 μm, that are formed at the chocolate surface [1–2]. Previous research has demonstrated that in the presence of these needle-like fat crystals, the cocoa butter TAG can be found in their most stable polymorph, i.e., form β_1VI [3–5]. Thus, fat bloom on chocolate is often related to this polymorphic form. Still, the development of fat bloom formation is not clearly understood and fat bloom can take various forms, from surface to internal structures, depending on the product and the storage conditions [2, 5–9]. Further, it has been shown that the polymorphic transition of form β_2V (the desired polymorph in chocolate) to form β_1VI may even occur without visual fat bloom development [3].

Fat bloom formation on chocolate products can be related to mainly three factors, i.e., poor tempering (polymorph and crystallization control) during production, storage at high temperatures (>23°C) and/or fluctuating temperature,

Correspondence: Hanna Dahlenborg, YKI, Institute for Surface Chemistry, Box 5607, SE-114 86 Stockholm, Sweden
E-mail: hanna.dahlenborg@yki.se
Fax: +46-8-20-89-98

Abbreviations: CB, cocoa butter; **CLSM,** confocal scanning laser microscopy; **LV SEM,** low vacuum scanning electron microscopy

[†]The online version of this article contains colour figures.

leading to melting and re-crystallization of cocoa butter (CB), and migration of filling oil into the surrounding chocolate shell in the case of center-filled chocolate products, which promotes crystal growth. The most cited mechanism by which TAG migrates to the surface of filled chocolate has been fat diffusion, where a diffusion equation derived from Fick's second law normally is used to model the migration [10–11]. The diffusive mobility in the mainly crystalline matrix can be expected to depend on the exchange rate at the liquid crystal interfaces as suggested by Lofborg et al. [12]. Lately, also capillary flow has been claimed to play a major role [13–15]. In a hypothesis paper by Aguilera et al. it is proposed that within the chocolate matrix, formed by an assembly of fat-coated particles, the liquid fraction of CB (which increases with temperature) is likely to move under capillary flow through interparticle passages and connected pores [13]. However, the mechanism of fat migration in chocolate pralines is until today not fully understood, and hence the detailed development of fat bloom remains unclear. Some recent studies have focused on the relationship between surface topology and fat migration, where atomic force microscopy, laser scanning microscopy, scanning electron microscopy, and optical profilometry have been used as main techniques [5–6, 16–23]. Some of these studies have reported chocolate surfaces featuring imperfections in form of pores and protrusions, and authors have suggested that these topological features could be related to fat migration and fat bloom development [6, 21–22]. In a study related to this present work, Dahlenborg et al. [6] suggest that there is a pressure driven convective flow leading to oil transportation through the chocolate matrix and to the chocolate surface, and that the oil migrates to the surface or goes back into the chocolate matrix depending on the temperature changes. Further, Loisel et al. have shown the presence of a porous matrix, that was partly filled with liquid CB fractions, in dark chocolate by using mercury porosimetry [24]. In this study it was suggested that the porous matrix is a network of cavities closed by multiple walls of fat crystals impregnated with liquid fat. Due to the difference in dilation coefficients between solid and liquid fat and further due to polymorphic evolution, the liquid phase leaves spaces and air fills pores close to the surface or makes empty cavities. During temperature variations the difference in dilation of air and liquid fat could push the liquid fat fraction to the surface and thus contribute to fat bloom formation.

Thus, it is of great relevance to investigate if there could be a connection between this porous matrix and the observed imperfections at chocolate surfaces, and hence, how the different components are distributed at and below the surface of a chocolate product. This can be investigated by using confocal Raman microscopy. This technique has evolved into a fast, direct and non-destructive method applicable in food research [25–31]. Confocal Raman microscopy offers the possibility to scan a sample to acquire a Raman spectrum providing chemical information, with a resolution down to the optical diffraction limit, i.e., the resolution limited by the wavelength of the used light. Further, the analysis can be performed at ambient conditions, without requiring any special sample preparation like addition of tracers or dyes, since the endogenic Raman scattering of the chocolate components is employed. Confocal Raman microscopy combines two different techniques, namely confocal microscopy and Raman spectrometry. In confocal microscopy a small pinhole, located in conjunction to the focus of the objective, allows only the light coming from the focal plane to pass into the detector. This focal plane can be moved several micrometers into the sample, which gives the opportunity of gaining 3D information. The possible depth of analysis depends on the properties of the material, in particular light absorption. Further, the Raman spectra allows us to differ between components as the energy of the Raman scattered light is the energy of the incoming light subtracted by the excitation energy, and as the excitation energies depends on the vibration properties of the molecular structures. Performing Raman microscopy, a Raman spectrum is recorded on every image pixel. Thus, when analyzing dedicated peaks of the spectra, a variety of images can be generated using only a single set of data. Post-processing of data enables identification of different components in the sample.

The objective of this study is to evaluate whether the former reported topological imperfections, observed as pores and protrusions at chocolate surfaces, are a part of a network of pore structures beneath and at the chocolate surface. This is done by using confocal Raman microscopy. In addition, low vacuum scanning electron microscopy (LV SEM) is used to identify the presence of topological imperfections. These results can lead to deeper understanding of the chocolate structure and thus, also extend the understanding of migration and thereby fat bloom development.

2 Materials and methods

2.1 Materials

White chocolate pralines with a hazelnut filling were manufactured by Ganache AB (Lilla Edet, Gothenburg, Sweden). The composition of the white chocolate and the hazelnut filling is listed in Table 1. The hazelnut mass consisted of caramelized and mixed hazelnuts, the milk chocolate had a cocoa level of 40% and contained whole milk powder, and the cream in the filling contained 40% fat. The white chocolate was tempered in a tempering unit (LCM 25 Twin), with melting temperature set to 43.0°C and tempering temperature set to 28.5°C. Since considerable fluorescence occurs when analyzing milk- and dark chocolate with confocal Raman microscopy (probably due to cocoa solids), white chocolate was used in this study.

Raman reference spectra were recorded for CB, sucrose, whole milk powder and skim milk powder. The CB (ADM Cocoa BV, The Netherlands) was supplied by Buhler AG

Table 1. Composition of white chocolate and hazelnut filling (wt%)

Components	White chocolate (wt%)	Hazelnut filling (wt%)
Cocoa butter	35	
Sugar	43	
Whole milk powder	21.5	
Emulsifier and vanilla	0.5	
Hazelnut mass		54
Cream		27
Milk chocolate		19
Total fat	41.1	36.1
Sugar	43	31.4
Water	<1	15

(Uzwil, Switzerland), the sucrose was supplied by AAK (Aarhus, Denmark), the whole milk powder was supplied by Arla Foods Ingredients (Viby, Denmark), and the skim milk powder was supplied by Semper AB (Sundbyberg, Sweden). The composition of the whole and skim milk powder is presented in Table 2.

2.2 Low vacuum scanning electron microscopy

Scanning electron microscopy (SEM) is a technique producing high resolution images of a sample surface. Due to the way in which the image is created, SEM images have a characteristic three-dimensional appearance and are useful for judging the surface structure of a sample. Philips XL30 environmental scanning electron microscope, equipped with a cold stage set to 5°C was used with mixed detectors (biased gaseous detector (GSE) 75% and backscattered electron detector (BSE) 25%), at 15 keV and at low vacuum mode with 0.7–0.9 Torr, which gives an RH of 13% approximately. These parameters were chosen considering that they cause minimal damage of the chocolate surface, and for optimizing the image quality. In this study, analyses of the samples were performed without sample preparation, i.e., without coating the sample surface with a conducting layer. This leads to a sacrifice in magnification and resolution; however, by analyzing without coating the true surface can be monitored. After each analysis the monitored samples were sacrificed due to the potential impact from the microscope such as electron beam, temperature, humidity, and pressure.

Table 2. Composition of whole milk powder and skim milk powder (wt%)

Components	Whole milk powder (wt%)	Skim milk powder (wt%)
Milk protein	24–34	36
Lactose	38–42	51
Milk fat	26	1

2.3 Confocal Raman microscopy

The measurements were performed with a WITec alpha300 system (Ulm, Germany) which has a lateral resolution of 300 nm and a vertical resolution of 500 nm, using a 532 nm laser for excitation. The objective was a 50× Nikon objective (NA = 0.75), and the integration time per Raman spectrum was 0.1 s, which gives a sufficient signal-to-noise ratio at the same time as it does not destroy the samples. Further, the microscope was equipped with a Linkam cold stage set to 3°C, preventing the samples from melting under the influence of the laser. Reference spectra were obtained for cocoa butter, sucrose, whole milk powder, and skim milk powder. The scan range for horizontal images was 60 μm × 60 μm with 140 × 140 pixels in *xy*-direction (nominal resolution 430 nm). For the depth images the scan range varied between 60 μm × 20 μm and 60 μm × 40 μm, with 45 × 140 to 90 × 140 pixels in *xz*-direction. The penetration depth, i.e., the focal plane, in the *xy*-scans varied between approximately 6 and 12 μm, depending on the signal strength. A total of 15 horizontal scans and 10 correlating depth scans were performed in this study, which generated representative result images. The data was evaluated using the software program WITec project 2.06 (Ulm, Germany).

3 Results and discussion

White chocolate pralines containing a hazelnut filling were manufactured with composition and tempering processing securing properties characteristic for high quality chocolate. The surface morphology was characterized using LV SEM 1 week after manufacturing. Result images from LV SEM are displayed in Fig. 1, where the figures show a surface that is partly covered by circular protrusions (P1) and pores (P2). The outer diameter of the protrusions was calculated to a mean of 20 μm, with SD 1.5 μm, and the pore diameter was calculated to a mean of 9.7 μm, with SD 1.2 μm. These dimensions are comparable to the ranges reported in earlier studies [6, 19, 21]. The sample surfaces were also monitored by LV SEM from a tilted angle in order to validate that the surface topological features resembling protrusions actually are protrusions. The results of the tilted samples support the interpretation that the surface displays protrusions of various sizes. Similar conclusions have also been reported earlier [6].

Confocal Raman microscopy was applied on the filled white chocolate samples with the objective of correlating the inner chocolate structure with the appearance of the protrusions. Reference spectra have been used to identify different components in the surface layer of the samples. When generating horizontal and depth scans a Raman spectrum is recorded in every image pixel and these spectra are compared to the reference spectra in order to acquire the local distribution of the components. The measured spectra were fitted
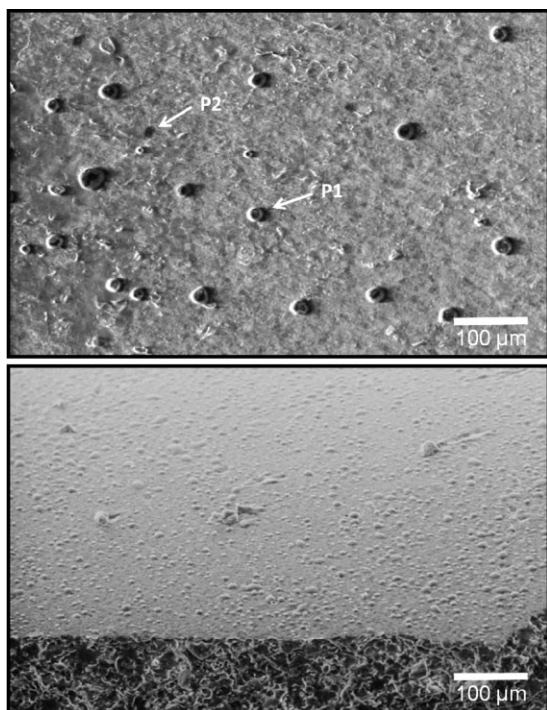
Figure 1. LV SEM images of white chocolate surface, enclosing a hazelnut filling, and a tilted chocolate sample (below), displaying imperfections observed as protrusions (P1) and pores (P2).

with a linear combination of the reference spectra. Essentially a least squares fit is made over the whole spectra, i.e., single peaks are not investigated, and images for the different components are overlaid. Thus, an area can consist of several components at the same time even though only one component is shown. Raman reference spectra of cocoa butter (CB), sucrose, whole milk powder, and skim milk powder have been recorded in order to identify the distribution of the components in the surface layer of the samples (Fig. 2). Further, Raman reference spectra of lactose and whey protein
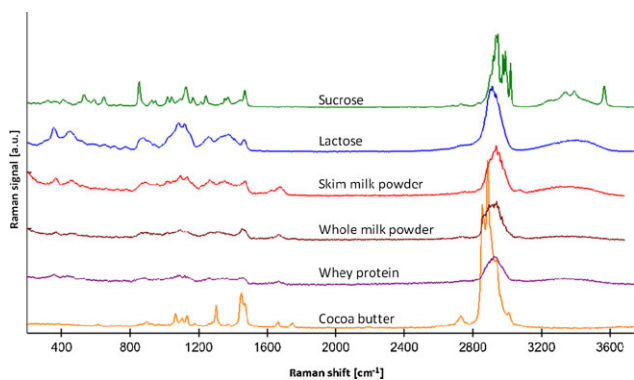

Figure 2. Recorded reference spectra of sucrose, amorphous lactose, skim milk powder, whole milk powder, whey protein, and cocoa butter.

were compared to the recorded reference spectra (Fig. 2). Assignments of the characteristic wave numbers to molecular groups are presented in Table 3. These assignments were achieved using the Refs. [30, 32–36]. The sucrose spectrum is characteristic with several distinguished peaks due to its crystallinity. A similar feature is visible in the CB spectrum. In the sucrose spectrum the main Raman signals are between 400 and 1550 cm^{-1}. Further, there is a strong hydrocarbon signal with several peaks between 2850 and 3050 cm^{-1} (v(CH)) and a broad hydroxyl band (v(OH)) between approximately 3200 and 3600 cm^{-1}, with a sharp peak at 3550 cm^{-1}. Lactose, as being chemically quite similar, although amorphous, has a similar pattern but with smoother regions of higher peaks. For instance the sharp peaks between 400 and 1550 cm^{-1} are all wider, the peak between 2830 and 3030 cm^{-1} is not split and the sharp peak at 3550 cm^{-1} is missing. Pure protein (whey protein) has a signal pattern that is fairly similar to the saccharides, however with a lower intensity and with a characteristic peak around 1670 cm^{-1} (the amide I signal (v(C=O)). Further, the broad peak between approximately 3150 and 3600 cm^{-1} includes amide functionalities (v(NH)). CB has less peaks below 1000 cm^{-1} and some more intense peaks between 1000 and 1500 cm^{-1} as well as a distinct peak at 1664 cm^{-1} (v(C=C)) and between 2800 and 3060 cm^{-1} (v(CH)). The compounded materials display features of several principal components. Skim milk powder mainly consists of milk proteins (36%) lactose (51%) and a lower amount of fat (in this case 1%). The skim milk powder spectrum displays the distinguished protein feature at 1678 cm^{-1} and the characteristic lactose features at around 400 and 850 cm^{-1}. The whole milk powder spectrum consists of milk proteins (24%), lactose (38%), and fat (26%), providing similar protein and lactose features and a characteristic intensity at 1755 cm^{-1} that was also observed for CB.

It is clear that the differences observed are vague compared to the chemical differences. Hence, the chemical resolution of the methodology is somewhat limited. However, it is also clear that there are possibilities to separate the principal components (milk powder, sucrose, and fat) from each other. Thus, the reference spectra of sucrose, CB, and skim milk powder were used to analyze the chocolate system. The skim milk powder was preferred over the whole milk powder as the butter fat contribution cannot be distinguished from the CB contribution.

Figure 3 represents light microscope images of the sample surfaces, i.e., white chocolate pralines containing a hazelnut filling. The images illustrate surfaces with fine roughness, including protrusions (Fig. 3A and B) and pores (Fig. 3C and D). The overlaid squares display the areas in which horizontal Raman images have been recorded, and the dashed lines indicate where the depth scans have been recorded. Thus, the images in Fig. 3 are connected to the representative Raman horizontal scans and depth scans in Figs. 4–5. The areas in the result scans in Figs. 4, 5 represent

Table 3. Observed approximate frequencies (cm^{-1}) and assignments for Raman spectra of sucrose, amorphous lactose, skim milk powder, whole milk powder, whey protein, and cocoa butter

Sucrose wavenumber (cm^{-1})	Lactose wavenumber (cm^{-1})	Skim milk powder wavenumber (cm^{-1})	Whole milk powder wavenumber (cm^{-1})	Whey protein wavenumber (cm^{-1})	Cocoa butter wavenumber (cm^{-1})	Assignment	Ref.
3200–3600	3150–3600					ν(OH)	[33, 35]
		3150–3600	3150–3600	3150–3600		ν(NH)	[35]
2850–3050	2830–3030	2800–3050	2830–3030	2830–3030	2800–3060	ν(CH)	[30, 32–34]
			1755		1750	ν(C=O)	[30, 32, 34–35]
					1664	ν(C=C)	[30, 34–35]
		1678	1668	1670		Amide I/ν(C=O)	[30, 32, 35]
1467	1465	1473	1455	1456	1449	δ(CH$_2$)	[32, 34–36]
1244		1355	1318		1303	τ(CH$_2$)	[32–34]
		1266	1266	1260		Amide III/δ(N–H)	[30, 35]
	1300–1420	1132	1132			δ(COH)	[32, 36]
1044	990–1180	1132	1132		1055–1145	ν(C–O)	[30, 32–33,35–36]
854		1132	1132			ν(C–C)	[32–33]
				880		ν(CNC)	[35]

ν, stretching mode; δ, bending mode, τ, twisting mode.

fat rich domains (yellow/light gray), sucrose rich domains (green/gray), milk powder rich domains (red/dark gray) and the black areas indicate that no signal was achieved, i.e., these areas represent air. The dashed lines across the horizontal scans (Figs. 4A1, 4B1, 5C1, and 5D1) show where the depth scans have been recorded (Figs. 4A2, 4B2, 5C2, and 5D2), and the dashed lines in the vertical scans show
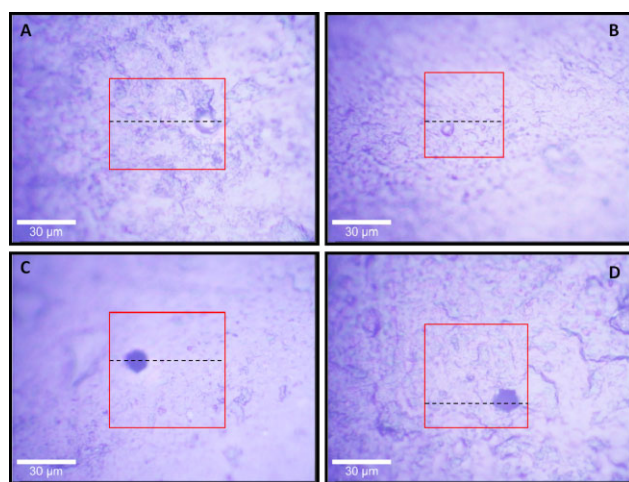

Figure 3. Light microscope images of white chocolate surfaces, enclosing a hazelnut filling. The overlaid squares represent the area over which Raman images have been recorded. (A, B) White chocolate surfaces including protrusions. These microscope images correlate to the horizontal and depth scans in Fig. 4A1 and 4A2, and in 4B1 and 4B2, respectively. (C, D) White chocolate surfaces including pores. These microscope images correlate to the horizontal and depth scans in Fig. 5C1 and 5C2, and in 5D1 and 5D2, respectively.

where the focal plane for the horizontal scans is. Thus, the horizontal scans do not show the upper surface, but approximately 6–12 µm below the average actual surface, in order to avoid effects of surface roughness in the images.

The images show that the technique allows us to clearly separate between the continuous CB matrix, the sucrose particles, the milk powder particles, and air filled pores. The images show quite well dispersed particles in agreement with the impression from images of milk chocolate that have been generated by using confocal scanning laser microscopy (CLSM) [37]. The CLSM provides a somewhat sharper distinction between the particles, but it demands a staining procedure that may cause structural changes such as recrystallization. The confocal Raman images also provide a very clear image of cavities that is more difficult to obtain with CLSM as the sucrose is non-stained in the matrix. It can be noted that the outer layer of the chocolate shell consists primarily of fat, with occasional sucrose particles and milk powder particles appearing close to the surface and sometimes almost penetrating the fat air interface (depth scans in Figs. 4 and 5). The microstructure that appears as a possible protrusion in Fig. 3A is observed as a clear dent in Fig. 4A1. However, from the depth scan in Fig. 4A2 it can be noted that this area is covered by fat, but also by sucrose and milk powder particles, leaving a hollow space underneath. The absence of this overlaying ''shell'' in the horizontal scan is most probably due to the location of the focal plane (10 µm below the actual chocolate surface). However, the protrusion illustrated in Fig. 3B shows a region enriched with fat in the horizontal image (Fig. 4B1, E). The depth scan connected to this image has been recorded on the border of this area where an indication of a protruding region can be observed (Fig. 4B2, F), and where the uppermost layer consists of fat
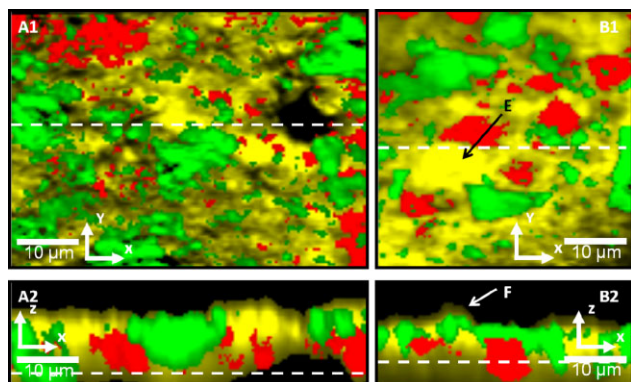
Figure 4. Horizontal scans, *xy* (A1 and B1), and depth scans, *xz* (A2 and B2), of white chocolate surfaces, enclosing a hazelnut filling. Yellow/light gray color represents fat rich domains, green/gray color represents sucrose rich domains, red/dark gray color represents milk powder rich domains, and black color represents air. The depth scans are performed over the dashed lines in the horizontal scans, and the position of the focal planes in the horizontal scans are shown with a dashed line in the depth scans. (A1) Scan range 60 μm × 60 μm with 140 × 140 pixels in *xy*-direction, and a penetration depth (focal plane) of 10 μm. (A2) Scan range 60 μm × 30 μm with 140 × 70 pixels in *xz*-direction. (B1) Scan range 60 μm × 60 μm with 140 × 140 pixels in *xy*-direction, and a penetration depth (focal plane) of 7 μm. (B2) Scan range 60 μm × 30 μm with 140 × 70 pixels in *xz*-direction. Integration time per Raman spectra is 0.1 s. E, F: Indicating a protrusion covered by a region enriched with fat.

Figure 5. Horizontal scans, *xy* (C1 and D1), and depth scans, *xz* (C2 and D2), of white chocolate surfaces, enclosing a hazelnut filling. Yellow/light gray color represents fat rich domains, green/gray color represents sucrose rich domains, red/dark gray color represents milk powder rich domains, and black color represents air. The depth scans are performed over the dashed lines in the horizontal scans, and the position of the focal planes in the horizontal scans are shown with a dashed line in the depth scans. (C1) Scan range 60 μm × 60 μm with 140 × 140 pixels in *xy*-direction, and a penetration depth (focal plane) of 8 μm. (C2) Scan range 60 μm × 40 μm with 140 × 90 pixels in *xz*-direction. (D1) Scan range 60 μm × 60 μm with 140 × 140 pixels in *xy*-direction, and a penetration depth (focal plane) of 9 μm. (D2) Scan range 60 μm × 30 μm with 140 × 70 pixels in *xz*-direction. Integration time per Raman spectra is 0.1 s.

and sucrose rich domains. Still, further down through the shell the region indicates an area enriched with fat. This area correlates with the focal plane in the horizontal image (7 μm below the chocolate surface). The pores in Fig. 3C and D can be observed as nothing but air in the corresponding horizontal scans (Fig. 5C1 and D1). Further, the depth scans in Fig. 5C2 and D2 show that these air filled pores continue further down through the chocolate shell, at least 10 μm, resembling a channel. In addition, these channels seem to expand a few microns below the surface.

The result images indicate that the protrusions are filled mainly with fat or that they have a fat enriched ''shell'', leaving a hollow channel underneath. This can further be connected to the structure of the protrusions that can be observed in the LV SEM images, as seen in Fig. 1. Further, it is shown that the pores are actually voids, consisting of neither fat nor sugar or protein. From the depth scans it seems as if these voids continue into the chocolate as channels, at least 10 μm. In addition, the mean pore size of the protrusions observed in the LV SEM images is estimated to 9.7 μm, with an SD of 1.2 μm, which correlates to the size range of the protrusions, pores, and channels detected in the Raman result images. If these channels continue even further into the chocolate, liquid fat from the filling and the chocolate matrix could be transported through these and up to the
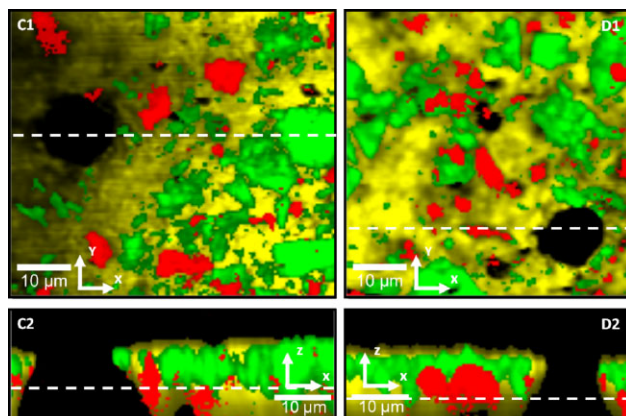
surface. The liquid fat might move through the channels, depending on the temperature, crystallize on the edge at the surface and then the liquid fat may return, leaving a hollow protrusion with a fat shell, which in some cases could collapse, leaving a pore at the surface. However, it could be argued that the empty protrusions, pores, and channels might be connected to gas filled bubbles lying under the surface of the chocolate shell. Still, the result images showing protrusions filled with mostly fat does not support this theory. The pressure driven convective flow theory is further supported by earlier studies [6, 21–22, 24]. In a recent study [6] designated protrusions at the surface were followed as a function of time and temperature, and the results showed that some of these protrusions disappear and then reappear, while some stay at the surface while changing their structure. Thus, this was interpreted as a pressure driven convective flow through pores and cracks in two directions, i.e., up to the surface and back into the shell. Smith and Dahlman [21] suggested that bloom growth in pralines is a two-step process, with drops initially forming at the surface and then bloom crystals nucleating and growing from them. In agreement with this study, Sonwai and Rousseau [22] found that cone-like structures might have formed at the surface of milk chocolate by welling and deposition of liquid-state fat pushed from within the matrix onto the surface during contraction. These cones

hardened with age, and crystal outcroppings protruded from the cones.

Thus, the findings from this study could provide evidence for the existence of pores in chocolate suggesting that they may play an important role in the development of fat bloom on filled chocolate products.

4 Conclusions

The objective of this study was to evaluate if the former reported topological imperfections, observed as pores and protrusions at chocolate surfaces, could be a part of a network of pore structures beneath and at the chocolate surface. This was done by investigating the appearance of these imperfections and the distribution of different components within them in white chocolate pralines by using confocal Raman microscopy. This study shows that there are actually protrusions at the chocolate surface (confirmed by LV SEM) having a base mean diameter of 20, with SD 1.5 μm, and an inner pore mean diameter of 9.7, with SD 1.2 μm. Further, Raman horizontal and depth scans indicate that these protrusions continue at least 10 μm in to the chocolate shell. Some of the analyzed protrusions and their continuing channels mainly consisted of fat, while some held a thin shell mainly consisting of fat, leaving a hollow space underneath. The analyzed pores and their continuing channels consisted of nothing but air, as characterized by Raman microscopy. We suggest that the protrusions might be connected to channels where a pressure driven convective flow of fat from within the chocolate matrix that, depending on pressure gradients caused by temperature changes, may be pressed up at the surface or drawn back into the matrix, leaving an empty pore with a shell of fat at the surface, which in some cases collapses and leaves a hollow pore and channel underneath. Thus, the findings from this study support the hypothesis that the pores could be connected to oil migration in filled chocolate products and, thus, further to fat bloom development.

The authors have declared no conflict of interest.

References

[1] Kinta, Y., Hatta, T., Composition and structure of fat bloom in untempered chocolate. *J. Food Sci.* 2005, *70*, 450–452.

[2] Lonchampt, P., Hartel, R. W., Fat bloom in chocolate and compound coatings. *Eur. J. Lipid Sci. Technol.* 2004, *106*, 241–274.

[3] Bricknell, J., Hartel, R. W., Relation of fat bloom in chocolate to polymorphic transition of cocoa butter. *J. Am. Oil Chem. Soc.* 1998, *75*, 1609–1615.

[4] Wille, R., Lutton, E., Polymorphism of cocoa butter. *J. Am. Oil Chem. Soc.* 1966, *43*, 491–496.

[5] Hodge, S. M., Rousseau, D., Fat bloom formation and characterization in milk chocolate observed by atomic force microscopy. *J. Am. Oil Chem. Soc.* 2002, *79*, 1115–1121.

[6] Dahlenborg, H., Millqvist-Fureby, A., Bergenstahl, B., Kalnin, D. J. E., Investigation of chocolate surfaces using profilometry and low vacuum scanning electron microscopy. *J. Am. Oil Chem. Soc.* 2011, *88*, 773–783.

[7] Hartell, R. W., Chocolate: Fat bloom during storage. *Manuf. Confect.* 1999, 89–99.

[8] James, B. J., Smith, B. G., Surface structure and composition of fresh and bloomed chocolate analysed using X-ray photo-electron spectroscopy, cryo-scanning electron microscopy and environmental scanning electron microscopy. *LWT–Food Sci. Technol.* 2009, *42*, 929–937.

[9] Kinta, Y., Hatta, T., Composition, structure, and color of fat bloom due to the partial liquefaction of fat in dark chocolate. *J. Am. Oil Chem. Soc.* 2007, *84*, 107–115.

[10] Miquel, M. E., Carli, S., Couzens, P. J., Wille, H. J., Hall, L. D., Kinetics of the migration of lipids in composite chocolate measured by magnetic resonance imaging. *Food Res. Int.* 2001, *34*, 773–781.

[11] Ghosh, V., Ziegler, G. R., Anantheswaran, R. C., Fat, moisture, and ethanol migration through chocolates and confectionary coatings. *Crit. Rev. Food Sci. Nutr.* 2002, *42*, 583–626.

[12] Lofborg, N., Smith, P., Furó, I., Bergenstahl, B., Molecular exchange in thermal equilibrium between dissolved and crystalline tripalmitin by NMR. *J. Am. Oil Chem. Soc.* 2003, *80*, 1187–1192.

[13] Aguilera, J. M., Michel, M., Mayor, G., Fat migration in chocolate: Diffusion or capillary flow in a particulate solid? A hypothesis paper. *J. Food Sci.* 2004, *69*, R167–R174.

[14] Choi, Y. J., McCarthy, K. L., McCarthy, M. J., Kim, M. H., Oil migration in chocolate. *Appl. Magn. Reson.* 2007, *32*, 205–220.

[15] Marty, S., Baker, K., Dibildox-Alvarado, E., Rodrigues, J. N., Marangoni, A. G., Monitoring and quantifying of oil migration in cocoa butter using a flatbed scanner and fluorescence light microscopy. *Food Res. Int.* 2005, *38*, 1189–1197.

[16] Briones, V., Scale-sensitive fractal analysis of the surface roughness of bloomed chocolate. *J. Am. Oil Chem. Soc.* 2006, *83*, 193–199.

[17] Briones, V., Aguilera, J. M., Brown, C., Effect of surface topography on color and gloss of chocolate samples. *J. Food Eng.* 2006, *77*, 776–783.

[18] Rousseau, D., On the porous mesostructure of milk chocolate viewed with atomic force microscopy. *LWT–Food Sci. Technol.* 2006, *39*, 852–860.

[19] Rousseau, D., Smith, P., Microstructure of fat bloom development in plain and filled chocolate confections. *Soft Matter* 2008, *4*, 1706–1712.

[20] Rousseau, D., Sonwai, S., Influence of the dispersed particulate in chocolate on cocoa butter microstructure and fat crystal growth during storage. *Food Biophys.* 2008, *3*, 273–278.

[21] Smith, P. R., Dahlman, A., The use of atomic force microscopy to measure the formation and development of chocolate bloom in pralines. *J. Am. Oil Chem. Soc.* 2005, *82*, 165–168.

[22] Sonwai, S., Rousseau, D., Fat crystal growth and microstructural evolution in industrial milk chocolate. *Cryst. Growth Des.* 2008, *8*, 3165–3174.

[23] Sonwai, S., Rousseau, D., Controlling fat bloom formation in chocolate – Impact of milk fat on microstructure and fat phase crystallisation. *Food Chem.* 2010, *119*, 286–297.

[24] Loisel, C., Lecq, G., Ponchel, G., Keller, G., Ollivon, M., Fat bloom and chocolate structure studied by mercury porosimetry. *J. Food Sci.* 1997, *62*, 781–788.

[25] Argov, N., Wachsmann-Hogiu, S., Freeman, S. L., Huser, T. et al., Size-dependent lipid content in human milk fat globules. *J. Agric. Food Chem.* 2008, *56*, 7446–7450.

[26] Fischer, H., Ibach, W., Dampel, H., A confocal Raman imaging study on emulsions. *Spectroscopy* 2010, *25*, 19–20.

[27] Fischer, H., Jauss, A., Food analysis with confocal Raman microscopy. *Spectroscopy* 2007, *22*, 29–30.

[28] Kaminskii, A. A., Stimulated Raman scattering by $C_{12}H_{22}O_{11}$ sugar (Sucrose). *Crystallogr. Rep.* 2003, *48*, 295–299.

[29] Liang, M., Chen, V. Y. T., Chen, H. L., Chen, W., A simple and direct isolation of whey components from raw milk by gel filtration chromatography and structural characterization by

[30] Thygesen, L. G., Lokke, M. M., Micklander, E., Engelsen, S. B., Vibrational microspectroscopy of food. Raman vs. FT-IR. *Trends Food Sci. Technol.* 2003, *14*, 50–57.

[31] Bresson, S., Rousseau, D., Ghosh, S., El Marssi, M., Faivre, V., Raman spectroscopy of the polymorphic forms and liquid state of cocoa butter. *Eur. J. Lipid Sci. Technol.* 2011, *113*, 992–1004.

[32] Almeida, M. R., Oliveira, K. D., Stephani, R., de Oliveira, L. F. C., Fourier-transform Raman analysis of milk powder: A potential method for rapid quality screening. *J. Raman Spectrosc.* 2011, *42*, 1548–1552.

[33] Max, J. J., Chapados, C., Sucrose hydrates in aqueous solution by IR spectroscopy. *J. Phys. Chem. A* 2001, *105*, 10681–10688.

[34] Sadeghijorabchi, H., Wilson, R. H., Belton, P. S., Edwardswebb, J. D., Coxon, D. T., Quantitative analysis of oils and fats by Fourier-Transform Raman spectroscopy. *Spectrochim. Acta, Part A* 1991, *47*, 1449–1458.

[35] Socrates, G., *Infrared and Raman Characteristic Group Frequencies*, Jhon Wiley & Sons Ltd, Chichester, UK 2001.

[36] Susi, H., Ard, J. S., Laser-Raman spectra of lactose. *Carbohydr. Res.* 1974, *37*, 351–354.

[37] Auty, M. A. E., Twomey, M., Guinee, T. P., Mulvihill, D. M., Development and application of confocal scanning laser microscopy methods for studying the distribution of fat and protein in selected dairy products. *J. Dairy Res.* 2001, *68*, 417–427.

III

Effect of shell microstructure on oil migration and fat bloom development in model pralines

Hanna Dahlenborg[a, b,*], Anna Millqvist-Fureby[a], and Björn Bergenståhl[b]

[a]SP Chemistry, Materials and Surfaces, Box 5607, SE-114 86 Stockholm, Sweden

[b]Lund University, Department of Food Technology, Engineering and Nutrition, P.O. Box 124, SE-221 00 Lund, Sweden

* Corresponding author. E-mail: hanna.dahlenborg@sp.se; Mobile: +46 70 587 60 62; Fax: +46 8 20 89 98

ABSTRACT

This study investigated the influence of shell microstructure on oil migration and fat bloom development in chocolate model systems. The microstructure of the model shells was varied by means of tempering or seeding cocoa butter and the addition of non-fat particles. Further, the behaviour at different storage conditions was studied. By using a set of novel analytical techniques the migration rate could be connected to the development of fat bloom at the surface. The non-seeded cocoa butter samples showed significantly higher rate of migration together with the highest rate of developed fat bloom, whereas the over-seeded cocoa butter samples showed low migration rate and low rate of fat bloom development. Addition of particles proved to have a significant impact on the microstructure, since these samples showed a substantially higher rate of migration and fat bloom development compared to seeded cocoa butter samples. Molecular diffusion could not explain the migration behaviour, thus, convective flow is suggested as an important contribution in addition to the molecular diffusion.

KEY WORDS

Microstructure, Cocoa butter, Cocoa particles, Sugar, Migration, Surface topology, Fat bloom

INTRODUCTION

Fat bloom on chocolate pralines is a commonly encountered problem in the confectionery industry leading to rejection by customers due to visual and textural quality loss. When chocolate surrounds a filling with high oil content (e.g. hazelnut oil in a praline filling) the quality loss can be related to migration of filling oil into the crystallised fat phase of the chocolate shell [1-5]. The driving force behind this oil migration is usually explained by a triacylglycerol (TAG) concentration gradient between the liquid filling fat and the liquid cocoa butter (CB) in the chocolate shell, aiming to reach a thermodynamic equilibrium [6-8]. The migrating liquid fat from the filling dissolves some of the crystallised CB TAGs in the shell which leads to a softer chocolate shell, while liquid CB from the shell fat matrix can migrate into the filling giving it a harder texture upon re-crystallisation [1, 5, 9]. In addition, liquid CB migrates to the chocolate surface where it re-crystallises into the most thermodynamically stable polymorphic form, $\beta_1 VI$ [4, 10]. These fat crystals have a needle-shaped form and due to their scattering of light when larger than 5 μm a dull, whitish haze is formed on the chocolate surface which can be correlated to fat bloom [2, 5, 11]. The mechanism of oil migration in chocolate pralines is not yet fully understood. However, it has been explained by molecular diffusion [1, 6-8, 12-16], capillary flow [17-22] and a pressure driven convective flow [23-26].

The rate of oil migration in pralines can be influenced by both storage conditions and product properties [18]. Several authors have found that the migration rate increases at higher storage temperatures [16, 19, 27-29]. Further, the migration rate of filling oil has been shown to be affected by the microstructure of the surrounding shell [13-14, 16, 30-32]. The shell microstructure is highly dependent on the crystallinity of the CB, which can be affected by varying the crystallisation regime. Generally, CB can crystallise into six different polymorphic forms named as form I-VI [10] or as form sub-α, α, β'_2, β'_1, β_2, β_1 [33], with respect to increasing stability and increasing melting points. Form $\beta_2 V$ is the desired form in chocolate, giving it the characteristics of gloss, fine texture, snap, a smooth melting in the mouth and relatively good fat bloom stability. This outcome is secured by a controlled crystallisation, where creation of nuclei induces the formation of $\beta_2 V$ crystals. There are two ways to achieve this; either by tempering or seeding. The tempering procedure is the conventional way to pre-crystallise chocolate, where liquid chocolate mass is treated mechanically and thermally, i.e. under shear and through a defined temperature profile. During this process crystals are formed that can act as seed crystals, from which the remaining fat in the chocolate solidifies. Pre-crystallisation by seeding can be realised in different ways, still, all procedures use seeds in order to induce formation of crystal form $\beta_2 V$ [34-36]. Zeng et al. [34] have developed a seeding technique where a premade seed CB crystal suspension, containing crystals of form $\beta_1 VI$, is added to the pre-cooled chocolate in quantities from 0.2-2%. This results in a large number of well defined nuclei, and

although the seed crystals are in form $\beta_1 VI$, the CB in the chocolate solidifies and develops into the desired form, $\beta_2 V$. In recent studies, this pre-crystallisation process has been shown to create chocolate products with increased fat bloom stability [30, 32, 34, 37-38]. Another way to affect the microstructure of the surrounding chocolate shell in a praline is by varying the size and amount of non-fat particles [23, 30-31, 37, 39]. Research done by Svanberg et al. [30, 37] indicated that addition of sugar and cocoa particles to CB affected the nucleation and growth of cocoa butter crystals and thus the microstructure of the shell. Further, Motwani et al. [31] investigated migration of peanut oil into samples composed of CB with or without the addition of cocoa particles, and observed that migration was enhanced when cocoa particles were present. Migration of TAGs in chocolate and model pralines has mostly been studied by using magnetic resonance imaging [13-14, 16, 18-19, 28-29, 40] and HPLC [27-28, 41-42]. Further, the relationship between surface microstructure and oil migration has been studied by using atomic force microscopy [28, 43-49], surface roughness measurements [21, 24, 44, 50-51], scanning electron microscopy [22, 24, 52] and confocal Raman microscopy [25].

Development of routes for quality improvement, leading to less oil migration from filling to chocolate shell is of importance for the confectionery industry. Therefore, it is of relevance to understand how the chocolate shell microstructure influences oil migration induced fat bloom in chocolate pralines. Thus, the objective of this study was to investigate the migration characteristics together with the fat bloom development in model pralines due to differences in shell microstructure by combining a set of novel analytical techniques. The microstructure in the chocolate shell is assumed to be possible to control by means of tempering or seeding protocols, addition of non-fat particles and storage conditions. Low vacuum scanning electron microscopy (LV SEM) and profilometry have been used to determine the fat bloom development at the shell surface as a function of time and temperature. Further, the migration between filling and shell was followed by energy dispersive X-ray spectroscopy (EDS), where brominated triacylglycerols (BrTAGs) were used as probe molecules for the migration. In addition, differential scanning calorimetry (DSC) results provided information of the polymorphic forms in the shells over time. Through these results we can achieve a deeper understanding of the influence of shell microstructure on oil migration and thus, also extend the understanding of fat bloom development in chocolate pralines.

MATERIALS AND METHODS

Materials. Model pralines, consisting of a filling layer in contact with a shell layer, were produced on a lab scale. The model filling consisted of 73 wt% cocoa butter (CB) (Bühler AG, Uzwil, Switzerland), 22 wt% triolein (Penta Manufacturing, New Jersey) and 5 wt% brominated

vegetable oil (BrTAG) (Penta Manufacturing, New Jersey) with an estimated molar mass of 978 g·mol^{-1}. This composition yielded a sufficiently hard filling with a solid fat content (SFC) of 53% at 20°C, without any separation of BrTAGs. In order to mimic a fat based filling the amount of added triolein was based on the assumption that hazelnut paste contains approximately 70% triolein [53-55]. This corresponds to 22% triolein of total fat content in a typical hazelnut based filling and thus, the model filling contained 22% triolein on a total fat basis. The shells consisted of CB (Bühler AG, Uzwil, Switzerland), CB and powdered sugar (AAK, Aarhus, Denmark), CB and cocoa particles (CP) (Bühler AG, Uzwil, Switzerland), and CB and defatted cocoa particles (dCP) (Bühler AG, Uzwil, Switzerland). The composition of both shells and filling is provided in Table 1. Further, the particle size distribution (PSD) was analysed using laser diffraction (Malvern Mastersizer 2000, Malvern, UK).Table 2 shows the PSD of sugar, CP and dCP. The premade seed CB crystal suspension used for seeding, containing crystals of form $\beta_1 VI$, was kindly supplied by Swiss Federal Institute of Technology, ETH (Zurich, Switzerland).

Table 1. Composition of shells and filling.

Model system	CB (wt%)	CB seeds (wt%)	Sugar (wt%)	CP* (wt%)	dCP (wt%)	Triolein (wt%)	BrTAG (wt%)	Fat content (wt%)
Non-seeded CB	100							100
Under-seeded CB	99.5	0.5						100
Seeded CB	96.4	3.6						100
Over-seeded CB	90	10						100
Sugar + CB	72.4	2.6	25					75
CP + CB	69.6	2.6		27.8				75
dCP + CB	72.4	2.6			25			75
Filling	69.4	3.6				22	5	100

*Fat content in CP = 10%

Table 2. Particle size distribution (PSD) represented by volume fractions 10%, D(v, 0.1); 50%, D(v, 0.5); 90%, D(v, 0.9), Sauter mean diameter, D[3.2], and specific surface area of sugar, cocoa particles (CP) and defatted cocoa particles (dCP).

Particles	D(v, 0.1) (µm)	D(v, 0.5) (µm)	D(v, 0.9) (µm)	D[3.2] (µm)	Specific surface area (m^2/g)
Sugar	14.53	42.68	99.78	12.42	0.48
CP	3.86	11.92	24.57	5.45	1.10
dCP	1.80	7.80	29.02	4.10	1.46

Production of model systems. The microstructure of the model shells was varied following two lines: addition of varied amount seed crystals, and addition of different particles. The CB seeds were stirred and heated in a sealed beaker in a water bath, and held a temperature of 33 - 33.7°C prior to mixing with shell and filling masses. The model systems consisted of a filling layer (a disc of 10 mm in diameter and 3 mm high) in contact with a shell layer (a disc of 10 mm in diameter and 1.5 mm high) (Figure 1A). The CB was kept at a temperature of 50°C for minimum 24hrs prior to production in order to eliminate any residual crystals.
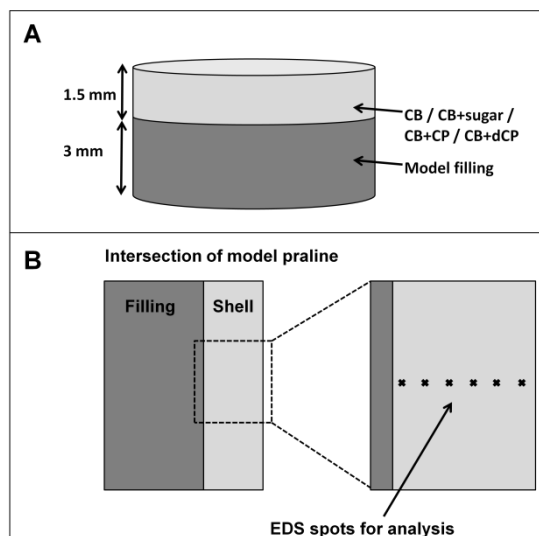

Figure 1. A: Model praline consisting of a shell layer (1.5 mm) in contact with a filling layer (3 mm). B: Intersection of model praline showing EDS spots for analysis.

In order to vary the crystal density and crystal structure the CB shells were prepared in four different manners (Table 1): i) non-seeded, ii) under-seeded, iii) seeded, and iv) over-seeded. In a first step, the shells were prepared. In the case of under-seeded, seeded and over-seeded shells, CB with a temperature of 50°C was cooled in a sealed water bath set to 31°C and stirred until the CB had reached a temperature of 33.8°C. This temperature was held for 2 minutes after which the pre-heated CB seeds were added to the CB. This was then stirred for 3 minutes at a temperature of 33.7-33.8°C. The seeded CB was poured into 1.5 mm high moulds, that were shaken to reduce air bubbles, and then the overload of CB was scraped of the moulds. In the case of non-seeded shells, CB with a temperature of 50°C was cooled in a water bath at 25°C and stirred until the CB had reached a temperature of 27°C. This temperature was held for 5 minutes and then the CB was placed in a water bath that kept 33°C, and was then stirred until a temperature of 31°C was reached. The moulds containing CB shells were stored at 15°C for 30 minutes and then allowed to rest at room temperature (20±0.5°C) for 20 minutes after which the filling was added to the shells. For preparation of the model filling CB, triolein and BrTAGs at 50°C were mixed in the proportions given in Table 1. The filling was prepared in the same way as the seeded shell mass. When a layer

of 3 mm seeded filling mass had been added to the shells, a process that mimics conventional praline preparation, the moulds were stored at 15°C for at least 1 hour before the samples were de-moulded. This was followed by storage at 15°C for 48 hrs approximately before distribution to final storage at 20°C and 23°C.

To evaluate the influence of particles, shells were prepared with tree different particles (Table 1and Table 2): i) sugar, ii) CP, and iii) dCP. All particles were stored in a desiccator over dry silica gel seven days before sample preparation in order to reduce the impact of moisture during pre-crystallisation. The mixtures of CB and particles were prepared and stirred at 50°C, 1 hour before production. Seeding was applied to keep a controlled production, and the shells together with filling were prepared and stored in the same way as the seeded CB shells.

The defatted cocoa particles (dCP) was prepared by extraction of TAGs and lecithin from the CP. This was carried out in two steps: Acetone and ethanol (70:30) was used as solvent in the first step. The solvent-CP mixture was stirred and heated to 30-35°C before it was shaken and filtered with a Büchner funnel under vacuum. In the second step hexane was used as solvent, and the mixture was once again shaken and filtered with a Büchner funnel under vacuum. Both steps were carried out twice.

Storage conditions. Two days after production, the model systems were stored for 12 weeks at two different temperature controlled environments. The samples were stored in heating cabinets (temperature accuracy ±0.5°C) where the temperature was kept at either 20°C or 23°C. The actual temperature was additionally controlled by a k-type thermocouple using a Picco Tc-08 interface for continuous measurement. At regular time intervals different analyses (LV SEM, Profilometry, EDS and DSC) were performed in order to follow the development of crystal form, surface topology and migration from filling to shell.

Differential scanning calorimetry. The differential scanning calorimeter (DSC) used in this study was a Mettler Toledo DSC 1 STARe System. Sample preparation was performed by scraping off layers from a cross section of the shells to represent the whole shell. The slices were then chopped into fine small pieces before it was weighed in a pan, after which a melting curve was recorded. The samples (approximately 5 mg) were hermetically sealed in an aluminium pan and an empty pan was used as reference. The time-temperature program used was: equilibration at 3°C below storage temperature and subsequent heating at a rate of 4°C/min to 50°C under a N_2 flow of 60 ml/min. Three replicates were performed at each analysis occasion.

Low vacuum scanning electron microscopy. Scanning electron microscopy (SEM) is a technique producing high resolution images of sample surfaces. Due to the way in which the image is created, SEM images have a characteristic three-dimensional appearance and are useful for judging the surface structure of a sample. Philips XL30 environmental scanning electron microscope, equipped with a cold stage set to 5°C was used with mixed detectors (biased gaseous detector (GSE) 75% and backscattered electron detector (BSE) 25%), at 15 keV and at low vacuum mode with 0.7 – 0.9 Torr, which corresponds to a RH of 10-15% approximately. These parameters were chosen considering that they cause minimal damage of the sample surface, and for optimising the image quality. In this study, analyses of the samples were performed without sample preparation, i.e. without coating the sample surface. This leads to a sacrifice in magnification and resolution; however, by analysing without coating the true surface can be monitored. Two samples from each environment were monitored on each analysis occasion, and the analyses were performed at different spots on the top of the pralines. After each analysis the monitored samples were sacrificed due to the possible impact from the microscope such as electron beam, temperature, humidity and pressure.

Profilometry. The surface topology of the shells was analysed using Profilometry Zygo New View 5010 (Middlefield, CT, USA), which is a non-contact profilometry method based on white light interferometry. Since profilometry uses reflective light, the degree of light absorption to the analysed sample has no impact on the results. Therefore this technique is applicable for light CB but also for dark chocolate and other light absorbing surfaces. In order to quantify the surface topology the surface roughness, Rq (μm), was analysed. Rq is the root-mean-square (rms) roughness, defined as the average of the measured height deviations taken within the evaluation length or area and measured from the mean linear surface (Eq. 1). $z(x)$ represents the height elements along the profile and L is the number of discrete elements.

$$rms = \sqrt{\frac{1}{L} \int_0^L z^2(x)dx} \qquad (\mu m) \qquad\qquad (1)$$

Through a digital filtering (cut-off filter) of the data, the surface characteristics of the investigated surface can be broken down into waviness and roughness results. This filter includes a high filter wavelength which defines the noise threshold; all shorter spatial wavelengths are considered noise. It also includes a low filter wavelength which defines the form threshold where all longer spatial wavelengths are considered form (waviness). Everything between these two wavelengths is assigned to roughness. The analysis set up used has previously been described by Dahlenborg et al.

. By using this set up we were able to analyse the same area (±20 μm) at each analysis occasion. This enabled us to follow and compare surface changes in that specific area of interest. As a result of this, we were able to reduce noise, normally observed due to the use of different spots for data collection. Two samples from each environment were monitored, and measurements were carried out at three different spots for each sample. The analyses were performed on the top of the model pralines, as for LV SEM, at room temperature (20°C approximately). After each measurement the samples were returned into their temperature-controlled environment for continued storage. The data was analysed using the advanced texture application in MetroProTM (Middlefield, CT, USA) analysis and control software.

Energy dispersive X-ray spectroscopy. Migration of BrTAGs from the filling into the shell was followed using energy dispersive X-ray spectroscopy (EDS). This is a powerful micro analytical tool that is compatible with scanning electron microscopes (SEM). EDS can be used to rapidly evaluate the elemental constituents of a sample. It is not only qualitative results that can be obtain with EDS, but also accurate quantitative results can be achieved. The generation of the electron beam is the same for EDS as for SEM. In this study, Philips XL30 environmental scanning electron microscope, equipped with a cold stage set to 5°C, was used at 15 keV and at low vacuum mode with 0.6 Torr, which corresponds to a RH of 10-15% approximately. These parameters were chosen considering that they cause minimal damage of the sample. The EDS detector used was an EDAX New XL-30, AMETEK together with the software program EDX control software. The EDS analyses were performed on an intersection of the model pralines, moving on a straight line from the filling-shell interface to the upper surface of the shells (Figure 1B). This intersection was obtained by slicing the samples with a razor blade, from one side to the other. Thus, mixing of shell and filling could be avoided. The wt% of C, O and Br was measured over a straight line on the shell intersection at different points with fixed distances to the shell-filling interface (H cannot be detected). From each measuring point, an EDS spectrum was obtained showing relative intensities for the different analysed elements in the shell. These relative intensities were converted into wt% by a software program. By measuring at different distances from the filling and over a straight line it was possible to follow the migration of the BrTAGs through the shell. The migration profile was obtained by plotting the amount of BrTAGs in the shell fat matrix as a function of the distance from the filling. Two samples from each storage environment were monitored at each analysis occasion, and measurements were carried out at two different lines for each sample.

8

Statistical analysis. All experiments were performed in replicates, reported in each analysis section. The numerical results are expressed as means ± the standard error of mean (s.e.m.). Statistical significance of the difference between the means of the Rq values was determined ($p < 0.05$) using analysis of variance (ANOVA). Further, representative results are presented in the LV SEM result images.

RESULTS

The samples with CB shells were produced by using different crystallisation regimes, where the non-seeded samples followed a tempering scheme without added shear, making it comparable with a conventional hand tempered product. The model shells containing particles were produced without the addition of emulsifiers in order to enable us to observe the direct influence of the particles. This affects the viscosity of the mixture and thus the total fat content could not be kept at a level of 32% as in a commercial chocolate product. Hence, a mixture with total fat content of 75% resulted in a manageable mixture without any observable macroscopic separation of particles.

A clear difference between the storage temperatures was observed over time for all model systems in terms of polymorphic development, migration of BrTAGs and development of the surface topology. Higher storage temperature, i.e. 23°C, resulted in higher rate of migration and development of surface crystals at an earlier stage compared to the lower storage temperature, i.e. 20°C. Further, macroscopic observations showed that after 12 weeks of storage at 23°C, the samples had swollen shells. This was especially evident for the non-seeded CB samples. Since most samples had the colour of CB it was impossible to determine by the eye at what time visible fat bloom developed.

Polymorphic development. The different model systems were analysed by using DSC in order to observe and compare how the CB crystal forms developed as a function of time and storage temperature. Figure 2 illustrates the temperatures of the peak maxima, i.e. the melting temperatures of the fat crystals, for all model systems as a function of storage time at the two different storage temperatures. It can be seen that all samples have similar melting points (32.2±0.4°C) at week 0, i.e. 2 days after production. The peak maxima for the samples stored at 20°C are still around 32°C after storage for 6 weeks, with only a minor increase, whereas the peak maxima have shifted towards higher values for the samples stored at 23°C. At this point, the most prominent differences can be seen for the non-seeded CB samples and the samples containing particles, where the peak maxima have shifted to noticeably higher values compared to the other samples. After storage for 12 weeks at 20°C the peak maxima for the non-seeded CB samples have shifted towards evidently higher

values compared to the other samples that stay at approximately the same melting temperatures. The samples stored at 23°C for 12 weeks show peak maxima that have shifted to even higher values, i.e. between 34 and 34.4°C, with no specific difference between the samples.
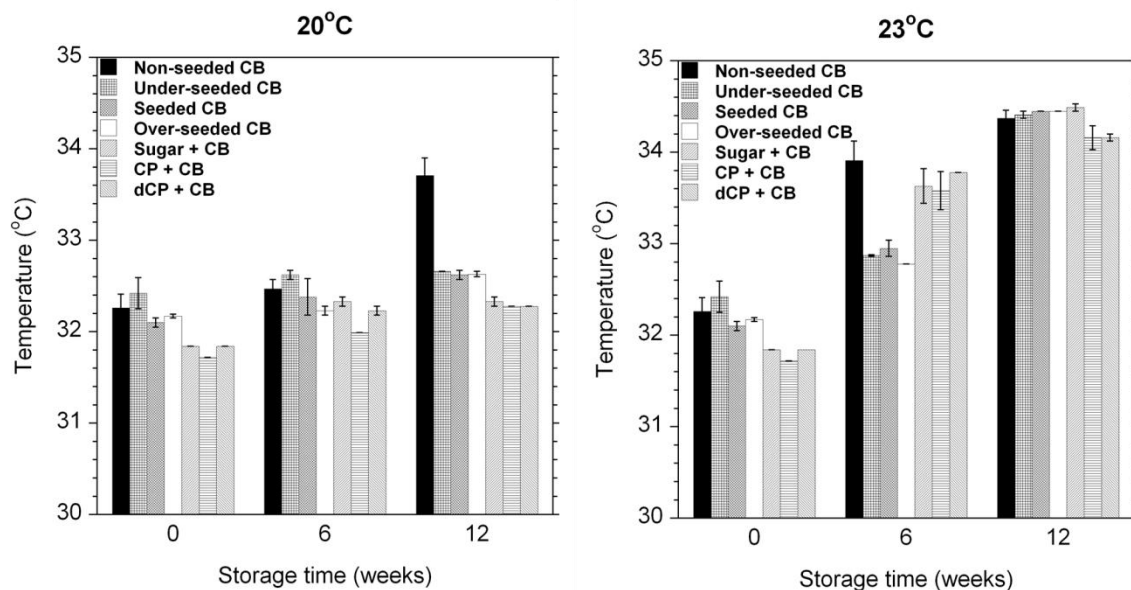

Figure 2. Peak maxima from DSC measurements showing melting temperatures of fat crystals in shells of model pralines stored at 20 and 23°C, presented as a function of storage time (weeks). Error bars represent the standard error of mean of 3 replicates.

To further elucidate the differences in melting enthalpy between the samples, Figure 3 illustrates the relative amount of melting enthalpy at the temperature intervals <30°C, 30-33°C and 33-40°C for samples stored at 20°C for 12 weeks and at 23°C for 6 weeks, respectively. At both storage temperatures samples containing particles show higher values at temperatures below 30°C. The non-seeded CB samples stored at 20°C for 12 weeks show significantly lower values in the range of 30-33°C compared to all other samples, and at the same time significantly higher values in the range of 33-40°C. The opposite can be seen for all the seeded CB samples. Further, the samples containing particles show the highest values in the range of 30-33°C and the lowest in the range of 33-40°C. After 6 weeks storage at 23°C the non-seeded CB samples show the same trend as when stored at 20°C for 12 weeks. The over-seeded CB samples show the lowest values in the range of 33-40°C, whereas the under-seeded and seeded CB samples together with the seeded samples containing sugar show slightly higher values. Further, it can be seen that the seeded samples containing dCP and CP show higher values in the range of 33-40°C compared to the previous mentioned samples. Thus, differences can be seen between the samples containing particles.
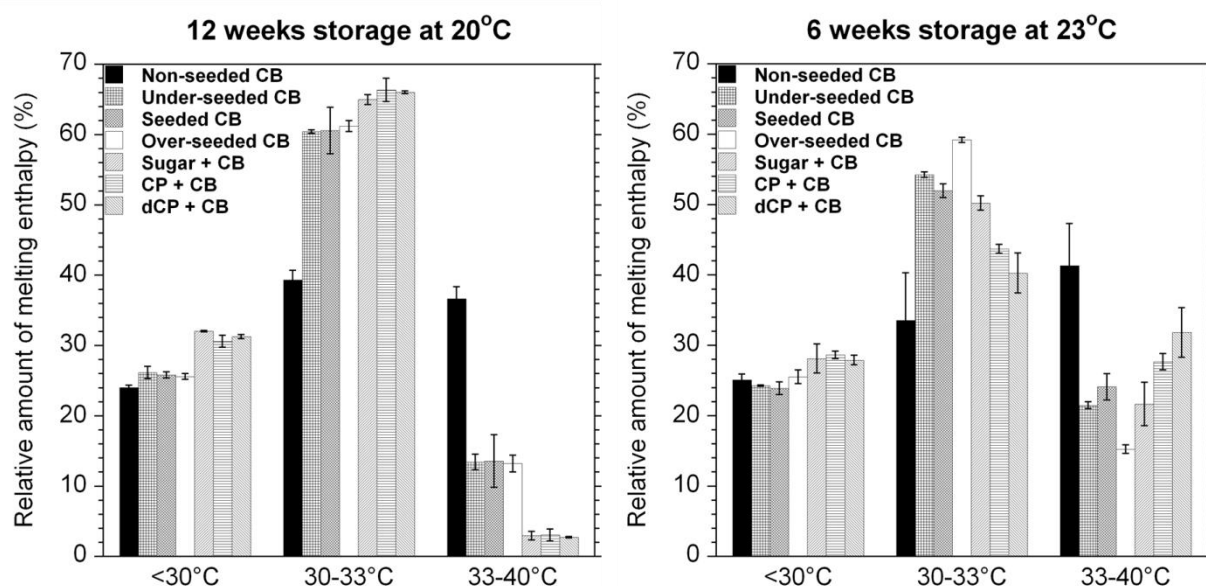
Figure 3. Relative amount (%) of melting enthalpy at the temperature intervals <30°C, 30-33°C and 33-40° for samples stored at 20°C for 12 weeks and at 23°C for 6 weeks, respectively. The melting enthalpy is expressed as J/g fat. Error bars represent the standard error of mean of 3 replicates.

Surface topology development. Figure 4 presents LV SEM images of the model shell surfaces after 12 weeks storage at 20°C. The non-seeded (A) and the under-seeded (B) CB samples show a development of surface crystals at this stage. In addition, the crystals on the non-seeded CB samples were clearly larger in size than the crystals on the under-seeded CB samples. On the other hand, the seeded CB samples (C) and the over-seeded CB samples (D) have developed almost no or low frequency of surface crystals by week 12. Instead these images show surfaces with some topological imperfections, which could be seen in LV SEM images already at the first analysis occasion (results not shown). Further, the frequency of these topological imperfections is evidently higher for the over-seeded CB samples than for the seeded samples. All samples containing particles (E, F, G) showed a low frequency of surface crystals after 12 weeks storage at 20°C.
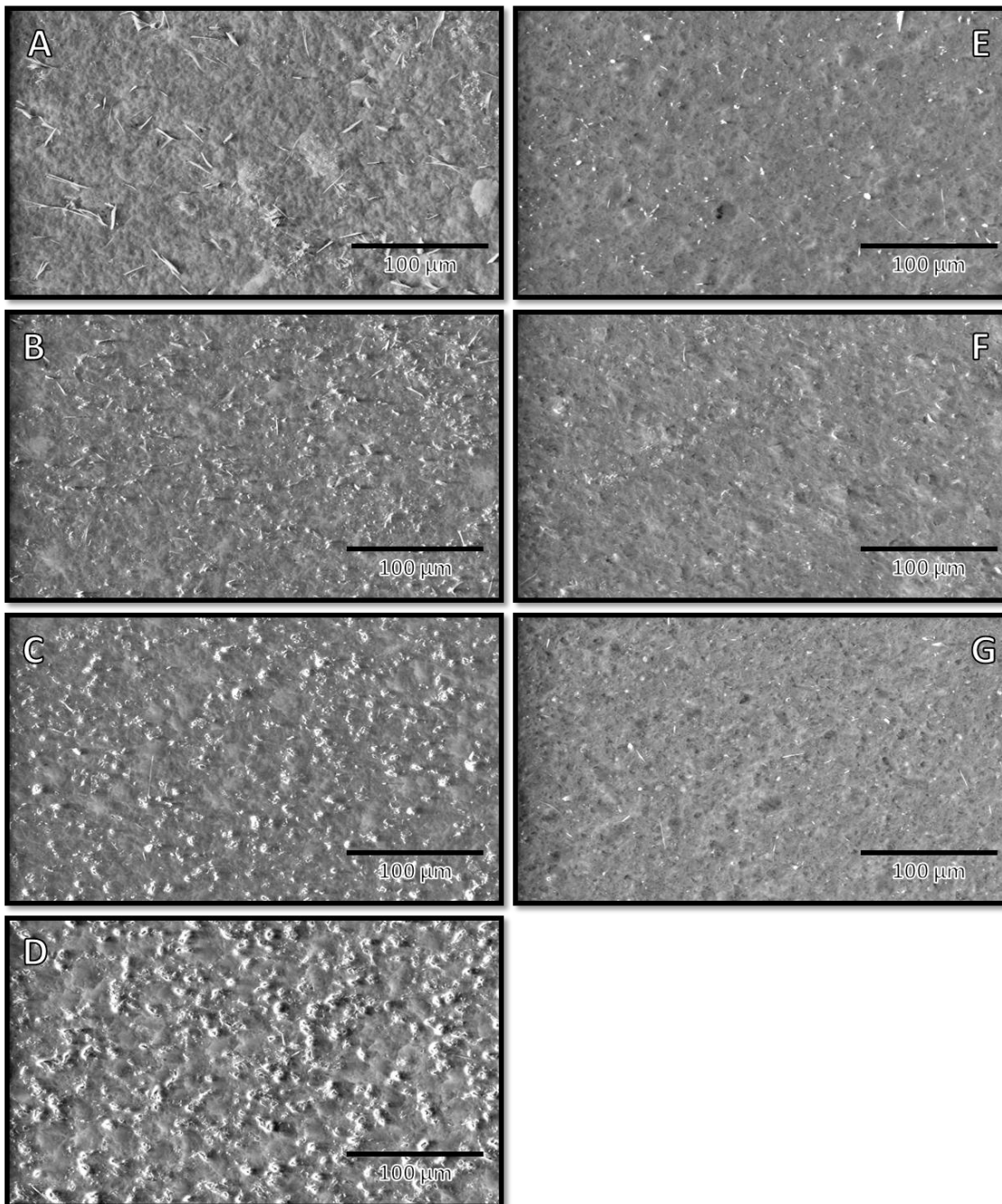
Figure 4. LV SEM images for samples stored at 20°C for 12 weeks. The shells in the samples are A: Non-seeded CB, B: Under-seeded CB, C: Seeded CB, D: Over-seeded CB, E: Seeded CB+sugar, F: Seeded CB+CP, G: Seeded CB+dCP. Scale bars represent 100 μm.

After 4 weeks of storage at 23°C all samples had developed crystals at the surface, still, to various quantities and of different sizes. Figure 5 shows LV SEM images of the different model samples stored at 23°C for 8 weeks. Here it is shown that the non-seeded CB samples (A) had developed the largest size and the highest frequency of surface crystals, followed by the under-seeded CB samples (B) and the seeded samples containing CP (F) and dCP (G). The seeded samples containing sugar (E) had developed a slightly lower frequency of surface crystals followed by the seeded CB samples (C). The over-seeded CB samples (D) showed the lowest frequency of

crystals at the surface. In addition, other topological features could be observed at the surface of the over-seeded CB samples.
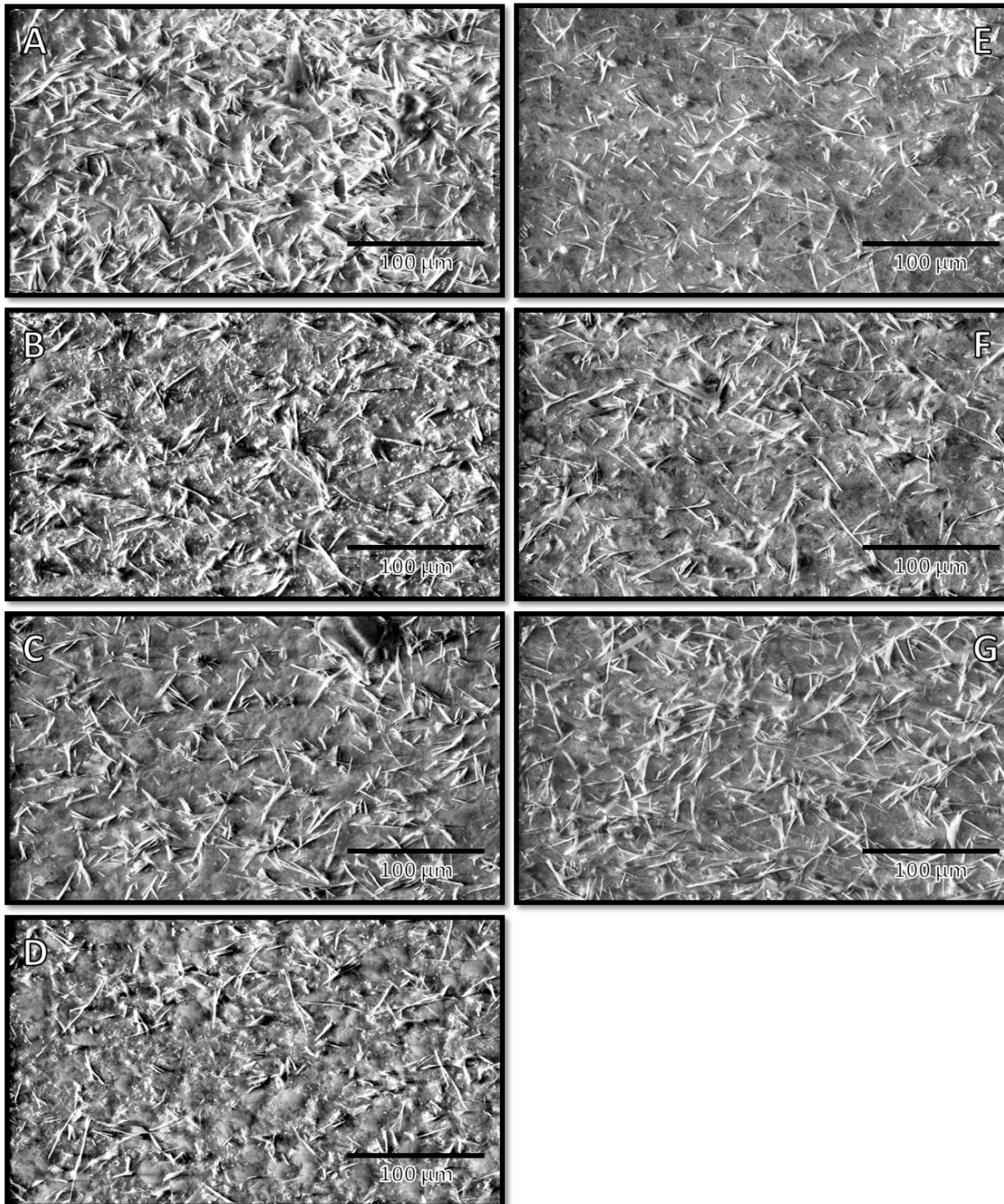
Figure 5. LV SEM images for samples stored at 23°C for 8 weeks. The shells in the samples are A: Non-seeded CB, B: Under-seeded CB, C: Seeded CB, D: Over-seeded CB, E: Seeded CB+sugar, F: Seeded CB+CP, G: Seeded CB+dCP. Scale bars represent 100 µm.

Table 3 presents profilometry Rq values from the first analysis occasion, i.e. t=0, which shows that the initial Rq value is higher by a factor of 4 for the over-seeded CB samples compared to the other samples, indicating on a rougher surface from the start. Still, the normalized Rq values presented in Figure 6 demonstrate that the roughness of the over-seeded CB samples

13

stayed constant over time at both storage temperatures. For the samples stored at 20°C the over-seeded and seeded CB samples stayed at a relatively constant level, compared to the non-seeded and under-seeded CB samples that showed slightly higher Rq values. However, for the samples stored at 23°C, the non-seeded CB samples showed a distinctly higher increase in roughness compared to the other samples, followed by seeded samples containing CP and dCP, which in their turn were followed by the under-seeded CB samples. The seeded CB samples and the seeded samples containing sugar showed a similar development of roughness, while the over-seeded CB samples showed the lowest increase in roughness over time. In addition, it can be seen from Figure 6 that the increase in surface roughness initiated after 4 to 6 weeks when stored at 23°C. Further, the roughness increased with a higher rate for the samples stored at 23°C compared to the samples stored at 20°C, with the exception for the over-seeded CB samples that stayed constant at both temperatures.

Table 3. Initial Rq values for the different model systems including standard error of mean (s.e.m.).

Model system	$Rq_{t=0}$	s.e.m.
Non-seeded CB	0.095	0.006
Under-seeded CB	0.100	0.004
Seeded CB	0.101	0.003
Over-seeded CB	0.421	0.009
Sugar + CB	0.094	0.005
CP + CB	0.053	0.004
dCP + CB	0.076	0.003
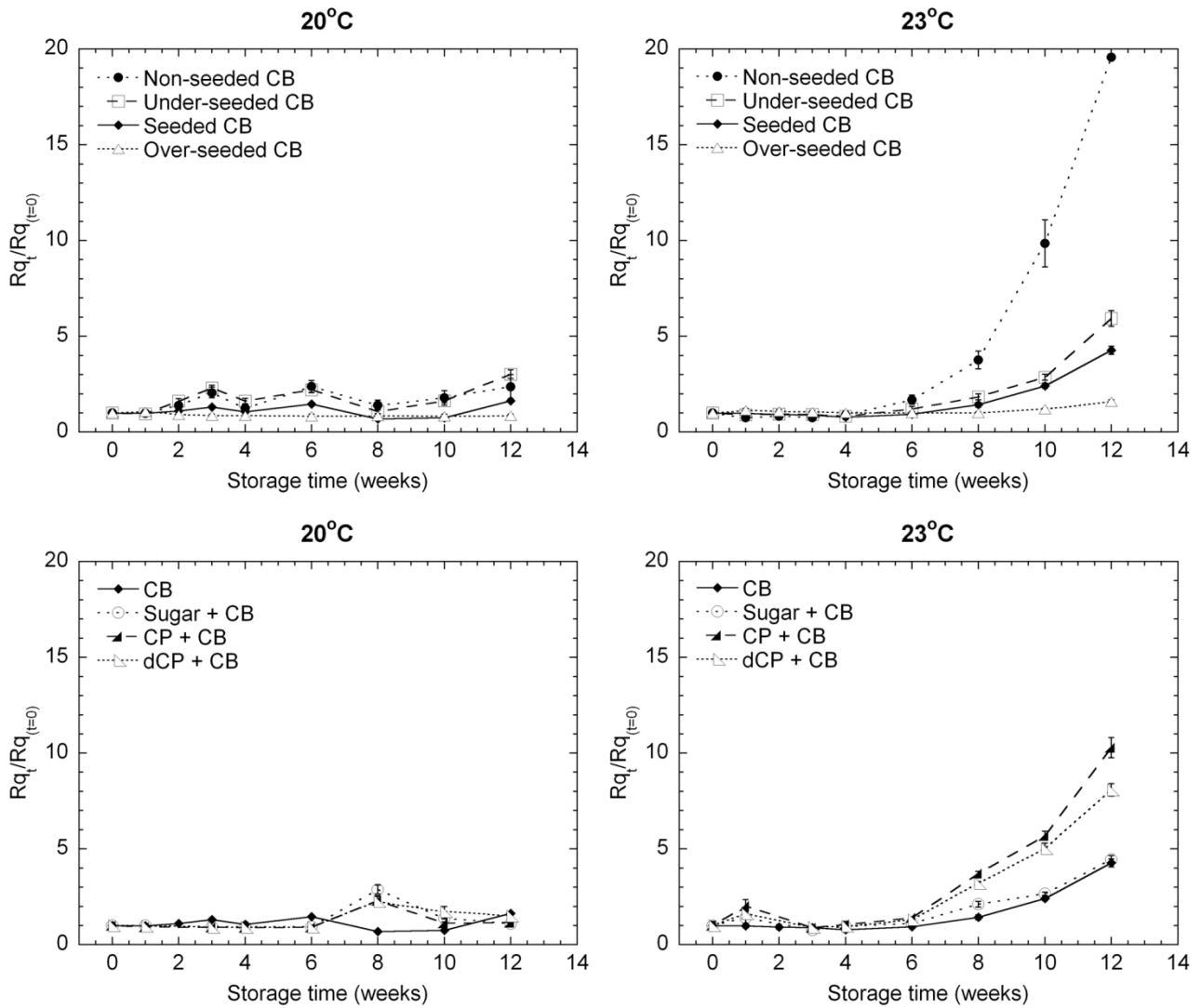
Figure 6. Normalized Rq values as a function of storage time for model pralines stored at 20 and 23°C. Error bars represent the standard error of mean of 6 replicates.

Oscillations in Rq values, mainly observed at 20°C storage temperature, are due to the presence of protrusions that appear, disappear and reappear over time, which can be identified on profilometry images shown in Figure 7 (note that these images represent the same area ±20µm). These images illustrate non-seeded CB samples stored at 20°C for 1, 3, 4 and 6 weeks, respectively. Comparing the images at the different storage times with Figure 6 explains the fluctuations of the Rq values.

Figure 7. Profilometry images of a model praline with non-seeded CB shell stored at 20°C for A: 1 week, B: 3weeks, C: 4weeks, D: 6 weeks. Note that the images represent the same area ±20µm.
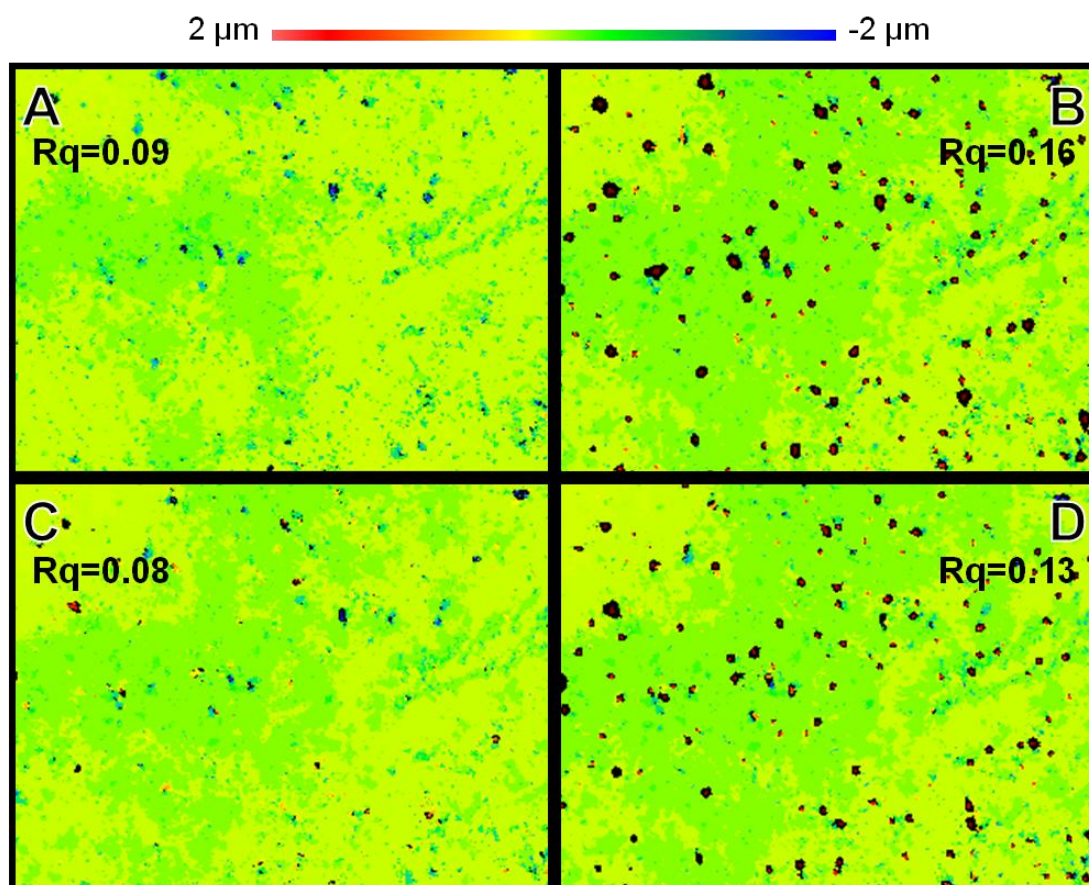
Migration. Migration profiles showed that the migration of BrTAGs into the shells developed over time, especially at larger distances from the filling-shell interface. Figure 8 displays migration profiles for non-seeded and seeded CB samples, and seeded samples containing sugar or CP, all stored at 23°C. The weight per cent of BrTAGs in the shell fat matrix is presented as a function of the distance from the filling. The results for the CB samples show that migration close to the filling-shell interface is initially high but decreases until a minimum is reached after 6 weeks storage. The same trend could be observed for all CB samples stored at 23°C. The non-seeded CB samples show a migration of BrTAGs up to a distance of 800 µm from the interface at 2 weeks storage, after which the migration goes deeper into the shell, i.e. further away from the filling-shell interface. After 4 weeks storage at 23°C the non-seeded CB samples show a BrTAG concentration of approximately 3 wt% of the total shell fat content close to the filling-shell interface. Further, after 12 weeks of storage fluctuations in the migration profile can be observed. For the seeded CB samples, migration of BrTAGs can be observed up to a distance of 800 µm from the interface during the first 6 weeks, compared to 2 weeks for the non-seeded CB samples. After 10-12 weeks storage the migration goes deeper into the shell. The samples containing sugar or CP also show an initially high migration close to the filling-shell interface. Migration of BrTAGs in the sugar

16

containing samples could be observed up to a distance of 800 μm from the interface after 6 weeks storage, after which the migration goes deeper into the shell. On the other hand, the samples containing CP show a migration up to 800 μm after only 3 weeks storage after which the migration goes deeper into the shell. The presence of particles is probably the cause of the relatively high error bars, compared to samples without particles. Thus, due to the presence of non-fat particles in chocolate, noise is inevitable.
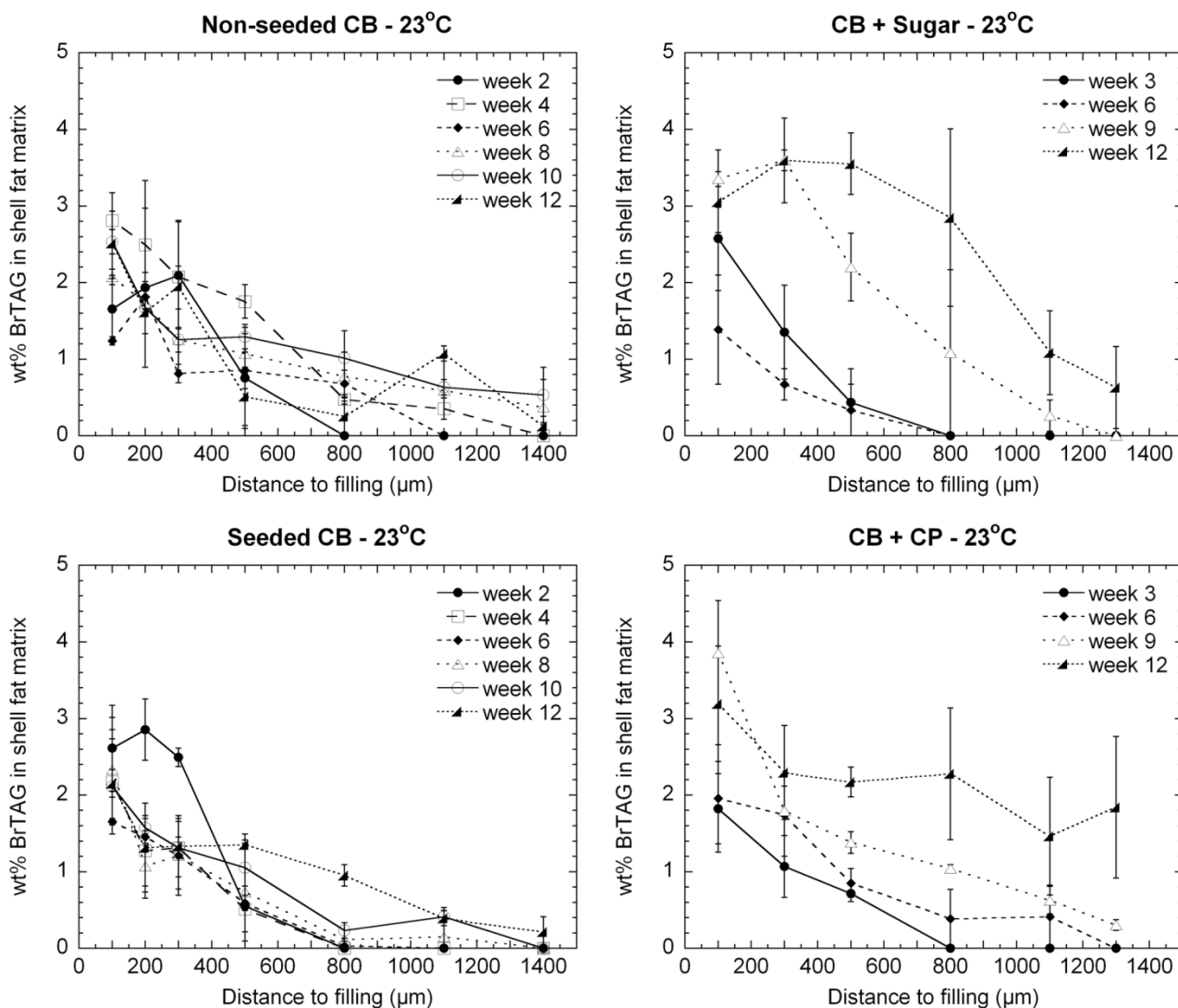
Figure 8. Migration profiles for non-seeded and seeded CB samples, and seeded samples containing CB+sugar or CB+CP, all stored at 23°C. Error bars represent the standard error of mean of 4 replicates.

To further elucidate the process of BrTAG migration into the shells of varied microstructure, the BrTAG concentration in the shell fat matrix at 300 and 1100 μm from the interface between filling and shell are shown in Figure 9 and Figure 10. Figure 9 shows the results for samples stored at 20°C and Figure 10 for samples stored at 23°C. From the results in Figure 9 it can be seen that the BrTAG concentration stays relatively constant over time for the CB samples at

17

300 µm from the filling, while at 1100 µm from the filling there is nearly no migration taking place. In contrast, the samples containing particles indicate on an increase in BrTAG concentration after 9 weeks of storage at a distance of 300 µm from the filling. This could also be observed at 1100 µm from the filling. Figure 10 shows the results for samples stored at 23°C. Here it can be seen that the concentration profiles for the samples containing CB at 300 µm from the interface indicate on a decrease in BrTAG concentration as a function of storage time, which levels out to a more stable value of approximately 1 wt% BrTAGs in the shell fat matrix (i.e. 20% of the initial value in the filling fat matrix). In addition, after 6 weeks storage a minimum could be observed. At 1100 µm from the interface the BrTAG concentration is initially low, but starts to increase after 6-8 weeks of storage. Further, the non-seeded CB samples show the highest concentration of BrTAGs, while the concentration in the over-seeded CB samples stays close to zero. The samples containing particles show a monotonous increase over time at 300 µm from the filling. At 1100 µm from the interface the BrTAG concentration increases after 6 weeks of storage, where the samples containing dCP indicate on the highest level of BrTAGs (approximately 2.5 wt% of the shell fat matrix, corresponding to 50% of the initial concentration in the filling fat matrix).
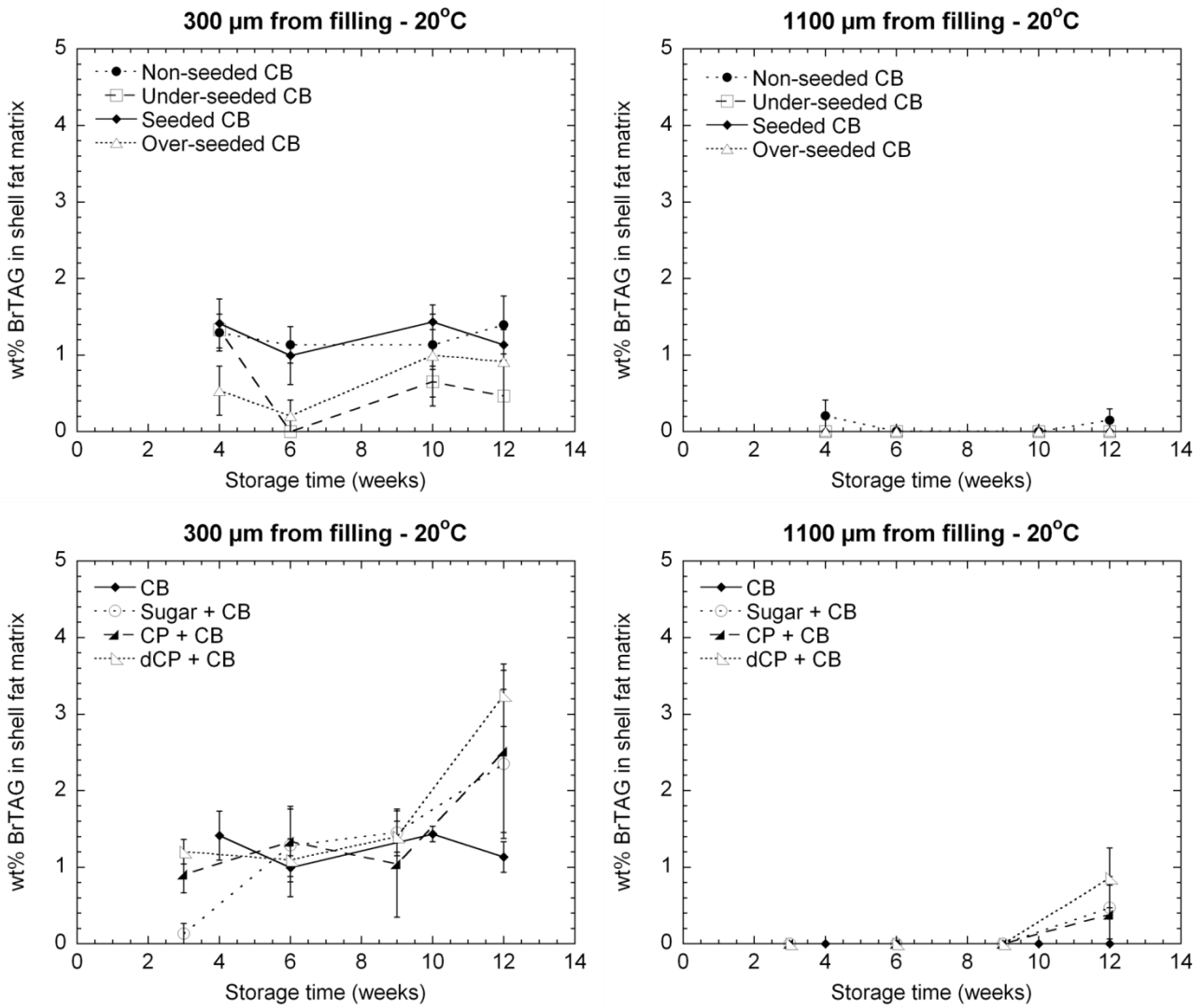
Figure 9. Wt% BrTAGs in shell fat matrix 300 and 1100 μm from filling as a function of storage time for model pralines stored at 20°C. Error bars represent the standard error of mean of 4 replicates.
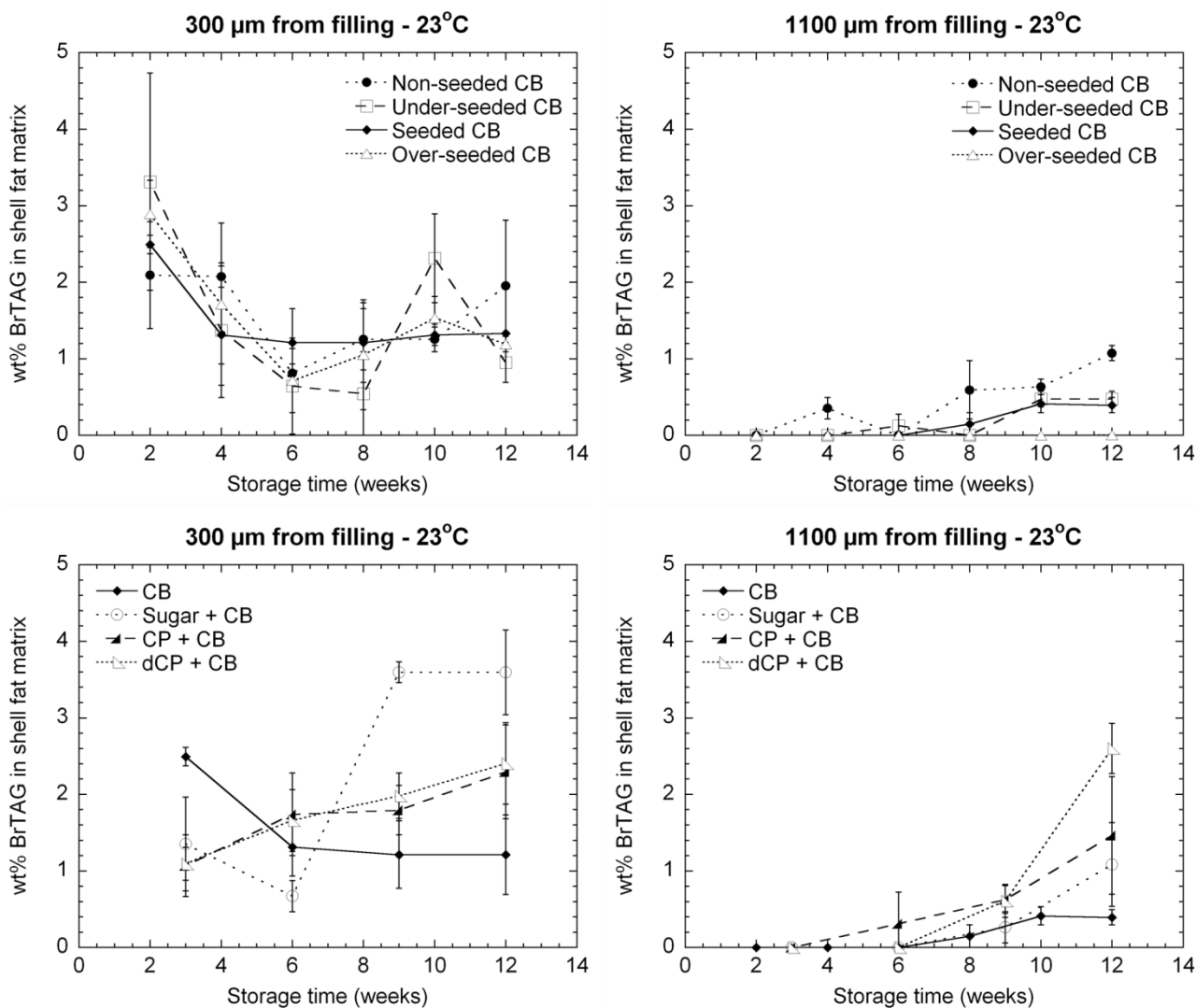
Figure 10. Wt% BrTAGs in shell fat matrix 300 and 1100 μm from filling as a function of storage time for model pralines stored at 23°C. Error bars represent the standard error of mean of 4 replicates.

Figure 11 presents the mean concentration of BrTAGs in the shell fat matrix as a function of storage time for all model systems stored at 20 and 23°C. The concentration of BrTAGs in the CB samples stored at 20°C stays relatively constant over time, while the samples containing particles show an increase in BrTAG concentration after 9 weeks of storage. In the case of storage at 23°C the CB samples indicate on a minimum in BrTAG concentration at 6 weeks storage, after which the concentration stays relatively constant over time with only minor increase. In contrast, the samples containing particles show a monotonous increase in concentration over time. After 12 weeks storage the mean concentration of migrated BrTAGs in the shell fat matrix has reached a value close to 3 wt% of the total shell fat matrix.
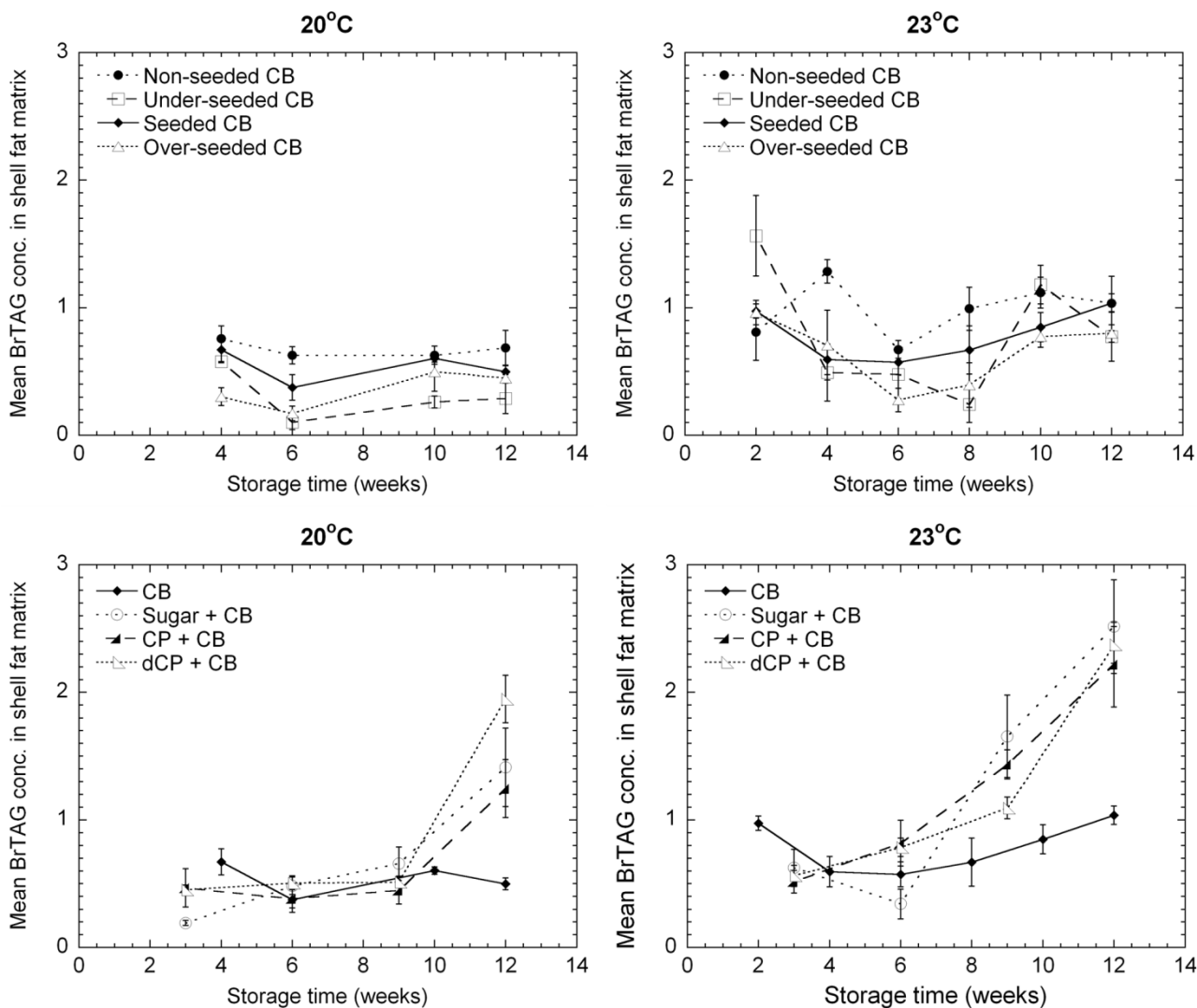
Figure 11. Mean BrTAG concentration in shell fat matrix as a function of storage time for model pralines stored at 20°C and 23°C. Error bars represent the standard error of mean of 4 replicates.

DISCUSSION

The microstructure of the model shells was varied with respect to amount and size of crystals and the addition of different particles. All samples stored at 23°C showed a higher rate of BrTAG migration from filling to shell compared to the samples stored at 20°C. Furthermore, the samples stored at 23°C showed a higher rate of polymorphic development into more stable crystals and also a higher rate of developing fat crystals at the surface compared to the samples stored at 20°C. Due to the size and shape of the developed surface crystals that can be seen in LV SEM images, these crystals are observed as fat bloom crystals. The DSC results in Figure 2 showed that the CB TAGs of all samples are mainly in form $\beta_2 V$, two days after production. Furthermore, after 12 weeks storage at 23°C the polymorphic behaviour has developed towards form $\beta_1 VI$ for all samples.

The non-seeded CB samples had developed the largest and highest frequency of fat bloom crystals at the surface compared to all other samples as was shown in Figure 4 and Figure 5. This could be observed for both storage temperatures. In addition, these samples had developed the highest amount of β_1VI crystals after 12 weeks storage at 20°C and after 6 weeks storage at 23°C, which could be connected to fat bloom development. Furthermore, at 23°C storage temperature the developed roughness was evidently higher for the non-seeded CB samples compared to all other samples. The under-seeded CB samples showed a higher development of roughness compared to the seeded and over-seeded CB samples at both storage temperatures. This was also the case regarding the frequency of developed fat bloom crystals at the surface, which could be observed in the LV SEM images (Figure 5). Still, the most obvious difference between the CB samples with varied amount of seed crystals was shown by the over-seeded CB samples where the roughness values stayed approximately at the same level over time at both storage temperatures. These samples also showed the lowest frequency of developed fat bloom crystals at the surface. The topological imperfections observed at the surface of the over-seeded CB samples and the initial Rq values (Table 3) could be a result of the more homogeneous fat crystal network created upon seeding. Thus, considering the CB samples, all results regarding surface topology development and polymorphic development point in the same direction, i.e. the non-seeded CB samples showed the highest rate of fat bloom development whereas the over-seeded CB samples showed the lowest rate of fat bloom development.

The seeded samples containing CP and dCP showed a higher development of roughness compared to the seeded samples with sugar, but most importantly, the particle containing samples showed a higher roughness than the seeded CB samples without particles at a storage temperature of 23°C. Further, CP and dCP samples indicated on a higher frequency of fat bloom crystals at the surfaces, when stored at 23°C, compared to the sugar samples and the seeded CB samples, as shown in the LV SEM results (Figure 5). In addition, the development of β_1VI crystals could be observed for all samples containing particles in the DSC results after 6 weeks storage at 23°C, indicating on fat bloom development (Figure 2 and Figure 3). The relative amount of β_1VI crystals was higher for the samples containing dCP and CP compared to the samples containing sugar and the seeded CB-samples. Thus, all these results coincide and clearly indicate that fat bloom development is enhanced in the presence of particles and further, that the presence of CP and dCP seem to influence the fat bloom development to a higher extent than the presence of sugar particles, which can be related to specific surface area.

The migration results show clear differences in migration rate between storage temperatures and between the samples with varied shell microstructure. CB samples stored at 20°C showed a low migration rate, which coincide with the polymorphic development, the low roughness

values and the insignificant fat boom development at the surface. Still, the non-seeded CB samples stored at 20°C developed $\beta_1 VI$ crystals and fat bloom crystals at the surface after 12 weeks storage, indicating on a fat bloom development which is rather due to the re-crystallisation of unstable, low-melting CB TAG crystals into form $\beta_1 VI$ than to migration induced fat bloom. On the other hand, CB samples stored at 23°C indicated on a rapid initial migration of filling fat into the shell close to the shell-filling interface. This initial migration appears to be pushed back into the filling during the first weeks until a minimum is reached after 6 weeks of storage when the migration continues deeper into the shell. At these larger distances from the interface a clear difference could be observed between the CB samples. The concentration of migrated BrTAGs is higher for non-seeded CB samples compared to the seeded CB samples, and especially compared to the over-seeded CB samples which show very low concentrations of migrated BrTAGs in the outer part of the shells. These results coincide with the roughness values, the polymorphic development and the development of fat bloom crystals at the surface.

The seeded samples containing particles show an evidently faster rate of migration compared to the seeded CB samples. The initial migration is still high close to the interface, but continues to increase over time and goes deeper into the shell at an earlier stage compared to the seeded CB samples. This observation is especially evident for the samples containing dCP and CP. These results coincide with the polymorphic development, the development of fat bloom crystals at the surface and the roughness values.

The differences in migration rate and fat bloom development between the storage temperatures could be explained by a higher liquid fat fraction in the shell and the filling at a higher storage temperature. Since the migration of TAGs takes place via the liquid fat portions, permeability increases and therefore migration-induced fat bloom development is enhanced when the storage temperature is increased. The observed effect of higher rate of migration during higher storage temperature agrees with results from earlier studies [16, 19, 27-29]. Further, the observed initial high migration rate for CB samples stored at 23°C and the differences in migration rate between seeded and non-seeded CB samples can be supported by research done by Svanberg et al. [30] where large differences in local diffusion rates could be observed immediately after cooling non-seeded and seeded CB samples. They observed that non-seeded samples had significantly higher diffusion rates, still, after one week of storage the differences between the seeded and the non-seeded samples were less pronounced as the local diffusion rate in the non-seeded samples had decreased significantly, and the local diffusion rate for the seeded samples remained constantly low. The differences in migration rate and fat bloom formation between the samples with varied crystallisation regimes could further be explained by the more uniform fat crystallisation when applying seeding where the CB contracts upon solidification. This would give a more homogeneous

23

crystal network compared to non- or under-seeded CB samples, which in contrast would create a more heterogeneous crystal network upon solidification with larger inter-crystalline spaces increasing the rate of migration and thus fat bloom development [1, 34]. A more homogeneous crystalline structure will retard migration, thus also the migration-induced fat bloom development due to higher resistance to entry of filling fat into the shell. Lower rates of migrating filling oil in well crystallised samples compared to under-tempered samples correlates with earlier studies [4, 14, 16, 30-32]. In addition, researches have shown that non-seeding and under-tempering give a wide crystal size distribution resulting in a more heterogeneous microstructure with domains of liquid fat, while seeded or optimally tempered samples create a more homogenous microstructure with crystals in a network with more defined inter-crystal connections [30, 37, 56]. The migration results show that the data of the non-seeded and under-seeded CB samples stored at 23°C are fluctuating to a high extent. This could be a result of a more heterogeneous, non-ordered crystal network where growing fat bloom crystals give rise to a coarse structure of the shells. The over-seeded CB samples indicate on having a fat crystal network consisting of a larger amount of $\beta_2 V$ crystals compared to the non-seeded CB samples which have a larger amount of $\beta_1 VI$ crystals, as could be seen in Figure 3. Thus, these differences can contribute to differences in the microstructure, where a CB shell consisting of a large amount of $\beta_1 VI$ crystals gives a more heterogeneous microstructure with liquid domains, while the over-seeded CB samples posses a more homogenous structure.

It has been suggested that non-fat particles such as CP and sugar retard the oil migration rate, mainly due to their contribution to increase of the tortuosity of the diffusion path for migrating lipids [57]. However, our observations show that after 12 weeks storage at both storage temperatures the amount of migrated BrTAGs had increased for samples containing CP, dCP and sugar compared to the seeded CB samples. These findings are supported by Motwani et al. [31] who found that the migration of peanut oil was enhanced upon addition of cocoa particles to CB. They suggested that the presence of cocoa particles could reduce the compactness of the fat crystal network resulting in higher rate of migration. We suggest that the particles could create pathways with higher permeability in the shell matrix where the migrating liquid fat could migrate, possibly along the surfaces of the particles. Furthermore, our results showed that samples containing sugar particles indicated on lower migration rates, developed lower frequency of fat bloom crystals and lower roughness values compared to the samples containing CP and dCP, but still higher than for samples without particles. Still, between the CP and dCP samples no evident differences could be observed regarding, migration rates, surface topology development or polymorphic development, suggesting that the included fat in CP does not influence the migration rate or fat bloom development to any higher extent. However, the CP had a larger specific surface area than the sugar particles, i.e. the CP were smaller (see Table 2), which suggests that the size of the added particles

has a higher impact on migration and fat bloom development than the character of the particles. In addition, Altimiras et al. [23] could show that samples containing particles of a smaller size had a higher oil migration rate than samples containing larger particles. Thus, it can be assumed that the particles create disturbances in the fat crystal network and that the particle surfaces can influence the fat crystallisation process. Further, it has been suggested that addition of particles to CB enhances crystal growth through heterogeneous nucleation [37, 58]. Dhonsi et al. [58] suggested that the presence of sugar promotes formation of lower melting polymorphs, by acting as an aid to heterogeneous nucleation on the sugar crystals. This can be supported from the DSC results in Figure 3, where a higher amount of unstable, low melting crystals could be observed in all samples containing particles. Thus, it may be speculated that the volume next to the surface of the particles represents a heterogeneity in the structure and that the fat crystal density is lower in the vicinity of the particles than on average. This would result in increased possibility for oil migration close to the particle surfaces, and hence more rapid development of fat bloom.

The BrTAG concentrations that can be observed in the model shells are relatively high compared to the initial BrTAG concentration in the filling, especially when stored at 23°C. The fat component in a chocolate system is a multi phase system, but we may consider it as a two phase system, with one migrating liquid phase and one solid resident, crystalline phase. The filling fat has a lower SFC than the shell fat phase due to the addition of liquid fat, i.e. triolein and BrTAGs. The solid fat content of the shell is $\varphi_{(SFC\text{-}shell,23°C)} = 73\%$ and of the filling fat $\varphi_{(SFC\text{-}ModelFilling,23°C)} = 47\%$ (SFC values were measured for equal samples according to the official AOCS Cd16b-93 method by using NMR, and obtained through personal communication with Ghent University, Belgium). Thus, the BrTAG content of the liquid phase of the filling is approximately 9.4%. The total liquid phase is distributed between the shell, 30%, and the filling, 70%. The average concentration of BrTAGs in the liquid fat phase at equilibrium between the liquid phase of the shell and the liquid phase of the filling will thus be 7.5%. However, we have observed the BrTAG concentration as the composition of the total shell fat matrix in our measurements which would be 2.1% BrTAGs, assuming that the liquid fraction remains constant. The observed concentrations are in several of the systems, particularly in the particle systems (Figure 8), well above the equilibrium level.

The main transport mechanism in confectionery systems is often referred to as molecular diffusion through the liquid phase, where the process is driven by a gradual equilibration of concentration differences [6-8, 12-16.] According to the diffusion laws we expect the triolein and the BrTAGs to diffuse in the direction of the shell while low melting CB TAGs would diffuse in the opposite direction. However, the liquid phase of the model filling is saturated by CB TAGs. Since the fat phase of the shell is further saturated by CB, dissolution of CB crystals in the shell fat matrix is not expected to occur to any substantial extent. The highest obtainable BrTAG concentration in

the liquid phase of the shell should correspond to the equilibrium concentration. From the profiles (Figure 8) and the averages (Figure 11) at 23°C, higher values could be observed, especially for the systems containing particles. Further, the migration profiles themselves at 23°C (Figure 8) disagree with a Fickian diffusion model. The slope of the concentration curve is high between 0 and 800 μm and the concentration is more or less constant between 800 and 1400 μm after 2-6 weeks, depending on the sample. After this storage time the complete curve has moved forward and upwards. A diffusion process following Fick´s second law should rather lead to a reduced slope, a constant or falling concentration close to the interface and the highest increase at the position were the second derivate of the concentration curve reaches its maximum. The profiles, the concentrations at different levels and the total flux leads to similar conclusion also at 20°C, although the magnitude of the migration is smaller and thereby the experimental certainty becomes more of a problem.

Another mechanism that has been discussed for oil migration in chocolate systems is capillary flow [17-22]. Observed protrusions originating from flow through surface pores have been characterised using profilometry, LV SEM and confocal Raman microscopy [24-25]. Still, measurements of the porosity of chocolate using mercury porosimetry [26] suggested that the pore volume is between 1 and 4%, which is a too small volume to explain the observed level of migration.

An additional model is a convective[*] flow mobilising liquid fat from the filling into the shell due to pressure differences. A convective flow just replacing the liquid fat in the penetrated fat matrix of the shell with the liquid fraction of the filling fat would lead to a BrTAG concentration rapidly reaching the maximum concentration possible, i.e. 2.1%. However, as observed, concentrations are above this level and it suggests that more than the initial level of liquid fat phase is entering into the shell matrix. The observed swelling of the shells and the increase of liquid fraction in the shells could be a possible explanation. Unfortunately, we did not characterise the relative volumes of shell and filling to confirm this hypothesis. However, swelling due to oil migration has been observed previously of CB matrixes in contact with liquid fat [12, 19, 24, 57, 59]. When storing white chocolate against a hazelnut filling at a cycled temperatures, Dahlenborg et al.[24] could observe a volume increase in the shells of approximately 40% after 36 weeks. Further, Galdamez et al. [57] observed an increase of approximately 25% in chocolate shell weight after storage against hazelnut oil at 23°C for one week, which corresponded to an increase of 61 wt% regarding the fat phase of the shell. We suggest that a likely scenario for a swelling could be crystal growth in the CB matrix due to Ostwald ripening and re-crystallisation into more stable

---

[*] We use the general definition of convective flow as a flow generated by a pressure gradient.

polymorphs. If the number concentration of the larger network forming crystals is constant while the crystals are growing in size the network will coarsen and absorb an increasing amount of liquid phase. This effect may be further strengthened by the presence of non-fat particles that may magnify the impact of a coarsening fat crystal network. Further, due to the possibly higher amount of low melting crystals and domains of liquid fat in the destructed fat crystal network, we suggest that the presence of particles would increase the permeability and thereby increase the consequences of a pressure driven convective flow of liquid fat resulting in fat bloom development at the surface. Thus we argue that there is an initial phase of molecular diffusion followed by re-crystallisation processes and crystal growth leading to a coarsening of the network and a convective oil migration into the expanding shell matrix.

This study shows that the microstructural changes, induced by means of different tempering or seeding, addition of different particles and storage conditions can be used to influence migration behaviour and thus, fat bloom development. Further, it is shown that migration of BrTAGs into the shells and the fat bloom development is highly correlated to the "quality" of crystallisation of the shells. A shell microstructure of a hand-tempered-like CB shell induced the highest initial migration rate of filling oil into the shell together with the highest frequency of developed fat bloom crystals and the highest rate of roughness development. When applying seeding to the CB shell lower migration rate, lower frequency of fat bloom crystals and lower rate of roughness development could be observed. However, when adding particles to the seeded CB shell there was a noticeably higher migration rate over time together with higher frequency of fat bloom crystals and higher rate of surface roughness development. This was especially evident for the samples containing cocoa particles, suggesting that particles and especially smaller particles enhance the migration rate of filling oil into the shell. Convective flow is suggested to be an important contribution to the migration in addition to molecular diffusion.

ABBREVIATIONS USED

TAG, triacylglycerols; CB, cocoa butter; CP, cocoa particles; dCP, defatted cocoa particles; LV SEM, low vacuum scanning electron microscope; EDS, energy dispersive X-ray spectroscopy; DSC, differential scanning calorimetry; Rq, roughness; BrTAG, brominated triacylglycerols; SFC, solid fat content; PSD, particle size distribution; HPLC, High Performance Liquid Chromatography.

AUTHOR INFORMATION

Corresponding author

*(H.D) E-mail: hanna.dahlenborg@sp.se

Notes

The authors declare no competing financial interest.

ACKNOWLEDGEMENT

REFERENCES

(1) Ghosh, V.; Ziegler, G. R.; Anantheswaran, R. C. Fat, Moisture, and Ethanol Migration through Chocolates and Confectionary Coatings *Critical Reviews in Food Science and Nutrition* **2002,** *42* (6), 583 – 626.

(2) Hartell, R. W. Chocolate: Fat bloom during storage. *The Manufacturing Confectioner* **1999**, 89-99.

(3) Talbot, G. Fat migration in biscuits and confectionery systems. *Confectionery production* **1990**, 265-272.

(4) Smith, K. W.; Cain, F. W.; Talbot, G. Effect of nut oil migration on polymorphic transformation in a model system. *Food Chemistry* **2007,** *102* (3), 656-663.

(5) Lonchampt, P.; Hartel, R. W. Fat bloom in chocolate and compound coatings. *European Journal of Lipid Science and Technology* **2004,** *106* (4), 241-274.

(6) Ziegleder, G., Moser, C., Geiger-Greguska, J. Kinetics of fat migration in chocolate products part I: Principles and analythical aspects. *Fett/Lipid* **1996,** *98*, 196-199.

(7) Ziegleder, G., Moser, C., Geiger-Greguska, J. Kinetics of fat migration in chocolate products part II: Influence of storage temperature, diffusion coefficient, solid fat content. *Fett/Lipid* **1996,** *98*, 253-256.

(8) Ziegleder, G.; Schwingshandl, I. Kinetics of fat migration within chocolate products. Part III: fat bloom. *Fett/Lipid* **1998,** *100* (9), 411-415.

(9) Ziegleder, G. Fat migration and bloom. *The Manufacturing Confectioner* **1997**, 43-44.

(10) Wille, R.; Lutton, E. Polymorphism of cocoa butter. *Journal of the American Oil Chemists Society* **1966,** *43* (8), 491-496.

(11) Kinta, Y.; Hatta, T. Composition and structure of f at bloom in untempered chocolate. *Journal of Food Science* **2005,** *70* (7), 450-452.

(12) Deka, K.; MacMillan, B.; Ziegler, G. R.; Marangoni, A. G.; Newling, B.; Balcom, B. J. Spatial mapping of solid and liquid lipid in confectionery products using a ID centric SPRITE MRI technique. *Food Research International* **2006,** *39* (3), 365-371.

(13) Lee, W. L.; McCarthy, M. J.; McCarthy, K. L. Oil Migration in 2-Component Confectionery Systems. *Journal of Food Science* **2010,** *75* (1), 83-89.

(14) Maleky, F.; McCarthy, K. L.; McCarthy, M. J.; Marangoni, A. G. Effect of Cocoa Butter Structure on Oil Migration. *Journal of Food Science* **2012,** *77* (3), 74-79.

(15) McCarthy, K. L.; McCarthy, M. J. Oil migration in chocolate-peanut butter paste confectionery as a function of chocolate formulation. *Journal of Food Science* **2008,** *73* (6), 266-273.

(16) Miquel, M. E.; Carli, S.; Couzens, P. J.; Wille, H. J.; Hall, L. D. Kinetics of the migration of lipids in composite chocolate measured by magnetic resonance imaging. *Food Research International* **2001,** *34* (9), 773-781.

(17) Choi, Y. J.; McCarthy, K. L.; McCarthy, M. J. Oil migration in a chocolate confectionery system evaluated by magnetic resonance imaging. *Journal of Food Science* **2005,** *70* (5), 312-317.

(18) Choi, Y. J.; McCarthy, K. L.; McCarthy, M. J.; Kim, M. H. Oil migration in chocolate. *Applied Magnetic Resonance* **2007,** *32* (1-2), 205-220.

(19) Guiheneuf, T. M.; Couzens, P. J.; Wille, H.-J.; Hall, L. D. Visualisation of Liquid Triacylglycerol Migration in Chocolate by Magnetic Resonance Imaging. *Journal of the Science of Food and Agriculture* **1997,** *73* (3), 265-273.

(20) Marty, S.; Baker, K.; Dibildox-Alvarado, E.; Rodrigues, J. N.; Marangoni, A. G. Monitoring and quantifying of oil migration in cocoa butter using a flatbed scanner and fluorescence light microscopy. *Food Research International* **2005,** *38* (10), 1189-1197.

(21) Quevedo, R.; Brown, C.; Bouchon, P.; Aguilera, J. M. Surface roughness during storage of chocolate: Fractal analysis and possible mechanisms. *Journal of the American Oil Chemists Society* **2005,** *82* (6), 457-462.

(22) Rousseau, D.; Smith, P. Microstructure of fat bloom development in plain and filled chocolate confections. *Soft Matter* **2008,** *4* (8), 1706-1712.

(23) Altimiras, P.; Pyle, L.; Bouchon, P. Structure-fat migration relationships during storage of cocoa butter model bars: Bloom development and possible mechanisms. *Journal of Food Engineering* **2007,** *80* (2), 600-610.

(24) Dahlenborg, H.; Millqvist-Fureby, A.; Bergenstahl, B.; Kalnin, D. J. E. Investigation of Chocolate Surfaces Using Profilometry and Low Vacuum Scanning Electron Microscopy. *Journal of the American Oil Chemists Society* **2011,** *88* (6), 773-783.

(25) Dahlenborg, H.; Millqvist-Fureby, A.; Brandner, B. D.; Bergenstahl, B. Study of the porous structure of white chocolate by confocal Raman microscopy. *European Journal of Lipid Science and Technology* **2012,** *114* (8), 919-926.

(26) Loisel, C.; Lecq, G.; Ponchel, G.; Keller, G.; Ollivon, M. Fat bloom and chocolate structure studied by mercury porosimetry. *Journal of Food Science* **1997,** *62* (4), 781-788.

(27) Ali, A.; Selamat, J.; Man, Y. B. C.; Suria, A. M. Effect of storage temperature on texture, polymorphic structure, bloom formation and sensory attributes of filled dark chocolate. *Food Chemistry* **2001,** *72* (4), 491-497.

(28) Khan, R. S.; Rousseau, D. Hazelnut oil migration in dark chocolate - kinetic, thermodynamic and structural considerations. *European Journal of Lipid Science and Technology* **2006,** *108* (5), 434-443.

(29) Altan, A.; Lavenson, D. M.; McCarthy, M. J.; McCarthy, K. L. Oil Migration in Chocolate and Almond Product Confectionery Systems. *Journal of Food Science* **2011,** *76* (6), 489-494.

(30) Svanberg, L.; Ahrne, L.; Loren, N.; Windhab, E. Effect of pre-crystallization process and solid particle addition on microstructure in chocolate model systems. *Food Research International* **2011,** *44* (5), 1339-1350.

(31) Motwani, T.; Hanselmann, W.; Anantheswaran, R. C. Diffusion, counter-diffusion and lipid phase changes occurring during oil migration in model confectionery systems. *Journal of Food Engineering* **2011,** *104* (2), 186-195.

(32) Svanberg, L.; Ahrne, L.; Loren, N.; Windhab, E. Impact of pre-crystallization process on structure and product properties in dark chocolate. *Journal of Food Engineering* **2013,** *114* (1), 90-98.

(33) Larsson, K. Classification of glyceride crystal forms. *Acta Chemica Scandinavica* **1966,** *20*, 2255-2260.

(34) Zeng, Y.; Braun, P.; Windhab, E. J. Tempering: Continous precrystallization of chocolate with seed cocoa butter crystal suspension. *The Manufacturing Confectioner* **2002,** *82* (4), 71-80.

(35) Hachiya, I.; Koyano, T.; Sato, K. Seeding Effects on Solidification Behavior of Cocoa Butter and Dark Chocolate.1. Kinetics of Solidification. *Journal of the American Oil Chemists Society* **1989,** *66* (12), 1757-1762.

(36) Hachiya, I.; Koyano, T.; Sato, K. Seeding Effects on Solidification Behavior of Cocoa Butter and Dark Chocolate. 2. Physical-Properties of Dark Chocolate. *Journal of the American Oil Chemists Society* **1989,** *66* (12), 1763-1770.

(37) Svanberg, L.; Ahrne, L.; Loren, N.; Windhab, E. Effect of sugar, cocoa particles and lecithin on cocoa butter crystallisation in seeded and non-seeded chocolate model systems. *Journal of Food Engineering* **2011,** *104* (1), 70-80.

(38) Windhab, E. J. New developments in crystallization processing. *Journal of Thermal Analysis and Calorimetry* **1999,** *57* (1), 171-180.

(39) Afoakwa, E., Ohene; Paterson, A.; Fowler, M.; Vieira, J. Microstructure and mechanical properties related to particle size distribution and composition in dark chocolate. *International Journal of Food Science & Technology* **2009,** *44* (1), 111-119.

(40) Walter, P.; Cornillon, P. Lipid migration in two-phase chocolate systems investigated by NMR and DSC. *Food Research International* **2002,** *35* (8), 761-767.

(41) Kinta, Y.; Hatta, T. Composition, structure, and color of fat bloom due to the partial liquefaction of fat in dark chocolate. *Journal of the American Oil Chemists Society* **2007,** *84* (2), 107-115.

(42) Depypere, F.; De Clercq, N.; Segers, M.; Lewille, B.; Dewettinck, K. Triacylglycerol migration and bloom in filled chocolates: Effects of low-temperature storage. *European Journal of Lipid Science and Technology* **2009,** *111* (3), 280-289.

(43) Nightingale, L. M.; Lee, S. Y.; Engeseth, N. J. Impact of Storage on Dark Chocolate: Texture and Polymorphic Changes. *Journal of Food Science* **2011,** *76* (1), 142-153.

(44) Sonwai, S.; Rousseau, D. Controlling fat bloom formation in chocolate - Impact of milk fat on microstructure and fat phase crystallisation. *Food Chemistry* **2010,** *119* (1), 286-297.

(45) Sonwai, S.; Rousseau, D. Fat crystal growth and microstructural evolution in industrial milk chocolate. *Crystal Growth & Design* **2008,** *8* (9), 3165-3174.

(46) Smith, P. R.; Dahlman, A. The use of atomic force microscopy to measure the formation and development of chocolate bloom in pralines. *Journal of the American Oil Chemists Society* **2005,** *82* (3), 165-168.

(47) Rousseau, D.; Sonwai, S. Influence of the dispersed particulate in chocolate on cocoa butter microstructure and fat crystal growth during storage. *Food Biophysics* **2008,** *3* (2), 273-278.

(48) Hodge, S. M.; Rousseau, D. Fat bloom formation and characterization in milk chocolate observed by atomic force microscopy. *Journal of the American Oil Chemists Society* **2002,** *79* (11), 1115-1121.

(49) Rousseau, D. On the porous mesostructure of milk chocolate viewed with atomic force microscopy. *Food Science and Technology* **2006,** *39* (8), 852-860.

(50) Briones, V. Scale-sensitive fractal analysis of the surface roughness of bloomed chocolate. *Journal of the American Oil Chemists Society* **2006,** *83* (3), 193-199.

(51) Rousseau, D.; Sonwai, S.; Khan, R. Microscale Surface Roughening of Chocolate Viewed with Optical Profilometry. *Journal of the American Oil Chemists Society* **2010,** *87* (10), 1127-1136.

(52) James, B. J.; Smith, B. G. Surface structure and composition of fresh and bloomed chocolate analysed using X-ray photoelectron spectroscopy, cryo-scanning electron microscopy and environmental scanning electron microscopy. *Food Science and Technology* **2009,** *42* (5), 929-937.

(53) Alasalvar, C.; Amaral, J. S.; Satir, G.; Shahidi, F. Lipid characteristics and essential minerals of native Turkish hazelnut varieties (Corylus avellana L.). *Food Chemistry* **2009,** *113* (4), 919-925.

(54) Amaral, J. S.; Cunha, S. C.; Santos, A.; Alves, M. R.; Seabra, R. M.; Oliveira, B. P. P. Influence of cultivar and environmental conditions on the triacylglycerol profile of hazelnut (Corylus avellana L.). *Journal of Agricultural and Food Chemistry* **2006,** *54* (2), 449-456.

(55) Bernardo-Gil, M. G.; Grenha, J.; Santos, J.; Cardoso, P. Supercritical fluid extraction and characterisation of oil from hazelnut. *European Journal of Lipid Science and Technology* **2002,** *104* (7), 402-409.

(56) Afoakwa, E. O.; Paterson, A.; Fowler, M.; Vieira, J. Influence of tempering and fat crystallization behaviours on microstructural and melting properties in dark chocolate systems. *Food Research International* **2009,** *42* (1), 200-209.

(57) Galdamez, J. R.; Szlachetka, K.; Duda, J. L.; Ziegler, G. R. Oil migration in chocolate: A case of non-Fickian diffusion. *Journal of Food Engineering* **2009,** *92* (3), 261-268.

(58) Dhonsi, D.; Stapley, A. G. F. The effect of shear rate, temperature, sugar and emulsifier on the tempering of cocoa butter. *Journal of Food Engineering* **2006,** *77* (4), 936-942.

(59) Svanberg, L.; Loren, N.; Ahrne, L. Chocolate Swelling during Storage Caused by Fat or Moisture Migration. *Journal of Food Science* **2012,** *77* (11), 328-334.

IV

Effect of particle size in chocolate shell on oil migration and fat bloom development

*Hanna Dahlenborg[a, b, *], Anna Millqvist-Fureby[a], and Björn Bergenståhl[b]*

[a]SP Chemistry, Materials and Surfaces, Box 5607, SE-114 86 Stockholm, Sweden

[b]Lund University, Department of Food Technology, Engineering and Nutrition, P.O. Box 124, SE-221 00 Lund, Sweden

* Corresponding author. E-mail: hanna.dahlenborg@sp.se; Mobile: +46 70 587 60 62; Fax: +46 8 20 89 98

Abstract

The effects of chocolate shell particle size were investigated by means of its influence on rate of oil migration and fat bloom development. The particle size of the non-fat particles in the chocolate, i.e. sugar and cocoa particles was varied between 15, 22 and 40 µm. A novel set of analytical techniques was used and by combining migration results with surface topology results clear differences could be observed between the samples. At 23°C storage the samples with a particle size of 15 µm showed significantly higher rate of oil migration and further, the earliest development of fat bloom at the surface. This could be observed both macroscopically and microscopically. Thus, it appears as a larger specific surface area of the non-fat particles facilitates migration of filling oil, possibly due to a more heterogeneous and coarser crystal network with higher permeability. Molecular diffusion cannot explain the level of oil migration observed and, thus, convective flow is assumed to be an important contribution in addition to the molecular diffusion.

Key words

Chocolate, Cocoa butter, Particle size, Fat bloom, Migration, Surface structure

1. Introduction

Migration of the internal filling fat into the surrounding chocolate shell in chocolate pralines is a major concern for the confectionery industry. This migration leads to textural quality loss in addition to fat bloom development, giving the product a dull, whitish haze resulting in rejection by the consumers (Ghosh et al., 2002; Hartell, 1999; Lonchampt & Hartel, 2004; Smith et al., 2007; Talbot, 1990). The driving force behind this migration is usually explained by a triacylglycerol (TAG) concentration gradient between the liquid filling fat and the liquid cocoa butter (CB) in the chocolate shell, tending towards a thermodynamic equilibrium (Ziegleder, 1996a; Ziegleder, 1996b; Ziegleder & Schwingshandl, 1998). However, the mechanism of oil migration in chocolate pralines is not yet fully understood, and it has been explained by molecular diffusion (Deka et al., 2006; Lee et al., 2010; Maleky et al., 2012; McCarthy & McCarthy, 2008; Miquel et al., 2001; Ziegleder, 1996a; Ziegleder, 1996b; Ziegleder et al., 1998), capillary flow (Aguilera et al., 2004; Choi et al., 2007; Guiheneuf et al., 1997; Marty et al., 2005; Quevedo et al., 2005; Rousseau & Smith, 2008) and a pressure driven convective flow (Altimiras et al., 2007; Dahlenborg et al., 2011; Dahlenborg et al., 2012; Loisel et al., 1997).

Due to migration of liquid fat from the filling, the solid fat content (SFC) is reduced in the chocolate shell in addition to polymorphic changes within the solid fat phase (Motwani et al., 2011; Timms, 1984). These polymorphic changes are usually connected to formation of fat bloom, where form $\beta_1 VI$, the most stable CB TAG polymorph, has developed within the chocolate fat matrix (Smith et al., 2007; Wille & Lutton, 1966). Further, when the needle shaped $\beta_1 VI$ crystals are formed on the chocolate surface and these are larger than 5 µm, a whitish haze, connected to fat bloom, appears due to scattering of light (Hartell, 1999; Kinta & Hatta, 2005; Lonchampt et al., 2004). In contrast, when producing chocolate products the desired crystalline form or polymorph of the CB TAGs is $\beta_2 V$, which is achieved when it undergoes a controlled crystallisation during production.

The rate of oil migration can be influenced by different parameters. Higher storage temperatures have shown to increase the migration rate (Ali et al., 2001; Altan et al., 2011; Dahlenborg et al., 2014; Guiheneuf et al., 1997; Khan & Rousseau, 2006; Miquel et al., 2001; Ziegleder et al., 1998), and the chocolate shell microstructure has also been shown to affect the migration rate (Dahlenborg et al., 2014; Lee et al., 2010; Maleky et al., 2012; Miquel et al., 2001; Motwani et al., 2011; Svanberg et al., 2011; Svanberg et al., 2013). Studies have demonstrated that by using different ways of pre-crystallisation, e.g. by following a defined tempering scheme or by using a seeding programme, differences in crystal size and crystal density of the product can be achieved, and thus, the rate of oil diffusion is affected (Svanberg et al., 2011; Svanberg et al., 2013).

Another way of changing the microstructure of the chocolate shell is by varying the particle size of the non-fat ingredients, i.e. sugar crystals and cocoa particles, and in some cases milk particles. It has been suggested that larger particles give rise to a higher migration rate (Choi et al., 2007). However, other researchers have also reported the opposite, i.e. that smaller particles give rise to a higher migration rate (Altimiras et al., 2007).

Thus, the objective of this study is to further investigate the influence of particle size on oil migration and fat bloom development in chocolate pralines by combining a set of novel analytical techniques. Model pralines with a chocolate shell of varied particle size were analysed as a function of time and storage temperature. By using profilometry combined with low vacuum scanning electron microscopy (LV SEM) the surface microstructure development could be monitored. This was further connected to the migration data produced by energy dispersive X-ray spectroscopy (EDS) analyses of labelled oil. The particle size in a chocolate product is an accessible parameter for the industry, thus the study of the particle size influence on migration and fat bloom is of relevant interest.

2. Materials and methods

2.1 Materials

Model pralines, consisting of a filling layer in contact with a shell layer, were produced on a lab scale. The model filling consisted of 73 wt% CB (Bühler AG, Uzwil, Switzerland), 22 wt% triolein (OOO) (Penta Manufacturing, New Jersey) and 5 wt% brominated vegetable oil (BrTAG) (Penta Manufacturing, New Jersey) with an estimated molar mass of 978 g·mol^{-1}. This composition yielded a sufficiently hard filling with a solid fat content (SFC) of 53% at 20°C, and without any separation of BrTAGs. In order to mimic a fat based filling the amount of added triolein was based on the assumption that hazelnut paste contains approximately 70% triolein (Alasalvar et al., 2009; Amaral et al., 2006; Bernardo-Gil et al., 2002). This corresponds to 22% triolein of total fat content in a typical hazelnut based filling and thus, the model filling contained 22% triolein on a total fat basis. The shells consisted of dark chocolate that was ground into varied particle size, i.e. 15, 22 and 40 μm, respectively. These particle sizes are referring to the largest particle size (D$_{90}$) from the analysed particle size distribution (PSD) of the ground chocolate masses by using laser diffraction (Malvern Mastersizer 2000, Malvern, UK). Table 1 shows the PSD of the non-fat particles (sugar and cocoa particles) included in the three chocolate masses. The chocolate masses were kindly produced and ground at Bühler AG, Uzwil, Switzerland. Table 2 shows the composition of the chocolate shells and the filling. The premade seed CB crystal suspension, containing crystals of

form $\beta_1 VI$, that was used for seeding was kindly supplied by Swiss Federal Institute of Technology, ETH (Zurich, Switzerland).

Table 1. Particle size distribution (PSD) represented by volume fractions 10%, D(v, 0.1); 50%, D(v, 0.5); 90%, D(v, 0.9), Sauter mean diameter, D[3.2], and specific surface area of chocolate masses.

Model system	D(v, 0.1) (µm)	D(v, 0.5) (µm)	D(v, 0.9) (µm)	D[3.2] (µm)	Specific surface area (m^2/g)
15 µm	1.268	5.009	14.547	3.002	2
22 µm	1.452	6.535	22.441	3.586	1.67
40 µm	1.633	8.034	40.302	4.141	1.45

Table 2. Composition of shells and filling.

Model system	CB (wt%)	CB seeds (wt%)	Sugar (wt%)	Cocoa particles (wt%)	Lecithin (wt%)	Triolein (wt%)	BrTAG (wt%)	Fat content (wt%)
15 µm	30.4	1.2	50	18	0.4			32
22 µm	30.4	1.2	50	18	0.4			32
40 µm	30.4	1.2	50	18	0.4			32
Filling	69.4	3.6				22	5	100

2.2 Production of model systems

In order to keep a controlled production, seed tempering was applied. The CB seeds were stirred and heated in a sealed beaker in a water bath, to a temperature of 33 - 33.7°C prior to mixing with the shell and filling masses. The model systems consisted of a filling layer (a disc of 10 mm in diameter and 3 mm high) in contact with a chocolate shell layer (a disc of 10 mm in diameter and 1.5 mm high) as can be seen in Figure 1A. By keeping the chocolate masses and the filling mixture in an oven, set to a temperature of 50°C for 24hrs, presence of crystal nuclei could be prevented. The chocolate shells, with particle sizes of 15, 22 and 40 µm, were prepared in a first step. The chocolate masses of 50°C were cooled in a sealed water bath at 31°C and stirred until the masses had reached a temperature of 33.8°C. This temperature was held for 2 minutes and then the heated CB seeds were added to the chocolate masses, which were then stirred for 3 minutes at a temperature of 33.7-33.8°C. The seeded chocolate was poured into 1.5 mm high moulds, that were shaken to reduce air bubbles, and then the overload was scraped of the moulds. The moulds containing chocolate shells were stored at 15°C for 30 minutes and then allowed to rest for 20 minutes at room temperature (20±0.5°C) after which the filling was added to the shells. For preparation of the model filling CB, triolein and BrTAGs at 50°C were mixed in the proportions given in Table 2. The filling was prepared in the same way as the seeded chocolate masses. Then a layer of 3 mm seeded filling was added to the shells, a process that mimics conventional praline

4

preparation. The moulds were stored at 15°C for at least 1 hour before the samples were de-moulded. This was followed by storage at 15°C for 48 hrs approximately before final storage at 20°C and 23°C.
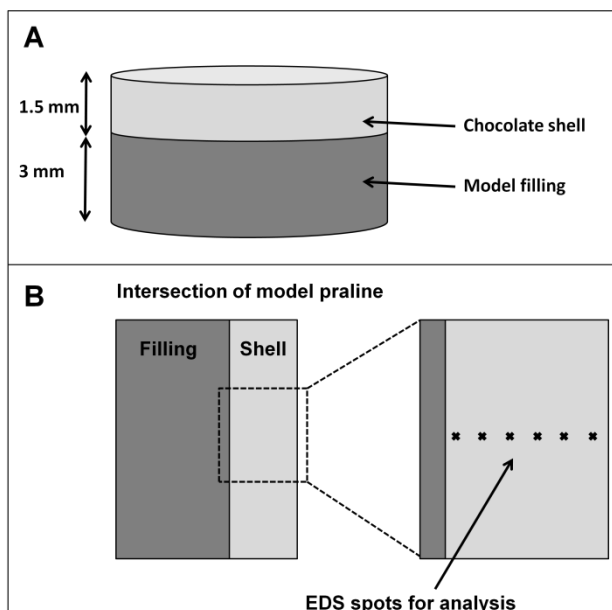

Figure 1. A: Model praline consisting of a chocolate shell layer (1.5 mm) and a model filling layer (3 mm). B: Intersection of model praline showing EDS spots for analysis.

2.3 Storage conditions

2 days after production, the model pralines were stored at two different temperature controlled environments. The samples were stored in heating cabinets (temperature accuracy ±0.5°C) where the temperature was kept at either 20°C or 23°C. The actual temperature was additionally controlled by a k-type thermocouple using a Picco Tc-08 interface for continuous measurement. At regular time intervals different analyses (LV SEM, profilometry, EDS and DSC) were performed in order to follow the development of crystal form, surface topology and migration from filling to shell.

2.4 Differential scanning calorimetry

The differential scanning calorimeter (DSC) used in this study was a Mettler Toledo DSC 1 STARe System. Sample preparation was performed by scraping off layers from a cross section of the shells to represent the whole shell. The slices were then chopped into fine small pieces before it was weighed in a pan and after which a melting curve was recorded. The samples (approximately 5 mg) were hermetically sealed in an aluminium pan and an empty pan was used as reference. The time-temperature program used was: equilibration at 3°C below storage temperature and subsequent

heating at a rate of 4°C/min to 50°C under a N$_2$ flow of 60 ml/min. Three replicates were performed at each analysis occasion.

2.5 Low vacuum scanning electron microscopy

Scanning electron microscopy (SEM) is a technique producing high resolution images of a sample surfaces. Due to the way in which the image is created, SEM images have a characteristic three-dimensional appearance and are useful for judging the surface structure of a sample. Philips XL30 environmental scanning electron microscope, equipped with a cold stage set to 5°C was used with mixed detectors (biased gaseous detector (GSE) 75% and backscattered electron detector (BSE) 25%), at 15 keV and at low vacuum mode with 0.7 – 0.9 Torr, which corresponds to a RH of 10-15% approximately. These parameters were chosen considering that they cause minimal damage of the chocolate surface, and for optimizing the imaging quality. In this study, analyses of the samples were performed without sample preparation, i.e. without coating the sample surface. This leads to a sacrifice in magnification and resolution; however, by analysing without coating the true surface can be monitored. Two samples from each environment were monitored on each analysis occasion, and the analysis was performed at different spots on the top of the pralines. After each analysis the monitored samples were sacrificed due to the possible impact from the microscope such as electron beam, temperature, humidity and pressure.

2.6 Profilometry

The surface topology of the shells was analysed using Profilometry Zygo New View 5010 (Middlefield, CT, USAL, which is a non-contact profilometry method based on white light interferometry. Since profilometry uses reflective light, the degree of light absorption to the analysed sample has no impact on the results. Therefore this technique is also applicable on dark chocolate and other light absorbing surfaces. In order to quantify the surface topology the surface roughness, Rq (μm), was analysed. Rq is the root-mean-square (rms) roughness. Thus, defined as the average of the measured height deviations taken within the evaluation length or area and measured from the mean linear surface (Eq. 1). z(x) represents the height elements along the profile and L is the number of discrete elements.

$$rms = \sqrt{\frac{1}{L}\int_0^L z^2(x)dx} \qquad (\mu m) \qquad\qquad (1)$$

Through a digital filtering (cutoff filter) of the data, the surface characteristics of the investigated surface can be broken down into waviness and roughness results. This filter includes a high filter

6

wavelength which defines the noise threshold; all shorter spatial wavelengths are considered noise. It also includes a low filter wavelength which defines the form threshold where all longer spatial wavelengths are considered form (waviness). Everything between these two wavelengths is assigned to roughness. The analysis set up used has previously been described by Dahlenborg et al. (Dahlenborg et al., 2011). By using this set up we were able to analyse the same area (±20 μm) at each analysis occasion. This enabled us to follow and compare surface changes in that specific area of interest. As a result of this, we were able to reduce noise, normally observed due to the use of different spots for data collection. Two samples from each environment were monitored, and measurements were carried out at three different spots for each sample. The analyses were performed on the top of the pralines, as for LV SEM, at room temperature (20°C approximately). After each measurement the samples were returned into their temperature-controlled environment for continued storage. The data was analysed using the advanced texture application in MetroProTM (Middlefield, CT, USA) analysis and control software.

2.7 Energy dispersive X-ray spectroscopy

Migration of BrTAGs from the filling into the chocolate shell was followed using energy dispersive X-ray spectroscopy (EDS). This is a powerful micro analytical tool that is compatible with scanning electron microscopes (SEM). EDS can be used to rapidly evaluate the elemental constituents of a sample. It is not only qualitative results that can be obtain with EDS, but also accurate quantitative results can be achieved. The generation of the electron beam is the same for EDS as for SEM. In this study, Philips XL30 environmental scanning electron microscope, equipped with a cold stage set to 5°C, was used at 15 keV and at low vacuum mode with 0.6 Torr, which corresponds to a RH of 10-15% approximately. These parameters were chosen considering that they cause minimal damage to the sample. The EDS detector used was an EDAX New XL-30, AMETEK together with the software program EDX control software. The EDS analyses were performed on an intersection of the model pralines, moving on a straight line from the filling-shell interface to the upper surface of the shells (Figure 1B). This intersection was obtained by slicing the samples with a razor blade, from one side to the other. Thus, mixing of the shell and filling could be avoided. The wt% of C, O and Br was measured over a straight line on the shell intersection at different points with fixed distances to the shell-filling interface (H cannot be detected). From each measuring point, an EDS spectrum was obtained showing relative intensities for the different analysed elements in the shell. These relative intensities were converted into wt% by a software program. By measuring at different distances from the filling and over a straight line it was possible to follow the migration of the BrTAGs through the shell. By plotting the amount of BrTAGs in the shell fat matrix as a function of the distance from the filling a migration profile could be achieved.

Two samples from each environment were monitored at each analysis occasion, and measurements were carried out at two different lines for each sample.

3. Results

3.1 Macroscopic observation

After 12 weeks of storage at 20°C no visible fat bloom could be observed, while the samples stored at 23°C had developed visible fat bloom already after 6 weeks of storage, still, to varied extent. After 8 weeks of storage at 23°C an obvious difference between the samples with varied particle size could be observed visually as can be seen in Figure 2. The samples with a particle size of 15 μm had developed the highest occurrence of fat bloom, followed by the samples with a particle size of 22 μm, and the lowest intensity of developed fat bloom was observed for the samples with a particle size of 40 μm. Further, after 15 weeks of storage at 23°C all samples showed swollen shells to some extent. Unfortunately, the relative volumes of the shells and the fillings were not characterised over time.
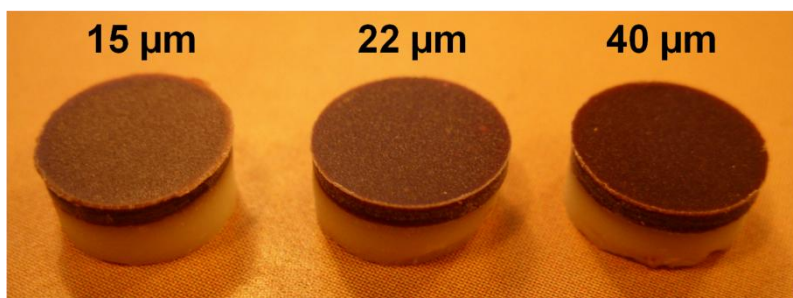

Figure 2. Model pralines with chocolate shells of varied particle size (15, 22, 40 μm), stored at 23°C for 8 weeks.

3.2 Polymorphic development

In order to compare the different samples and see how the crystal forms developed as a function of time and storage temperature, DSC was used. The DSC melting peaks were comparably wide having a single peak maximum. Figure 3 illustrates the temperatures of the peak maxima for the three different shells as a function of storage time at 20 and 23°C, respectively. It can be seen that the CB TAGs of all samples melt at approximately 32°C by week 0, i.e. 2 days after production. After storage for 14 weeks, the peak maxima for the samples stored at 20°C have increased slightly to 32.5°C, whereas for the samples stored at 23°C the peak maxima have shifted towards higher values around 34.5°C.
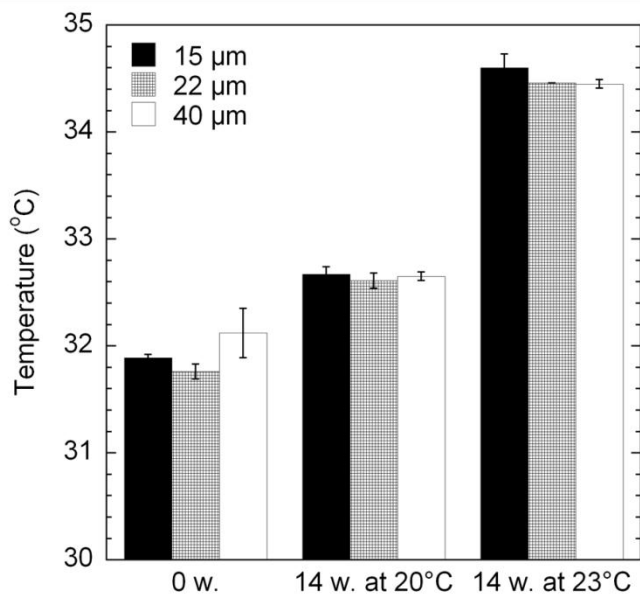
Figure 3. Peak maxima from DSC measurements showing melting temperatures of fat crystals in the different shells stored at 20 and 23°C, presented as a function of storage time (weeks). Error bars represent the standard error of mean of three replicates.

3.3 Surface topology development

Figure 4 shows representative LV SEM images of the sample surfaces stored at 20 and 23°C. A low frequency of surface crystals could be observed for the 15 µm samples stored at 20°C for 12 weeks (Figure 4 A-B), while the 22 and 40 µm samples stored at 20°C showed no development of visible surface crystals by week 12 (Figure 4 A-B). However, already after 4 weeks of storage at 23°C a low frequency of crystals could be observed at the surface of all model pralines (results not shown). Further, after 6 weeks of storage at 23°C the frequency of surface crystals had increased, and the result images indicate that this frequency is higher for the samples with a particle size of 15 µm, followed by samples with a particle size of 22 and 40 µm, as can be seen in Figure 4 C-D. Further, the surface crystals on the 15 µm samples are larger than on the other samples. As can be seen in Figure 4 E-F, after 8 weeks of storage at 23°C the development of surface crystals was even more pronounced and the difference in frequency could still be observed for the samples with different particle size.
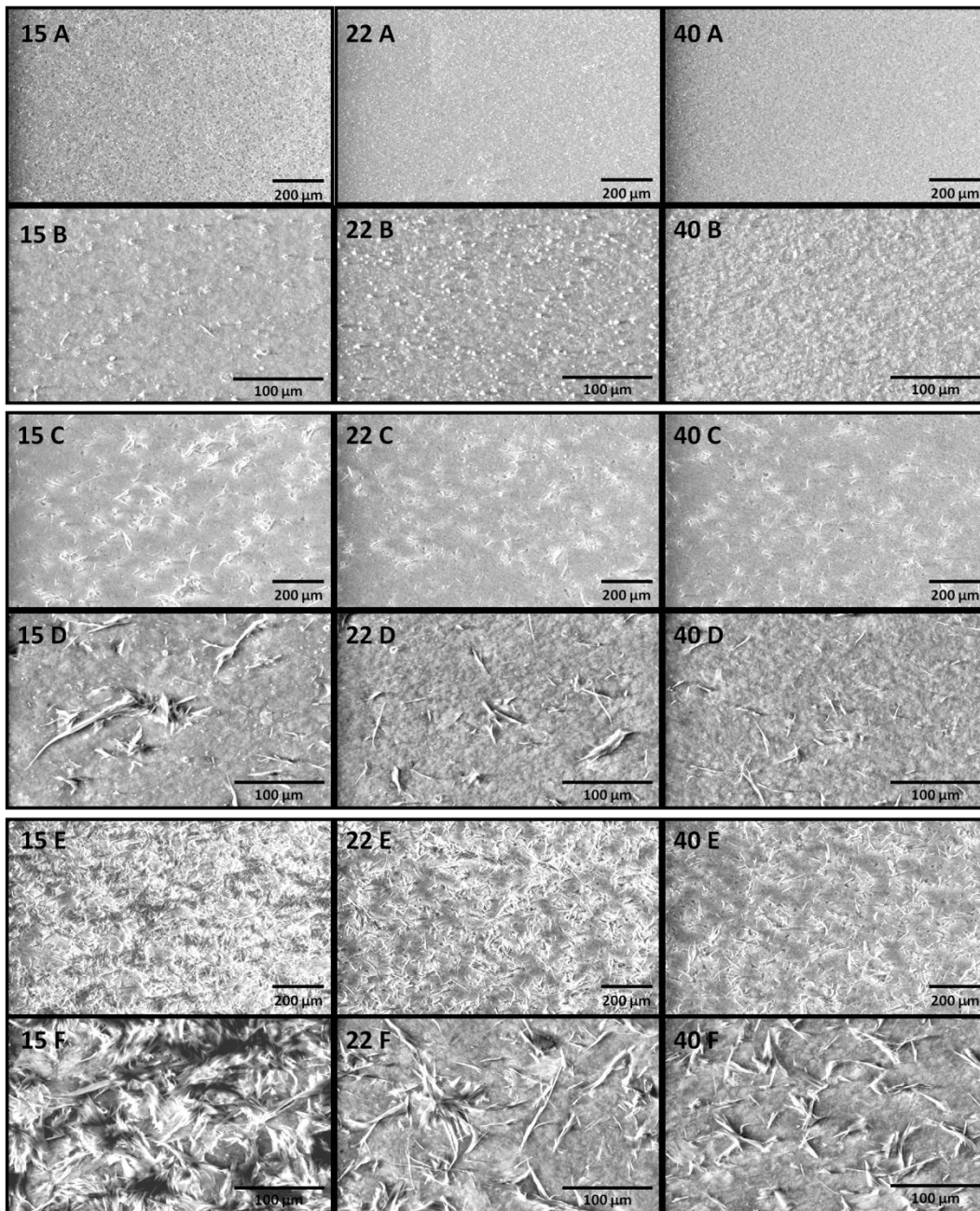
9

Figure 4. LV SEM images showing development of fat bloom crystals at the surface of the chocolate shells. 15A-B / 22A-B / 40A-B: Model samples with particle size 15, 22 and 40 μm, respectively, stored at 20°C for 12 weeks. 15C-D / 22C-D / 40C-D: Model samples with particle size 15, 22 and 40 μm, respectively, stored at 23°C for 6 weeks. 15E-F / 22E-F / 40E-F: Model samples with particle size 15, 22 and 40 μm, respectively, stored at 23°C for 8 weeks.

The roughness (Rq) increased over time for all samples and at both storage temperatures, still with varied rates. The results are reported as the relative increase in roughness compared to the starting value at t=0, i.e. $Rq_{(t)}/Rq_{(t=0)}$. From the results in Figure 5 it is shown that the 15 μm samples, stored at 23°C, have a higher increase in Rq than the other samples after week 4 and onward, whereas the other samples follow each other to a great extent. Further, the roughness values for the samples stored at 23°C increase to higher values than for the samples stored at 20°C. Oscillations in Rq values, mainly observed at 20°C storage temperature, are due to the presence of protrusions that appear, disappear and reappear over time, which have been reported in recent

studies (Dahlenborg et al., 2011; Dahlenborg et al., 2014). Statistical significance of the difference between the means of the samples could be determined ($p < 0.05$) using analysis of variance (ANOVA).
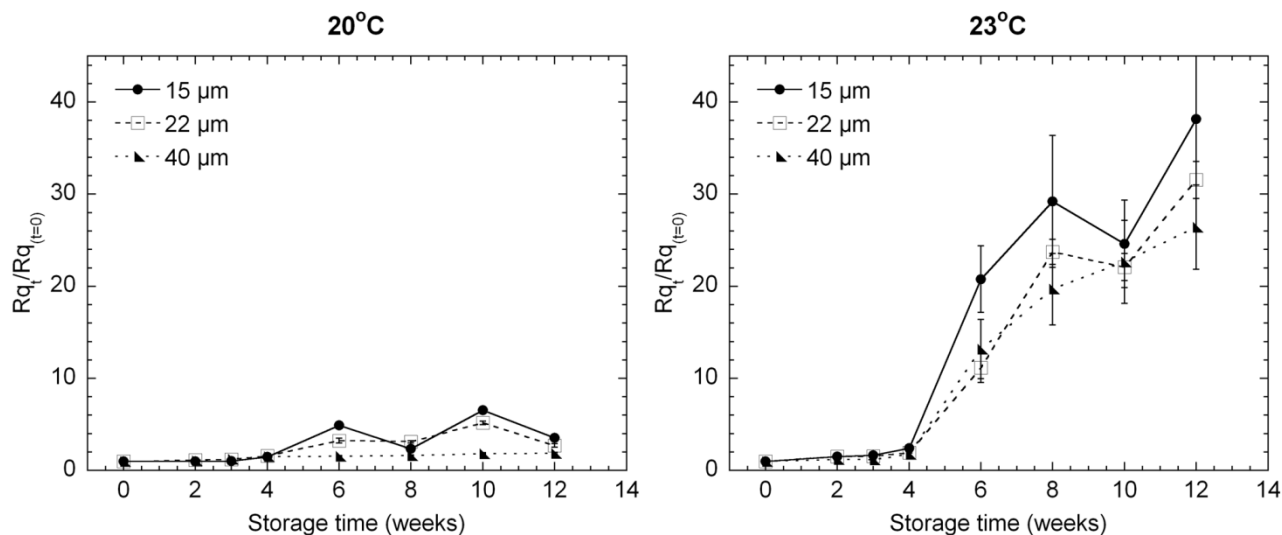

Figure 5. Normalized Rq values as a function of storage time for model samples stored at 20 and 23°C. Error bars represent the standard error of mean of 6 replicates.

3.4 Migration

Migration profiles are presented for the samples with particle size of 15, 22 and 40 μm stored at 23 °C. These can be seen in Figure 6, where they are presented as wt% BrTAGs in shell fat matrix as a function of distance to the filling (μm). It can be seen that close to the filling-shell interface the BrTAG migration is initially high for all samples. After 3 weeks storage the concentration of BrTAGs in the shell fat matrix close to the filling is approximately 4 wt% for all samples. Further, there is a gradual decay of the concentration. After 6 weeks of storage the BrTAG concentration is higher for all samples at all distances from the interface and it appears as if the gradient from 3 weeks has moved 600 μm into the samples. After 15 weeks storage the concentration closest to the filling decreases and an even concentration is obtained throughout the shells.
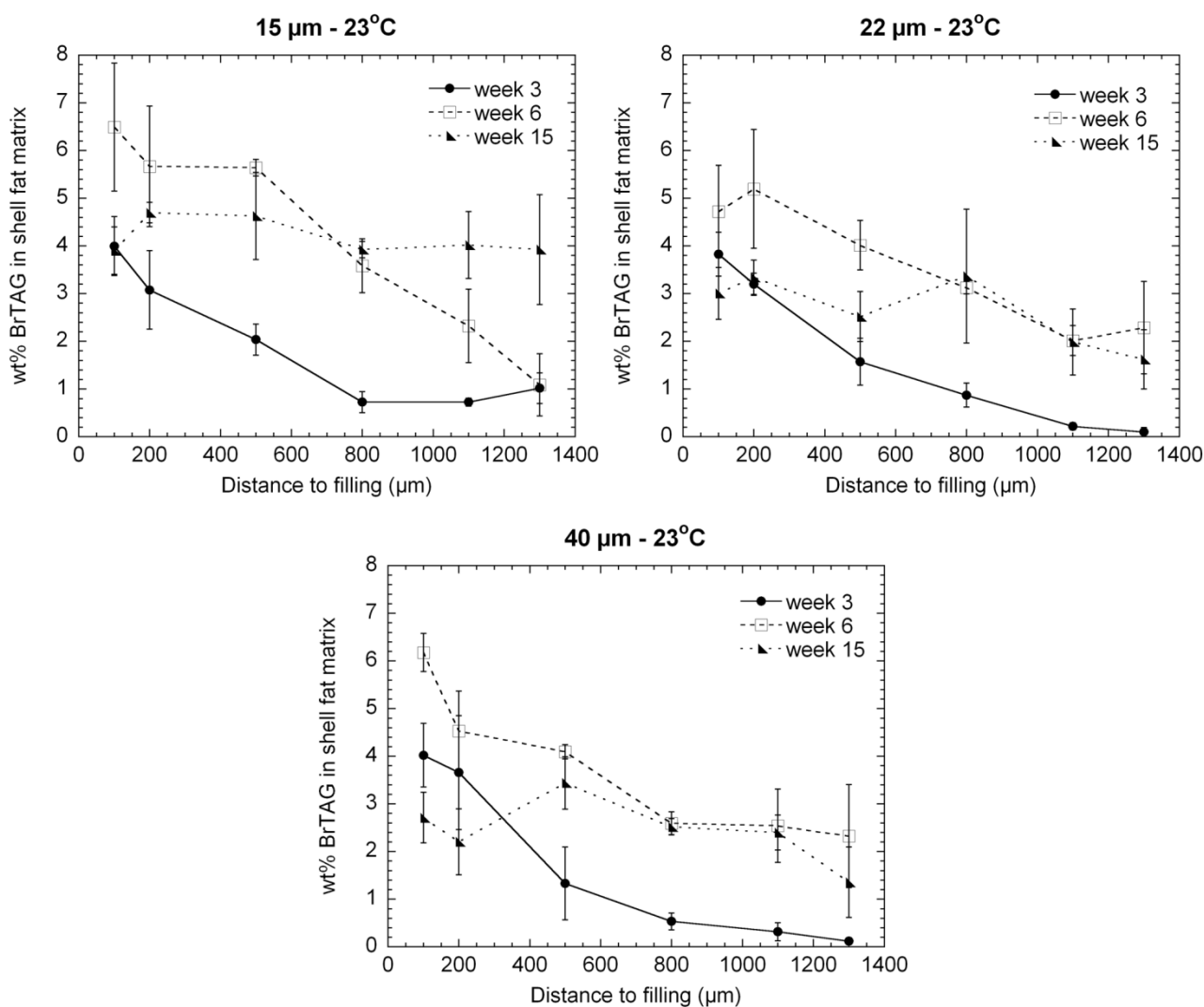
Figure 6. Migration profiles for model samples with chocolate shells of particle size 15, 22 and 40 μm, respectively, stored at 23°C. Error bars represent the standard error of mean of 4 replicates.

To further elucidate the process of BrTAG migration into the shells the mean BrTAG concentration in the shell fat matrix of all samples stored at 20 and 23°C at the distances 500 and 1100 μm from the interface between filling and shell are presented in Figure 7. From these results it can be seen that at 500 μm from the filling there is no significant difference between the samples stored at 20°C. At 1100 μm a slightly higher BrTAG concentration can be observed for the 15 μm samples after 15 weeks storage at 20°C. However, the 15 μm samples stored at 23°C show a higher concentration of BrTAGs in the shell fat matrix at a distance of 500 μm from the filling compared to the other samples over the whole storage period. Further, at 6 weeks storage a maximum in BrTAG concentration can be observed for all samples. At 1100 μm from the filling-shell interface the 15 μm samples show the highest mean concentration of BrTAGs after 15 weeks storage at 23 °C, while the 22 and 40 μm samples stay at the same level as at 6 weeks storage.
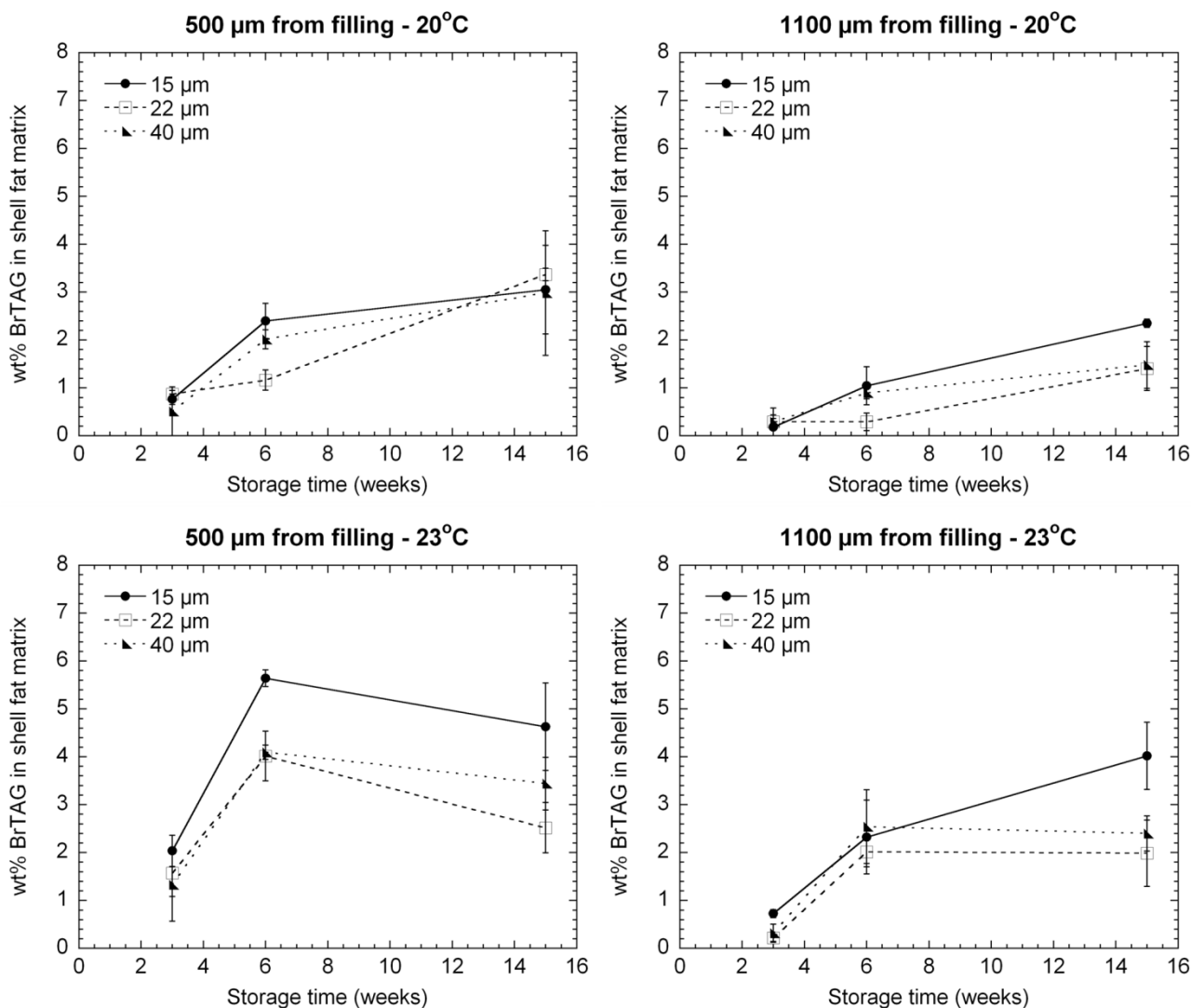
Figure 7. Wt% BrTAGs in shell fat matrix 500 and 1100 µm from filling as a function of storage time for model pralines stored at 20 and 23°C. Error bars represent the standard error of mean of 4 replicates.

Figure 8 represents the mean concentration of BrTAGs in the fat phase of the shells as a function of storage time for the model systems with varied particle size, stored at 20°C and at 23°C. The samples stored at 20°C show an increase in BrTAG concentration over time, still the mean concentration does not vary to any higher extent between the different samples except at 6 weeks of storage. After 15 weeks storage at 20°C the mean concentration of BrTAGs show an approximate value of 2.5% in the shell fat matrix which corresponds to 50% of the initial concentration in the filling fat phase. For the samples stored at 23°C the 15 µm samples show the highest mean concentration of BrTAGs over the whole storage period. Further, the BrTAG concentration of the 15 µm samples does not change to any great extent between 6 and 15 weeks of storage. On the other hand, it appears that the concentration of BrTAGs for the 22 and 40 µm samples goes through a maximum after 6 weeks of storage, still, the decrease in BrTAG concentration after 6 weeks of storage is not statistically significant. Further, the BrTAG concentration in the shell fat matrix of the

13

samples containing particles of 22 and 40 µm is shown to be relatively similar for both samples over the storage period. In addition, it can be seen that the samples stored at 23°C show a higher increase in BrTAG concentration that the samples stored at 20°C, where the mean BrTAG concentration in the shell fat matrix is approximately 4% for the 15µm samples after 15 weeks storage.
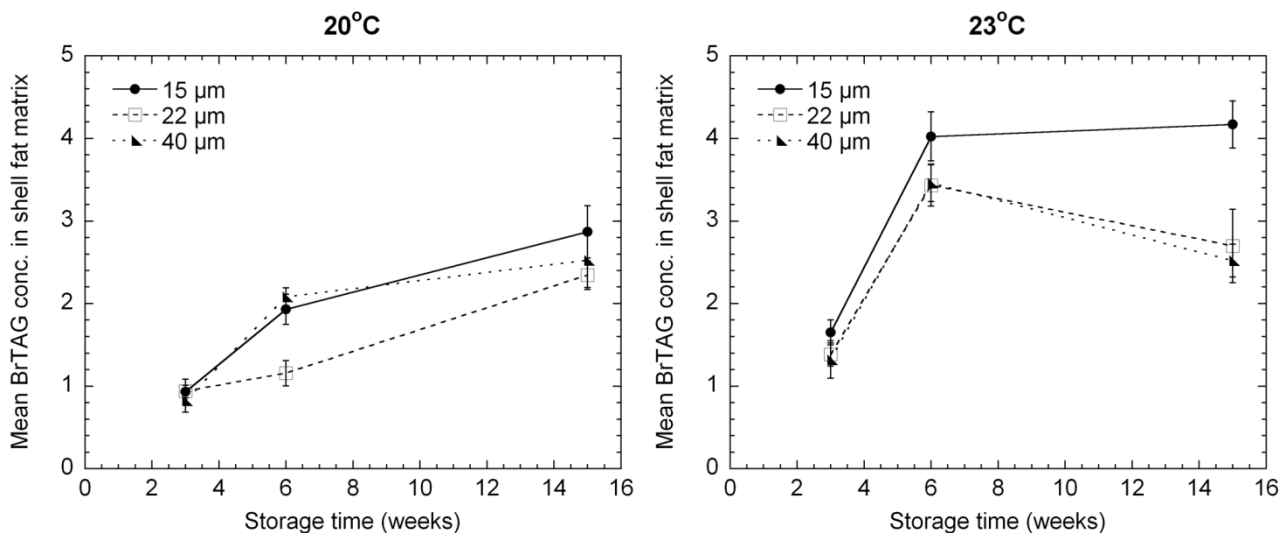

Figure 8. Mean BrTAG concentration in shell fat matrix as a function of storage time for model pralines stored at 20°C and 23°C. Error bars represent the standard error of mean of 4 replicates.

4. Discussion

All samples stored at 23°C showed a higher rate of polymorphic development into more stable crystals than the samples stored at 20°C, as could be seen from the results in Figure 3. The samples stored at 23°C also showed the highest rate of BrTAG migration from filling to shell. Further, these samples showed a higher rate of developing crystals at the surface compared to the samples stored at 20°C. Due to the size and shape of the crystals that could be seen in LV SEM images (Figure 4) they are observed as fat bloom crystals.

No significant difference in polymorphic development could be observed between the samples after 14 weeks of storage at 20 or 23°C. Still, it could be concluded that the CB TAGs of all samples initially were mainly in form $\beta_2 V$ and that all samples had developed CB crystals of polymorph $\beta_1 VI$ after 14 weeks storage at 23°C, indicating on fat bloom development. Further, the distribution of the $\beta_2 V$ and $\beta_1 VI$ crystals appears to be equal after 14 weeks storage irrespectively of the particles size, indicating that the polymorphic transformations for the samples stored at 23°C took place at an earlier stage. This could be supported by the macroscopic results (Figure 2) and the results from LV SEM and profilometry analyses (Figure 4 and Figure 5).

All results from surface topology development point in the same direction. At 20°C nearly no fat bloom or roughness development could be observed. On the other hand, at 23°C storage the frequency of developed fat bloom crystals at the surface and the roughness values were evidently higher for the 15 μm samples compared to the 22 and 40 μm samples. In addition, the frequency of fat bloom crystals appeared to be higher for the 22 μm samples compared to the 40 μm samples.

The differences in migration rate and fat bloom development between the storage temperatures could be explained by a higher liquid fat fraction in the shell and the filling at a higher storage temperature. Since the migration of TAGs takes place via the liquid fat portions, permeability increases and therefore migration induced fat bloom development is enhanced when the storage temperature is increased. The higher rate of migration during higher storage temperature agrees with results from earlier studies (Ali et al., 2001; Altan et al., 2011; Guiheneuf et al., 1997; Khan et al., 2006; Miquel et al., 2001; Ziegleder et al., 1998). Further, results from migration data, particularly at higher storage temperature, suggest that the samples with the smallest particle size, i.e. 15 μm (d(3.2)=3.0 μm), and thus with the largest specific surface area undergo a higher rate of oil migration from the filling compared to the samples with larger particle size, i.e. 22 and 40 μm (d(3.2) equal to 3.6 and 4.1 μm, respectively). Thus, combining the surface topology results with the migration results indicate that all results support each other, i.e. that the samples containing the smallest non-fat particles show the highest migration rate and the highest rate of fat bloom development. These findings can be supported by earlier studies, where Altimiras et al. (Altimiras et al., 2007) produced CB bars with sand particles of varied size. They could demonstrate that the bars made with the smallest sand particle fraction (~5 μm) showed the highest rate of oil migration and the biggest whiteness index change. The study by Choi et al. (Choi et al., 2007) with the opposite effect was performed with much larger particles (~50 μm), and the impact of the particles was actually quite small. Further, Montwani et al. (Motwani et al., 2011) stated that the interfaces of particles could be covered with liquid oil and thereby oil migration increases. Additionally, they suggested that the non-fat particles do not support the growth of fat crystal clusters leading to a more heterogeneous crystal network possibly resulting in higher permeability and enhanced migration of oil. Thus, specific surface area of the non-fat particles could play a role for possible migration pathways, where smaller particle size contributes to more surface area and thus, more passages for migration.

In a recent study (Dahlenborg et al., 2014), CB samples containing 25 wt% non-fat particles without added emulsifier were analysed regarding surface topology development and rate of oil migration. In this present study there were 2-3 times higher amount of non-fat particles present in the chocolate shells, i.e. 68 wt%. By observing the results obtained from these two studies it can be seen that the rate of fat bloom development at the surface, the roughness development and the oil

migration rate is significantly higher for the samples containing 68 wt% non-fat particles compared to the samples containing 25 wt% non-fat particles. After 12 weeks storage at 23°C the relative Rq values are a factor 2-3 times higher for the samples including 68 wt% particles compared to the samples including 25 wt% particles, and after 6 weeks storage the mean concentration of BrTAGs in the shell fat matrix is approximately three times higher for the samples containing 68 wt% particles than for the samples including 25 wt% particles. Figure 9 illustrates results from these two studies, where the effect of specific surface area of non-fat particles on oil migration is shown. A larger specific surface area corresponds to a higher migration rate of BrTAGs. Thus, a higher amount of non-fat particles with a larger specific surface area appear to increase the rate of migration and fat bloom development. These findings further support that the amount of non-fat particles together with the specific surface area of the non-fat particles affects the migration rate of liquid filling fat into the chocolate shell, and thus fat bloom development is also affected.
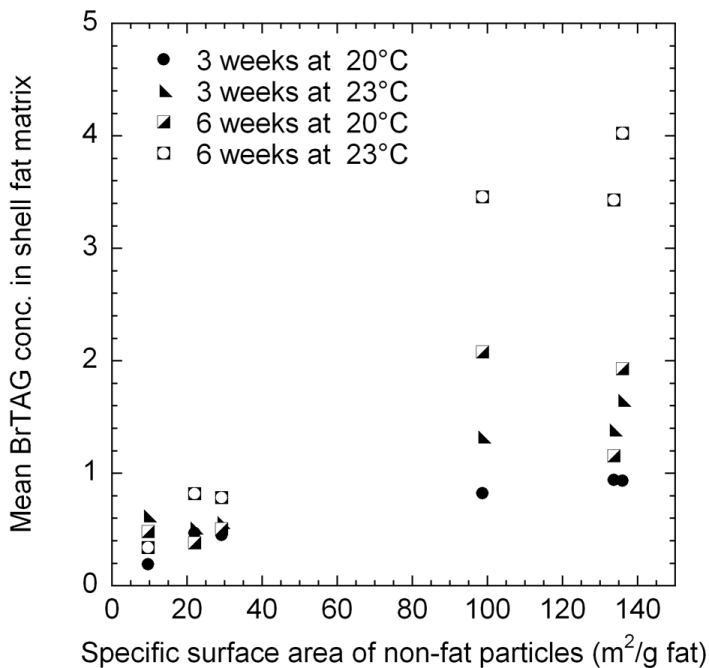

Figure 9. Mean BrTAG concentration in shell fat matrix as a function of specific surface area of non-fat particles (m^2/ g fat) for model pralines stored at 20°C and 23°C.

The initially observed high migration of BrTAGs close to the interface which declines with the distance from the interface (Figure 6) can be supported by earlier studies (Smith et al., 2007). Further, an interesting observation is the high concentration of BrTAGs in the shells, especially for samples stored at 23°C. In the first 200 μm of the shell between 5-7% of BrTAGs is observed at week 6, which is even above the actual concentration in the filling (5% of the total fat content in the filling). The fat matrix is a multiphase system, although, in this context, we may consider it as a two phase system with a liquid phase and a solid phase. We may assume that the solid phase is resident

16

and that all migration occurs in the liquid phase. Using $\varphi_{(SFC\text{-}Chocolate,\ 23°C)} = 67\%$ and $\varphi_{(SFC\text{-}ModelFilling,\ 23°C)} = 47\%$ we obtain a BrTAG concentration of the liquid fat phase in the filling of 9.4% (SFC values were measured for equal samples according to the official AOCS Cd16b-93 method by using NMR, and obtained through personal communication with Ghent University, Belgium). The ratio of the liquid fat phase in the filling relative to the liquid fat phase in the shell is very much in favour of the filling, as the fat content in the shell is low as well as the liquid fat fraction. Further, the liquid phase in the model filling is saturated by CB TAGs. The average concentration of BrTAGs in the liquid fat phase at complete equilibrium between the liquid fat phase in the filling and the liquid fat phase in the shell will thus be 8.3% for the whole model praline, which would give 2.7% BrTAGs counted on the total fat phase in the shell.

A common assumption is that the main transport mechanism is molecular diffusion through the liquid phase (Deka et al., 2006; Lee et al., 2010; Maleky et al., 2012; McCarthy et al., 2008; Miquel et al., 2001; Ziegleder, 1996a; Ziegleder, 1996b; Ziegleder et al., 1998), where the diffusion process is driven by a gradual equilibration of concentration differences. The liquid phase of the filling contains approximately of 9.4% BrTAGs, 42% triolein and 48% liquid CB components while the liquid phase in the shell contains 100% liquid CB components. According to the diffusion laws we expect triolein and BrTAGs to diffuse in the direction of the shell while liquid CB components diffuse in the opposite direction. The highest obtainable BrTAG concentration in the liquid phase of the shell is thus 8.3% which counted on the total fat content in the shell gives 2.7% of BrTAGs. From the profiles (Figure 6) as well as from the averages (Figure 7) it is clear that we obtain values well above this level. Although individual data points display large errors, the assembled mass of the data support that the concentration is well above what could be expected from diffusion. In addition, the profiles themselves (Figure 6) disagree with a Fickian diffusion model. The slope of the concentration curve is high between 0 and 600 μm and the concentration is more or less constant between 600 and 1400 μm after 3 weeks. After 6 weeks the complete curve has moved forward (about 600 μm) and upwards (about 2%). A diffusion process following Fick´s second law should lead to a reduced slope and a constant or falling concentration close to the interface. At week 15 the concentration gradient almost has disappeared, and the concentration close to the filling is comparable to the rest of the system.

Capillary penetration has also been suggested as an explanation for fat migration in chocolate systems (Aguilera et al., 2004; Choi et al., 2007; Guiheneuf et al., 1997; Marty et al., 2005; Quevedo et al., 2005; Rousseau et al., 2008). Further, protrusions originating from flow through surface pores have been characterised using profilometry, LV SEM and confocal Raman microscopy (Dahlenborg et al., 2011; Dahlenborg et al., 2012). However, measurements of the

porosity using mercury porosimetry (Loisel et al., 1997) suggests that the pore volume is between 1 and 4%, which is a too small volume to explain the observed penetration.

A suggested third model is a convective[1] flow that mobilizes liquid fat from the filling into the shell due to pressure differences. A convective flow that replaces the liquid fat in the penetrated fat matrix of the shell with the liquid fraction of the filling fat would lead to a BrTAG concentration rapidly reaching 2.7%. Still, as the observed concentrations are above this level it suggests that more than the initial level of liquid fat phase is entering into the shell matrix. A possible explanation could be that the shell is swelling and that the liquid fraction in the shell increases. To reach the maximum observed BrTAG levels of 5-7% the shells need to absorb about 80-140 % (calculated on the fat content) additional liquid fat of the filling fat composition which would lead to a swelling of between 35-60% of the shell (note that the peek values only have been obtained in limited domains of the shell). Unfortunately, we did not characterise the relative volumes of shell and filling to confirm this hypothesis, still, swelling of the shells was observed. Further, swelling has been observed previously of CB matrixes put in contact with liquid fat (Dahlenborg et al., 2011; Deka et al., 2006; Galdamez et al., 2009; Guiheneuf et al., 1997; Svanberg et al., 2012). Dahlenborg et al. (Dahlenborg et al., 2011) observed a volume increase in white chocolate shell, that was stored against a hazelnut filling, of approximately 40% after 36 weeks storage at cycled temperatures. Further, Galdamez et al. (Galdamez et al., 2009) observed an increase of approximately 25% in chocolate shell weight after storage against hazelnut oil at 23°C for one week, which corresponded to an increase of 61 wt% regarding the fat phase of the shell. We suggest that a possible reason for a swelling could be crystal growth in the CB matrix, due to Ostwald ripening and re-crystallisation into more stable polymorphic forms. If the crystals are growing in size while the number crystal concentration is constant, the network will get coarser and absorb an increasing amount of liquid phase. This effect may be further strengthened by the presence of non fat particles that may magnify the impact of a coarsening fat crystal network. Thus our picture of the processes is that there is an initial phase of molecular diffusion followed by a re-crystallisation processes and crystal growth leading to coarsening network and convective oil migration into the expanding shell matrix.

5. Conclusions

The effects of particle size regarding oil migration and fat bloom development on chocolate model pralines have been evaluated. Combined results from LV SEM, profilometry, EDS and DSC strongly indicate that model pralines, stored at 23°C, with a non-fat particle size of 15 µm undergo a higher rate of oil migration from filling to shell and thus a higher rate of developing fat bloom,

---

[1] We use the general definition of convective flow as a flow generated by a pressure gradient.

compared to model pralines with a non-fat particle size of 22 or 40 μm. Thus, the specific surface area of the non-fat particles seems to be an important parameter for oil migration and fat bloom development in chocolate pralines. From the migration experiments with the brominated probe it is clear that the results cannot only be explained using diffusive migration. Hence we concluded that convective migration most likely contributes to the migration process.

Acknowledgements

References

Aguilera, J. M., Michel, M., & Mayor, G. (2004). Fat migration in chocolate: Diffusion or capillary flow in a particulate solid? A hypothesis paper. *Journal of Food Science*, *69* (7), 167-174.

Alasalvar, C., Amaral, J. S., Satir, G., & Shahidi, F. (2009). Lipid characteristics and essential minerals of native Turkish hazelnut varieties (Corylus avellana L.). *Food Chemistry*, *113* (4), 919-925.

Ali, A., Selamat, J., Man, Y. B. C., & Suria, A. M. (2001). Effect of storage temperature on texture, polymorphic structure, bloom formation and sensory attributes of filled dark chocolate. *Food Chemistry*, *72* (4), 491-497.

Altan, A., Lavenson, D. M., McCarthy, M. J., & McCarthy, K. L. (2011). Oil Migration in Chocolate and Almond Product Confectionery Systems. *Journal of Food Science*, *76* (6), 489-494.

Altimiras, P., Pyle, L., & Bouchon, P. (2007). Structure-fat migration relationships during storage of cocoa butter model bars: Bloom development and possible mechanisms. *Journal of Food Engineering*, *80* (2), 600-610.

Amaral, J. S., Cunha, S. C., Santos, A., Alves, M. R., Seabra, R. M., & Oliveira, B. P. P. (2006). Influence of cultivar and environmental conditions on the triacylglycerol profile of hazelnut (Corylus avellana L.). *Journal of Agricultural and Food Chemistry*, *54* (2), 449-456.

Bernardo-Gil, M. G., Grenha, J., Santos, J., & Cardoso, P. (2002). Supercritical fluid extraction and characterisation of oil from hazelnut. *European Journal of Lipid Science and Technology*, *104* (7), 402-409.

Choi, Y. J., McCarthy, K. L., McCarthy, M. J., & Kim, M. H. (2007). Oil migration in chocolate. *Applied Magnetic Resonance*, *32* (1-2), 205-220.

Dahlenborg, H., Millqvist-Fureby, A., Bergenstahl, B., & Kalnin, D. J. E. (2011). Investigation of Chocolate Surfaces Using Profilometry and Low Vacuum Scanning Electron Microscopy. *Journal of the American Oil Chemists Society*, *88* (6), 773-783.

Dahlenborg, H., Millqvist-Fureby, A., & Bergenståhl, B. (2014). Effect of Shell Microstructure on Oil Migration and Fat Bloom Development in Model Pralines. *Submitted*.

Dahlenborg, H., Millqvist-Fureby, A., Brandner, B. D., & Bergenstahl, B. (2012). Study of the porous structure of white chocolate by confocal Raman microscopy. *European Journal of Lipid Science and Technology*, *114* (8), 919-926.

Deka, K., MacMillan, B., Ziegler, G. R., Marangoni, A. G., Newling, B., & Balcom, B. J. (2006). Spatial mapping of solid and liquid lipid in confectionery products using a ID centric SPRITE MRI technique. *Food Research International*, *39* (3), 365-371.

Galdamez, J. R., Szlachetka, K., Duda, J. L., & Ziegler, G. R. (2009). Oil migration in chocolate: A case of non-Fickian diffusion. *Journal of Food Engineering*, *92* (3), 261-268.

Ghosh, V., Ziegler, G. R., & Anantheswaran, R. C. (2002). Fat, Moisture, and Ethanol Migration through Chocolates and Confectionary Coatings *Critical Reviews in Food Science and Nutrition*, *42* (6), 583 – 626.

Guiheneuf, T. M., Couzens, P. J., Wille, H.-J., & Hall, L. D. (1997). Visualisation of Liquid Triacylglycerol Migration in Chocolate by Magnetic Resonance Imaging. *Journal of the Science of Food and Agriculture*, *73* (3), 265-273.

Hartell, R. W. (1999). Chocolate: Fat bloom during storage. *The Manufacturing Confectioner*, 89-99.

Khan, R. S., & Rousseau, D. (2006). Hazelnut oil migration in dark chocolate - kinetic, thermodynamic and structural considerations. *European Journal of Lipid Science and Technology*, *108* (5), 434-443.

Kinta, Y., & Hatta, T. (2005). Morphology of fat bloom in chocolate. *Journal of the American Oil Chemists Society*, *82* (9), 685-685.

Lee, W. L., McCarthy, M. J., & McCarthy, K. L. (2010). Oil Migration in 2-Component Confectionery Systems. *Journal of Food Science*, *75* (1), 83-89.

Loisel, C., Lecq, G., Ponchel, G., Keller, G., & Ollivon, M. (1997). Fat bloom and chocolate structure studied by mercury porosimetry. *Journal of Food Science*, *62* (4), 781-788.

Lonchampt, P., & Hartel, R. W. (2004). Fat bloom in chocolate and compound coatings. *European Journal of Lipid Science and Technology*, *106* (4), 241-274.

Maleky, F., McCarthy, K. L., McCarthy, M. J., & Marangoni, A. G. (2012). Effect of Cocoa Butter Structure on Oil Migration. *Journal of Food Science*, *77* (3), 74-79.

Marty, S., Baker, K., Dibildox-Alvarado, E., Rodrigues, J. N., & Marangoni, A. G. (2005). Monitoring and quantifying of oil migration in cocoa butter using a flatbed scanner and fluorescence light microscopy. *Food Research International*, *38* (10), 1189-1197.

McCarthy, K. L., & McCarthy, M. J. (2008). Oil migration in chocolate-peanut butter paste confectionery as a function of chocolate formulation. *Journal of Food Science*, *73* (6), 266-273.

Miquel, M. E., Carli, S., Couzens, P. J., Wille, H. J., & Hall, L. D. (2001). Kinetics of the migration of lipids in composite chocolate measured by magnetic resonance imaging. *Food Research International*, *34* (9), 773-781.

Motwani, T., Hanselmann, W., & Anantheswaran, R. C. (2011). Diffusion, counter-diffusion and lipid phase changes occurring during oil migration in model confectionery systems. *Journal of Food Engineering*, *104* (2), 186-195.

Quevedo, R., Brown, C., Bouchon, P., & Aguilera, J. M. (2005). Surface roughness during storage of chocolate: Fractal analysis and possible mechanisms. *Journal of the American Oil Chemists Society*, *82* (6), 457-462.

Rousseau, D., & Smith, P. (2008). Microstructure of fat bloom development in plain and filled chocolate confections. *Soft Matter*, *4* (8), 1706-1712.

Smith, K. W., Cain, F. W., & Talbot, G. (2007). Effect of nut oil migration on polymorphic transformation in a model system. *Food Chemistry*, *102* (3), 656-663.

Svanberg, L., Ahrne, L., Loren, N., & Windhab, E. (2011). Effect of pre-crystallization process and solid particle addition on microstructure in chocolate model systems. *Food Research International*, *44* (5), 1339-1350.

Svanberg, L., Ahrne, L., Loren, N., & Windhab, E. (2013). Impact of pre-crystallization process on structure and product properties in dark chocolate. *Journal of Food Engineering*, *114* (1), 90-98.

Svanberg, L., Loren, N., & Ahrne, L. (2012). Chocolate Swelling during Storage Caused by Fat or Moisture Migration. *Journal of Food Science*, *77* (11), 328-334.

Talbot, G. (1990). Fat migration in biscuits and confectionery systems. *Confectionery production*, 265-272.

Timms, R. E. (1984). Phase behaviour of fats and their mixtures. *Progress in Lipid Research*, *23* (1), 1-38.

Wille, R., & Lutton, E. (1966). Polymorphism of cocoa butter. *Journal of the American Oil Chemists Society*, *43* (8), 491-496.

Ziegleder, G., Moser, C., Geiger-Greguska, J. (1996a). Kinetics of fat migration in chocolate products part I: Principles and analythical aspects. *Fett/Lipid*, *98*, 196-199.

Ziegleder, G., Moser, C., Geiger-Greguska, J. (1996b). Kinetics of fat migration in chocolate products part II: Influence of storage temperature, diffusion coefficient, solid fat content. *Fett/Lipid*, *98*, 253-256.

Ziegleder, G., & Schwingshandl, I. (1998). Kinetics of fat migration within chocolate products. Part III: fat bloom. *Fett/Lipid*, *100* (9), 411-415.